AD-A193 787 MODELING OF SPRAY COMBUSTION IN DIRECT INJECTION DIESEL 1/1
ENGINE(U) NORTH CAROLINA AGRICULTURAL AND TECHNICAL
STATE UNIV GREENSBO.. H SINGH ET AL. 30 JAN 88
UNCLASSIFIED ARO-21329.3-EG-H DAAG29-84-G-0001 F/G 21/2 NL

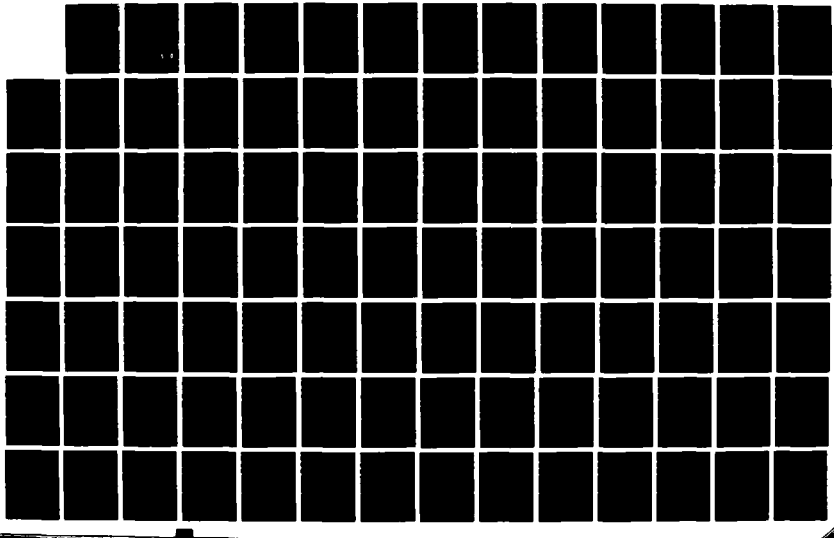

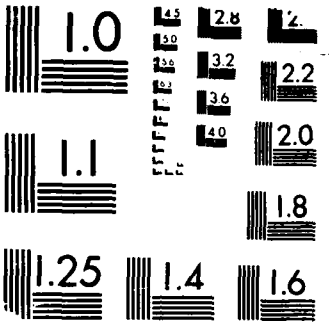

MODELING OF SPRAY COMBUSTION IN DIRECT INJECTION DIESEL ENGINE

FINAL REPORT

Dr. H. Singh
Dr. D. E. Klett

January 30, 1988

U. S. ARMY RESEARCH OFFICE

DAAG29-84-G-0001

NORTH CAROLINA A&T STATE UNIVERSITY
GREENSBORO, NC 27411

UNCLASSIFIED

SECURITY CLASSIFICATION OF THIS PAGE (When Data Entered)

REPORT DOCUMENTATION PAGE		READ INSTRUCTIONS BEFORE COMPLETING FORM
1. REPORT NUMBER ARO 21329.3-EG-H	2. GOVT ACCESSION NO. N/A	3. RECIPIENT'S CATALOG NUMBER N/A
4. TITLE (and Subtitle) Modeling of Spray Combustion in Direct Injection Diesel Engine		5. TYPE OF REPORT & PERIOD COVERED FINAL Jan. 84 to Dec. 87 6. PERFORMING ORG. REPORT NUMBER
7. AUTHOR(s) H. Singh D. E. Klett		8. CONTRACT OR GRANT NUMBER(s) DAAG29-84-G-0001
9. PERFORMING ORGANIZATION NAME AND ADDRESS North Carolina A&T State University Greensboro, NC 27411		10. PROGRAM ELEMENT, PROJECT, TASK AREA & WORK UNIT NUMBERS N/A
11. CONTROLLING OFFICE NAME AND ADDRESS U. S. Army Research Office Post Office Box 12211 Research Triangle Park, NC 27709		12. REPORT DATE Jan. 30, 1988 13. NUMBER OF PAGES 93
14. MONITORING AGENCY NAME & ADDRESS(if different from Controlling Office)		15. SECURITY CLASS. (of this report) Unclassified 15a. DECLASSIFICATION/DOWNGRADING SCHEDULE

16. DISTRIBUTION STATEMENT (of this Report)

Approved for public release; distribution unlimited.

17. DISTRIBUTION STATEMENT (of the abstract entered in Block 20, if different from Report)

NA

18. SUPPLEMENTARY NOTES

The view, opinions, and/or findings contained in this report are those of the author(s) and should not be construed as an official Department of the Army position, policy, or decision, unless so designated by other documentation.

19. KEY WORDS (Continue on reverse side if necessary and identify by block number)

Diesel Combustion
Combustion Modeling
Cross Flow
Fuel Injection
Spray Penetration
Equivalence Ratio

20. ABSTRACT (Continue on reverse side if necessary and identify by block number)

(SEE ATTACHED SHEET)

DD FORM 1 JAN 73 1473 EDITION OF 1 NOV 65 IS OBSOLETE

UNCLASSIFIED

SECURITY CLASSIFICATION OF THIS PAGE (When Data Entered)

20. ABSTRACT CONTINUED

A mathematical model has been developed to predict the penetration of a transient fuel spray, the temporal and spatial distribution of air fuel mixture before the end of ignition delay and the subsequent pressure rise during combustion in a Direct Injection Diesel Engine with and without swirl. The model accounts for the non-isothermal and non-isobaric character of processes during fuel injection resulting from continuous motion of the piston. The effects of various engine operating variables on spray have been studied and graphically presented. The calculated spray penetration with and without crossflow of air has been compared with the available experimental data of other researchers and good agreement between the two is noticed.

The model can predict the rate of combustible mixture formation, the rate of heat release and cylinder pressure as a function of time in direct injection (DI) diesel engine. A single cylinder D.I. research diesel engine was operated with N-hexadecane as the engine fuel to validate the mathematical model. However, a leaking head gasket rendered the data unusable, so comparisons between modeled and measured cylinder pressure rise data are not included in this report. As soon as such data is available, it will be forwarded as a supplement to this report.

SCIENTIFIC PERSONNEL EMPLOYED ON THE PROJECT:

Dr. Harmohindar Singh, Principal Investigator

Dr. David E. Klett, Co-Investigator

Vijay Vasandani, Graduate Assistant (received MSME Degree, May 1986)

David Indire, Graduate Assistant

TABLE OF CONTENTS

TABLE OF CONTENTS

LIST OF TABLES AND FIGURES

NOMENCLATURE

		Units*
A_l	: Surface area of droplet	cm^2
C_d	: Coefficient of discharge	
C_D	: Coefficient of drag for fuel droplet	
d	: Nozzle diameter	cm
d_s	: Sauter mean diameter of droplet	μm
d_l	: Mass averaged diameter of droplet	μm
g	: Gravitational constant	cm/sec^2
K_o	: Evaporation rate constant in stagnant air	cm^2 /sec
K	: Evaporation rate constant	cm^2 /sec
L	: Length of nozzle hole	cm
m_l	: Mass of liquid fuel	gm
n	: Number of droplets	
P_a	: Chamber gas pressure	atm
P_{cyl}	: Cylinder charge pressure	atm
P_{inj}	: Injection pressure	atm
Q	: Discharge from nozzle	mm^3 / stroke
Re	: Reynolds number	
Sc	: Schmidt number	
t	: Time from start of injection	sec
T_a	: Chamber gas temperature	K
T_{inj}	: Injection timing	deg BTDC
V_l	: Liquid fuel velocity	cm/sec
V_{lo}	: Jet velocity at nozzle exit	cm/sec

* Indicates units used in the text unless stated otherwise

V_r	: Relative velocity of fuel droplet (wrt air velocity)	cm/sec
V_{or}	: Relative velocity of droplet at the beginning of any interval of time	cm/sec
X	: Penetration	cm
ΔP	: Pressure differential across nozzle	atm
ρ_a	: Chamber gas density	gm/cc
ρ_l	: Liquid fuel density	gm/cc
θ	: Spray cone angle	degrees
τ_i	: Ignition delay period	seconds
μ_a	: Viscosity of chamber gas	gm/cm-sec
μ_l	: Viscosity of liquid fuel	gm/cm-sec
ν_a	: Kinematic viscosity of chamber gas	cm^2/sec

DEFINITIONS

$$ds = \frac{\Sigma n_i d_i^3}{\Sigma n_i d_i^2}$$

$$d_l = \left(\frac{\Sigma n_i d_i^3}{\Sigma n_i}\right)^{0.33}$$

Re = Reynolds number

$$= \frac{\text{velocity of droplet x droplet diameter}}{\text{kinematic viscosity of ambient gas}}$$

Sc = Schmidt number

$$= \frac{\text{kinematic viscosity of ambient gas}}{\text{diffusivity coefficient}}$$

1. INTRODUCTION

Diesel Engines are used for a wide variety of applications, not only for the purpose of transport but also as a source of power for stationary systems. Their wide acceptance as prime movers is attributed to their superior fuel consumption characteristics in heavy duty vehicles, and low hydrocarbon and carbon monoxide emissions in lighter duty vehicle applications although they exhibit somewhat higher nitric oxide and particulate emission. The purpose of this research project was to create a computer model of the spray combustion process in a direct injection diesel engine which could then be used to study the parameters necessary to optimize engine performance.

Computer modeling of the combustion process is a valuable complement to engine design and testing since it allows the investigation of varying engine design parameters without the expense of building and testing numerous possible design alternatives. The model developed here takes a phenomenological approach to combustion analysis and relies on previous results of experiments on various fundamental aspects of the combustion process. A fully detailed simulation of engine operation is not yet possible due to a lack of understanding of all the complex phenomena occurring in an operating engine.

To achieve improvements in the performance of Direct Injection (D.I.) Diesel Engines, the process of combustion needs to be better understood. The complicated mechanisms involved in diesel combustion are the subject of on-going research by many individuals. From what is known, there are strong indications that the diesel spray and mechanics of its formation preceeding combustion significantly influence the entire process and thus

calls for primary attention in any investigation.

Fuel spray injection from a nozzle into a combustion chamber is followed by the division of liquid fuel into a large number of fine droplets to ensure good distribution of fuel in the chamber and to increase the surface area through which rapid heat transfer rates may be accomplished. Atomization, phenomenon responsible for fuel breakup, is a direct result of any one or combination of the following: cavitation, turbulence, roughness of nozzle, pressure variation across the nozzle and the formation of surface waves. The emerging droplets come into contact with hot swirling air above the piston. They exchange and conserve mass, momentum and energy while traveling away from the nozzle tip, overcoming drag and vaporizing to form a well distrubuted fuel air mixture in the combustion chamber. Combustion then takes place in three recognizable stages. The first stage, at the beginning of autoignition, corresponds to the process of burning of premixed fuel and air existing within specific flammability limits at the end of ignition delay. A rapid rate of pressure rise is the result of this process. The second stage is the burning of the combustible mixture formed during the rapid pressure rise period. Finally, in the third stage, fuel still in the liquid phase and a very rich mixture of fuel and air at the core of the spray, burns in a diffusion flame.

In the present study, efforts were focused on developing a computer model to predict spray characteristics during its formation, locate the regions where autoignition commences and then analyze combustion in the stages described above for environmental conditions obtaining in actual engines. The computer model is capable of predicting the rate of heat

release and cylinder pressure with respect to the engine crank shaft rotation. The model predictions with and without crossflow of air for spray penetration were verified from available experimental data of other researchers. Work is presently under way to conduct experiments on a Ricardo - Hydra Direct Injection Diesel Research Engine procured by the department to validate the results of the model.

2. LITERATURE REVIEW

An extensive survey of the literature was done to review previous work on studying the various processes occuring within the cylinder and other modeling techniques adopted. Beginning with Schwietzer in 1938, efforts have been directed at understanding the complexities of interactions between processes that follow the injection of fuel in diesel engines. To form a reasonably strong basis for any further investigation, it was necessary to review the opinions of other researchers regarding the nature of spray penetration, effect of various engine parameters on penetration, mixing of fuel vapor in air and finally the process of combustion.

2.1 NATURE AND GEOMETRY OF SPRAY

Work done to date can broadly be classified as either analytical or experimental or a combination of both. The analytical approach adopted by Ogasawara and Sami[1]* and Elkotb and Rafat [2] treated the spray as an agglomerate of droplets with their studies confined to one such droplet. On the other hand, Oz [3] and Melton [4] opted in favor of a "Mixing Jet Theory" by regarding the spray as fuel vapor injected at high pressure into lower pressure air. Experiments conducted on diesel engines have revealed the coexistence of liquid and vapor phases in actual fuel sprays. In fact Hiroyasu and Kadota [5] successfully demonstrated that fuel droplets never attain critical temperature even when injected into a supercritical environment, thereby confirming the heterogeneous character of fuel sprays inside diesel engines.

---

*Numbers in brackets denote the reference found at the end of this report.

There appears to be no general consensus among researchers regarding the geometry of spray, especially in the presence of swirling air. Chiu, Shahed, and Lyn [6] of Cummins Engine Company have assumed the shape to be like that of a blunt body whereas Hiroyasu and Kadota [7] have considered the spray as a right circular cone under no swirl conditions.

2.2 AIR MOTION

Air motion in a high speed direct injection diesel engine cylinder consists of swirl motion, an inward radial component of air motion, commonly called "Squish", and an axial component of air velocity due to the motion of the piston. The role of moving air is to facilitate proper mixing of the fuel vapor with air and enhance the subsequent process of combustion.

The inlet valve geometry and the extent of its opening affect the generation of swirl in a combustion chamber. For the purpose of analysis, swirl can be assumed as solid body rotation about the cylinder axis [8]. Squish tends to cause swirl to deviate from true solid body rotation. Squish has a maximum value close to TDC and depends largely on the shape of the combustion chamber.

2.3 SPRAY DEVELOPMENT

Schweitzer [9] was among the first to investigate the penetration of sprays. Using oil in his experiments conducted in a pressure chamber with stagnant air, he determined the factors that have considerable impact on spray tip penetration. Dimensional analysis served to establish a relation between penetration and injection pressure, chamber pressure, orifice size and shape, and viscosity. It was a good beginning, considering that sophisticated photography equipment was not available in 1938, and the fact

that he ignored many important factors such as evaporation, effect of elevated temperatures and air swirl. Schweitzer's correlation, along with those of others discussed below, have been summarized in tabular form in Table 1.

Since the 1960's a lot of research has been conducted on this topic. Parks, et al [10] performed experiments which helped them conclude that higher gas temperature reduces the penetration of spray because of rapid evaporation, provided the chamber density remains constant. They also found that a larger orifice diameter increases penetration due to increased droplet size. The effects of varying injection pressure and chamber pressure were also included in the scope of their investigation. While higher injection pressure increases the velocity of droplets which tends to increase the penetration, it also results in the formation of smaller droplets thereby reducing the time of evaporation and consequently the penetration of droplets. The net effect is a small increase in the value of penetration. Similarly, a lower chamber pressure increases the pressure differential across the nozzle, producing smaller droplets and tending to decrease penetration. But, as drag is also decreased the final result is a slight increase in penetration. By curve fitting their experimental data, they modified Schweitzer's correlation. However, they failed to recognize the importance of momentum exchange between fuel and surrounding air.

Ogasawara and Sami [1] proposed an expression to evaluate spray tip penetration after studying the behavior of a single droplet. While viscous drag and exchange of momentum with the surrounding air was kept in mind, the effect of any evaporation of the droplet during motion in a high temperature and pressure environment was assumed to be negligible.

Oz [3] in 1969 was among the first few to advocate the concept of analyzing fuel sprays in diesel engines as being equivalent to injecting vapors at high speed into air. The empirical formula that Oz presented gave a fairly good match with experimental values for low back pressures.

Melton [4] proposed that at a distance from the source of about 30 nozzle diameters, a diesel spray is essentially an air jet bearing a fog of fuel droplets. As such, Melton applied the "Theory of Submerged Jets" to spray mechanics and derived an expression for spray penetration.

In 1971, Dent [11] reviewed all the experimental work done in cold and hot bombs and utilized the information to generate an equation for fuel penetration under cold bomb, hot bomb, and engine working conditions. Later Hay and Jones [12] recommended the use of this equation for all conditions except for very high gas densities.

An attempt to model fuel spray trajectory under conditions pertinent to actual engine cylinders was made in 1977 by Elkotb and Rafat [2]. The effect of shape of the combustion chamber, air velocity pattern, heat transfer and drag force variations were all considered in the model to predict the location of a fuel droplet at any instant. Using basic equations of mass, momentum and energy conservation, non-linear differential equations were developed. These were solved numerically and the results were verified by experimental investigation. Their model sought to improve upon the ballistic approach adopted by Ogasawara in 1966.

All experimental work done before 1978 gave poor results for the initial part of the injection. But it is this initial period of about one millisecond (MS) that is of interest in an actual diesel engine since it corresponds closely to the ignition delay period. Hiroyasu, et al [13]

developed techniques to overcome this drawback. They performed experiments with quiescent air as well as with swirling air. Study of fuel penetration was done under varying ambient gas pressure, injection pressure, nozzle geometry and ambient gas temperature. It was concluded that spray penetration is proportional to time in the early stage of injection and thereafter to the square root of time. Thus the fuel jet was divided into a developing region and a fully developed region, with transition occurring at a time called the breakup time.

Photographs taken by Kuniyoshi, et al [14] in 1980 revealed that the spray is composed of two distinct zones, namely the main jet region and a mixing region. The main jet region lies towards the core of the spray and holds small sized droplets moving at high velocities, while the mixing region, containing somewhat larger droplets moving with lower velocity, encircles the main jet region. They observed that the total penetration could be subdivided into an initial part, a mixing part and a dilution portion. Further, for high charge pressure and varying elevated temperatures the initial part of the penetration remained unchanged.

A new dimension was added by Varde, Popa and Varde [15] in the search for independent parameters that influence penetration. They established the dependence of penetration on nozzle L/D ratio in addition to the indirect effect it has on altering the coefficient of discharge. Working at extremely high injection pressures, they also found that the decay in velocity was directly proportional to the injection pressure for high penetration values but showed a reversed trend for smaller values of penetration.

A study of the process of atomization using diesel fuel injection at

high pressure and high temperature into a quiescent gaseous environment was undertaken by Takeuchi, et al [16] in 1983. They explained that fuel, when injected from any nozzle, has a jet cone which grows in a wavy form then breaks up into thin threads. Finally small droplets are formed from these filaments. The spray tip penetration was seen by them to be composed of 3 linear relations. The first corresponded to the period required for jet breakup, the second was present till the disappearance of wavy flow and the third gave the spray tip penetration beyond that period. All three equations, one for each phase, are given in Table 1.

A "Stochastic Thick Spray Model" has been developed in the form of a computer code by Kuo, Yu, and Shahed [17] to quantify fuel and air in different regions in space. The analysis treats the spray as being composed of discrete computational particles representing a group of droplets and follows them along Lagrangian trajectories accounting for mass, momentum and energy exchange at every time step.

Fragoulis and Henein, in a recent publication [18], have examined most of the existing expressions for spray penetration and derived a correlation of their own by "averaging" the powers to which independent parameters have been raised in these expressions. They also introduced a new concept of "Mean Penetration Diameter" allowing description of spray tip penetration by knowing the initial diameter of the droplets.

Work is under progress at the University of Manchester England [19] to examine the formation of spray in stagnant air as well as air moving in a direction perpendicular to the direction of injection. The latter has been achieved in a wind tunnel with induced air velocities of 8 and 12 m/s. The experimental data has shown spray penetration to be mainly dependent on gas

density with a relatively weak dependence on gas temperature. At room temperature, no substantial difference was recorded in the values with and without crossflow.

2.4 IGNITION DELAY AND RATE OF BURNING

Although numerous definitions for ignition delay have been given by different authors, all seem to agree that it is the period extending from the beginning of injection to the time of measurable combustion. Henein and Bolt [20] found that pressure rise was the first noticeable change occurring in diesel combustion and emphasized the use of measuring ignition delay in terms of pressure rise. Their engine tests demonstrated that increase in cylinder air pressure, fuel/air ratio, cooling water temperature and engine speed, all work towards shortening the delay period.

The same authors, in 1969 [21], suggested an exponential correlation for evaluating ignition delay in terms of apparent activation energy and mean integrated temperature of air charge. An increase in activation energy as per that correlation, increases ignition delay but any increase in temperature decreases ignition delay.

Spontaneous ignition delay of fuel droplets and fuel spray in a high pressure gaseous environment was examined closely by Hiroyasu and Kadota in two separate experiments [5]. The effect of charge pressure, temperature and oxygen concentration of the ambient gas on ignition delay was recorded and used to yield an expression for finding ignition delay. The constants in the expression were found to be functions of fuel properties and their values have been determined for various fuels. Similar effects of varying intake air pressure and temperature, cooling water temperature and engine speed on ignition delay in a single cylinder, direct injection, 4 stroke

diesel engine were observed by Wong and Steere in 1982 [22].

A number of ignition delay models for heterogeneous charge engines were compared by Primus and Wong [25] in 1985. They observed that there is widespread agreement that the physical delay is very short relative to the chemical delay; and, therefore, the total delay may be measured using the Arrhenius equation. In the majority of cases, mean cylinder pressure and temperature are used for computing the ignition delay period. As far as heat release is concerned, many of the existing models consider an apparent heat release diagram as a part of their program input to calculate the actual heat release by iterating to satisfy the burning rate equation and the equations of conservation of energy simultaneously.

TABLE 1

Author and year	Nature of Work	Expression Derived	Fluid Used	Ambient Gas	Injection Pressure	Back Pressure	Ambient Temp.	Remarks
Schweitzer 1938	Experimental	$X_{(in)} = \frac{(d)}{1+\rho_a} f\left(\frac{t}{d}\rho_a(\Delta P)^{1/2}\right)$ d = nozzle dia in inch ρ_a = density of chamber gas in units of atm density ΔP = pressure differential across nozzle in lb/sq in. t = time from start of injection in seconds	Oil	Air	1000-8000 psia	-	-	Ambient air density was 1 to 275 unit of atm density
Parks et al 1966	Experimental	$X_{(in)} = \frac{200d[\rho_a (P)^{1/2}]\{1-(1-\frac{d}{d_o})1.12\times10^{-3}(Ta-70)\}^{0.6} t^{0.6}}{1+\rho_a}$ d = nozzle dia in inch ρ_a = density of chamber gas in units of atm density P = pressure differential across nozzle in lbs/sq in. d_o = reference orifice dia = 0.0236 in. Ta = ambient gas temperature in F t = time from start of injection in seconds	Diesel	Air	6500-11000 psia	upto 1000 psia	70-1000 F	Constant gas properties were used
Ogasawara et al 1966	Analytical and Experimental	$X_{(m)} = \left(\frac{\rho_l d^2 V_{lo}}{\mu_a}\right)\left(\frac{10}{36_v Re_o}\right)[\ln\{1+Re_o(1-\exp(-37.58\beta_v N_t))\}]$ ρ_l = liquid fuel density in Kg sec^2/m^4 d = droplet size in m V_{lo} = relative velocity of droplet at the time of injection μ_a = viscosity of air in Kg sec/m^2 Re_o = Reynolds no. for droplet at the time of injection β_v = 0.85 t = time from the start of injection in seconds $N = t\mu_a/\rho_l d^2$	Kerosene, gas oil	Air	-	33 atm	700-800 K	Exit velocity at nozzle = 72 m/s

TABLE 1 (cont)

I.Z. OZ 1969	Theoretical (Mixing jet Theory)	$X_{(m)} = ae\text{-}bp^n t^{1/2}$ $p = P_a / P_{atm}$ $a = 5$ $b = 0.04$ $n = 1$ t = time in seconds from start of injection	Diesel	Air	-	atm pressure	-	Gives good results for low values o P_a / P_{atm}
Dent 1970	Analytical	$X_{(in)} = 13.6((\frac{\Delta P}{\rho_a})^{1/2} dt)^{1/2} (\frac{530}{T_a})^{1/4}$ P = pressure differential across nozzle in lbf/sq.in ρ_a = ambient gas density in lbm/cubic in d = nozzle diameter in inch T_a = ambient gas temperature in K t = time from start of injection in ms	Diesel	Air	upto 20000 psia	100 atm	-	Valid for lo ambient gas $2 < L/d < 4$ and $t > 0.5m$
Melton Jr 1971	Theoretical (Theory of submerged jet)	$X = \frac{d/2}{\alpha} [\frac{2\alpha V_{lo}}{d/2} (\frac{\rho_s}{\rho_l})^{1/2} t+1^{1/2} -1]$ d = nozzle dia V_{lo} = velocity of jet at nozzle exit ρ_s = jet density ρ_l = 0.85 t = time from start of injection	Diesel	Air	-	-	-	
Hiroyasu et al 1978	Experimental	$X_{(m)} = Cd (\frac{2\Delta P}{\rho_l})^{1/2} t$ for $0 < t < t_b$ $= 2.95 (\frac{\Delta P}{\rho_a})^{1/4} (dt)^{1/2}$ for $t > t_b$ Cd = coefficient of discharge P = pressure differential in Pa ρ_a = ambient gas density in Kg/m^3 ρ_l = fuel density in Kg/m^3 d = nozzle dia in m t = time from start of injection in seconds	Diesel fuel, Light oil, Kerosene	Air and Nitrogen	upto 25 MPa	upto 10 MPa	Room temp to 320 C	Air swirl was also considered

TABLE 1 (cont)

Kuniyoshi et al 1980	Experimental	$X_{(mm)} = 418\ t^{0.375}\ \gamma_a\ ^{0.092 \log t - 0.409}\ d^{0.538}$ d = dia of nozzle in mm γ_a = specific weight of fuel in Kgf/m^3 t = time from start of injection in ms	Diesel	Air, Air + N	35.4 MPa	upto 8 MPa	upto 900 k	
Varde et al 1983	Experimental	$X_{(cm)} = 1.1\ (A1)^{0.3}(A2)^{-0.008}(A3)^{0.5}(A4)^{0.16} t^{0.55}$ $A1 = \Delta P \rho_l d^2 / \mu_l^2$ $A2 = \rho_l \sigma_l d / \mu_l^2$ $A3 = \rho_l / \rho_a$ A4 = L/d ΔP = pressure differential across nozzle ρ_l = fuel density d = nozzle dia μ_l = fuel viscosity σ_l = surface tension L = length of nozzle	Diesel # 2	Air + N	upto 150 MPa	upto about 5 MPa	-	Establishes significance of L/d ratio
Takeuchi et al 1983	Experimental	$X1_{(mm)} = 3.25\ \Delta P^{1.01}\ \rho_a^{-0.238}\ t^{1.04}$ $X2 = 1.75\ \Delta P^{0.631}\ \rho_a^{-0.544} t^{0.524}$ $X3 = 3.93\ \Delta P^{0.231}\ \rho_a^{-0.591} t^{0.233}$ ΔP = pressure differencial across nozzle in MPa ρ_a = ambient gas density in Kg/m^3 t = time in ms from the start of injection	Diesel	Air, Air + CO CO	11.9 MPa	4-5 MPa	Room temp	
Apostoles and Henien 1984	Analytical and Experimental	$X = C\ V_{lo}^{1/4} \left(\frac{\rho_l}{\rho_a}\right)^{1/4} d^{1/4}\ t^{1/4}$ V_{lo} = initial droplet velocity ρ_l = liquid fuel density ρ_a = ambient gas density d = nozzle dia t = time from the start of injection	Diesel # 2, Jet propulson fuel, Indolene	Air	6.9 to 27.6 MPa	atm conditions	Room temp	

3. DIESEL ENGINE COMBUSTION CHARACTERISTICS

Inspite of the complexities involved in diesel combustion, a large number of correlations and models have been proposed in the past, but very seldom do we find them being applied under actual engine conditions. Most theoretical work assumes the properties of chamber gas and fuel to be a constant and experiments have invariably been performed in cold or hot chambers, having constant volume, fixed temperature and non varying pressure drop across the nozzle for each test run. Furthermore, the photographic technique employed in all experiments gives good results for time greater than 1 ms from the start of injection. As mentioned earlier, it is the time prior to 1 ms that is of significance since high speed diesel engines rarely display an ignition delay of over 1 ms. Thus, the relationships are seldom used in determining spray characteristics during time less than one millisecond from the start of injection.

The expressions for spray penetration summarized in Table 1 cannot be compared directly, as each was derived under a different set of environment conditions. Nevertheless, a close examination of each expression provides insights about the effects of various parameters on spray penetration. These parameters are listed on the next page and a brief discussion on each follows in the next section.

ΔP : Mean effective pressure across the nozzle

C_d : Coefficient of discharge for the nozzle

d : Diameter to nozzle opening

L/d : Length to diameter ratio of the nozzle

ρ_a : Ambient gas density

T_a : Ambient gas temperature

ρ_l : Liquid fuel density

SMD : Sauter mean diameter of droplets

θ : Spray cone angle

K : Evaporation rate constant

t : Time from the start of injection

In addition to the variables listed above, penetration in an actual diesel engine may also be affected by engine dimensions, engine speed, duration of injection, swirl ratio, angle of inclination of nozzle, distribution of SMD in spray cone, distribution of fuel by mass across the cone and some fuel properties.

3.1 EFFECT OF SOME PARAMETERS ON PENETRATION

(1) Pressure differential across nozzle

The pressure differential across a nozzle can be altered either by changing the injection pressure or by varying the chamber pressure.

(a) Changing injection pressure: An increase in injection pressure increases the velocity of droplets which tends to increase the penetration. At the same time, higher injection pressure also results in the formation of smaller droplets having shorter life and hence less penetration. The net effect, as noticed by many, is a slight increase in the value of penetration.

(b) Altering chamber pressure: Higher chamber pressure results in the formation of larger droplets capable of travelling farther, but since the drag on the droplets also increases, the net result is a slight decrease in the penetration.

(2) Coefficient of discharge for the nozzle

Coefficient of discharge has a very obvious effect on

penetration. Penetration increases as coefficient of discharge is increased.

(3) Orifice diameter

With an increase in orifice diameter, larger sized droplets are formed. They can survive longer, and even though the drag they experience escalates, they move much further as compared to smaller droplets.

(4) L/d ratio of the nozzle

A higher L/d ratio, in addition to increasing the coefficient of discharge for the nozzle, also inhibits the decay in center line velocity thereby increasing the penetration.

(5) Ambient gas density

For all other parameters remaining unchanged, an increase in chamber gas density increases the drag on fuel droplets, resulting in smaller penetration.

(6) Ambient gas temperature

Although an increase in the ambient gas temperature decreases the life of fuel droplets, the ambient gas density is also decreased and subsequently reduced drag enhances penetration.

The remaining parameters affecting penetration are dependent variables and can be expressed in terms of the above discussed parameters. Knowing their relationship to the above six, their effects can also be predicted.

The variables mentioned in (1) through (6) above are characteristics of the engine or the working environment. Their value serves as an essential input to any model that portrays the development of fuel sprays.

3.2 AN INSIGHT TO PROBABLE INPUTS

Sauter Mean Diameter (SMD), the spray cone angle (θ), the evaporation rate constant (K), and the ignition delay period (τ) are the few other possible inputs that need to be scrutinized. Vital information is available on them and deserves individual inspection in the following paragraphs.

3.2.1 SAUTER MEAN DIAMETER

Several mean diameters of droplets in a spray have been used to describe the quality of atomization, but Sauter Mean Diameter is of particular interest in combustion application. The definition of SMD relates the surface area to the volume of the droplets, thereby providing a very essential relationship between surface area and volume that is required for analyzing evaporation.

The variation of SMD with location in a spray, and the effect of injection pressure, chamber pressure and nozzle geometry on this variation have been studied by Hiroyasu and Kadota [26]. The empirical formula proposed by them, and commonly accepted for use, is given by

$$SMD = C\ (\Delta P)^{-0.135}\ (\rho)^{0.121}\ (Q)^{0.131} \qquad (3.1)$$

where,

SMD = Sauter Mean Diamter in μm

ΔP = Mean effective pressure drop in MPa

ρ_a = Air or chamber gas density in Kg/m^3

Q = Amount of fuel delivered in mm^3/stroke

C = Constant depending on nozzle type

= 25.1 for pintle nozzle

= 23.9 for hole nozzle

= 22.4 for throttling nozzle

A typical distribution of the SMD across the spray as obtained from the above reference is shown in Figure 1.

3.2.2 SPRAY CONE ANGLE

Bracco [27] has shown that in the case of high speed diesel engines the atomization of liquid fuel is spontaneous and the breakup length is practically non-existent. In other words, divergence of spray begins immediately at the exit of the nozzle. The same observation has, however, not been reported for low speed diesel engines or for injection into constant volume hot and cold chambers. The angle of divergence is also known as the spray cone solid angle. This angle is a function of nozzle dimensions, chamber gas density and the pressure differential across the nozzle [15].

Varde, Popa and Varde [15] recently studied the effect of chamber gas density and ΔP on the spray cone angle. Their results are represented graphically in Figure 2. A significant change in the behavior of the curves is noticed as the nozzle L/d ratio is increased. The transition in the trend was found to occur at an L/d value of about 4.

3.2.3 EVAPORATION RATE CONSTANT

The evaporation rate constant for the liquid droplets of fuel is a function of the pressure and temperature of the medium surrounding the droplets. As expected, the effect of higher temperature is to increase the value of the evaporation rate constant and consequently decrease the life span of a droplet. At higher temperatures, an increase in gas pressure further increases the evaporation rate, whereas just the opposite happens if the gas temperature is low. The dependence of the evaporation rate on

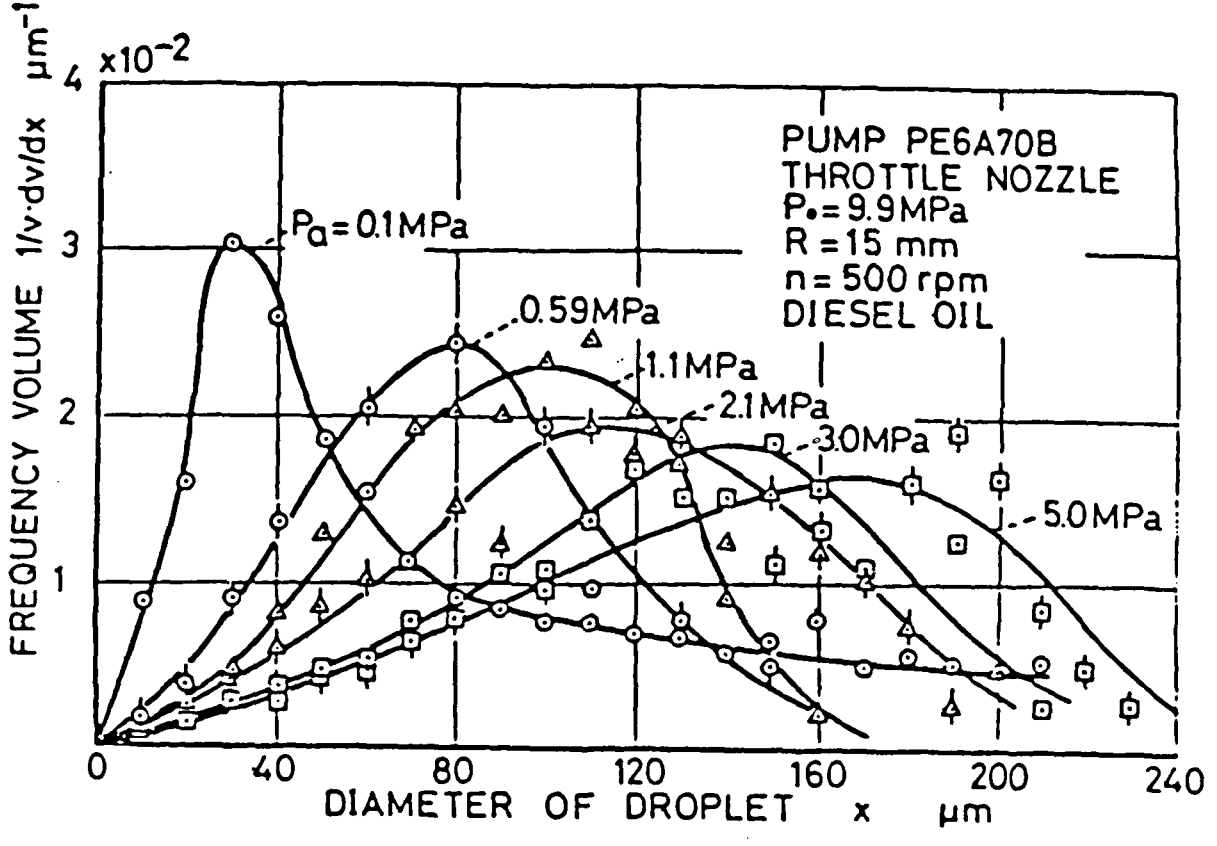

FIG. 1 **Droplet size distribution at various back pressure** (from ref 13)

SPRAY CONE ANGLE = f(nozzle dia, L/D ratio, ΔP, ρ_g)

$$\theta = 1.32 \left(\frac{d_o^2 \rho_a \Delta P}{\rho_g^2 \nu_a^2} \right)^{1/4}$$

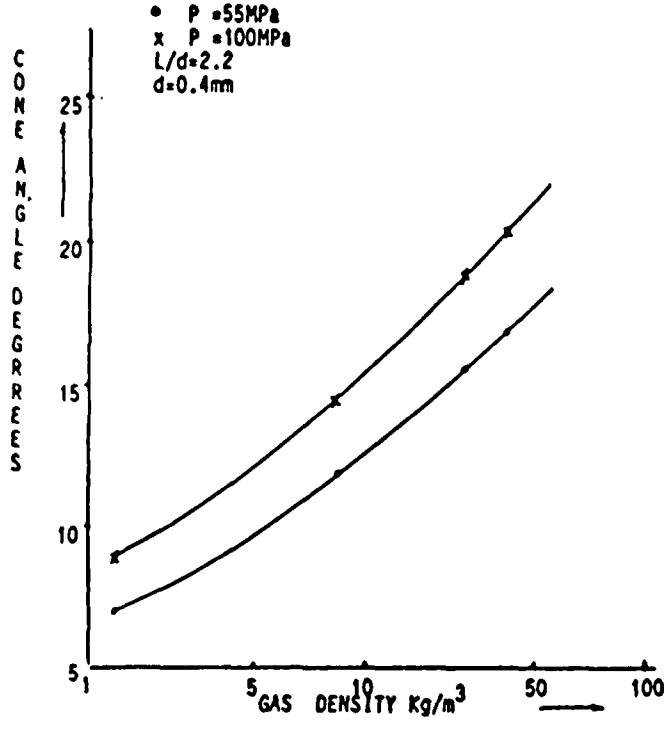

EFFECT OF GAS DENSITY ON SPRAY CONE ANGLE
(from ref 15)

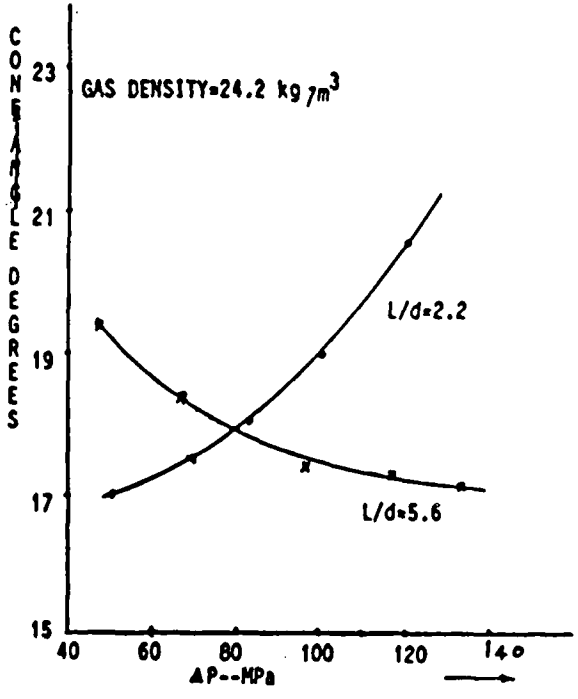

EFFECT OF INJ.PRESSURE ON CONE ANGLE
(from ref 15)

FIG. 2

temperature and pressure for various types of fuel in a quiescent air environment has been determined by Hiroyasu and Kadota [5] and is reproduced graphically in Figure 3.

3.2.4 IGNITION DELAY PERIOD

Depending on the definition of ignition delay various correlations for computing the delay period have been proposed. Since it is widely accepted to consider the beginning of rapid pressure rise to be the end of ignition delay, the work done by Hiroyasu and Kadota [5] is of particular interest. They have conducted experiments with liquid sprays and single droplets at high temperature and pressure to establish the degree of influence of chamber gas pressure, gas temperature and oxygen concentration in the ambient gas on ignition delay. The following equation is the outcome of their efforts:

$$\tau = A\ (P_a)^B\ (\Phi)^C\ \exp\ (D/T_a) \qquad (3.2)$$

where,

P_a = Chamber gas pressure

Φ = Oxygen concentration in ambient gas

T_a = Mean temperature of gas

A, B, C, and D are constants, whose values for some commonly available fuels are also given in reference 5.

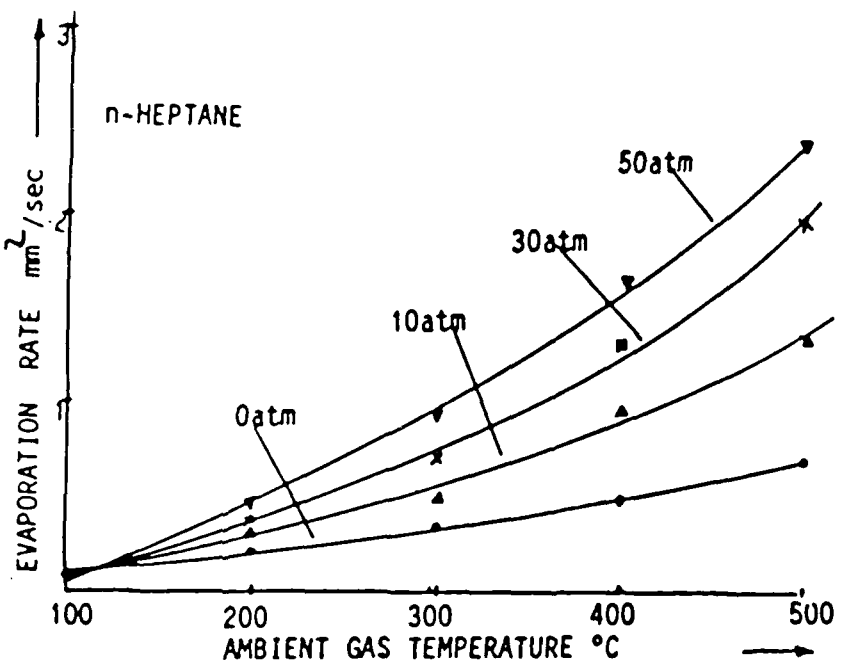

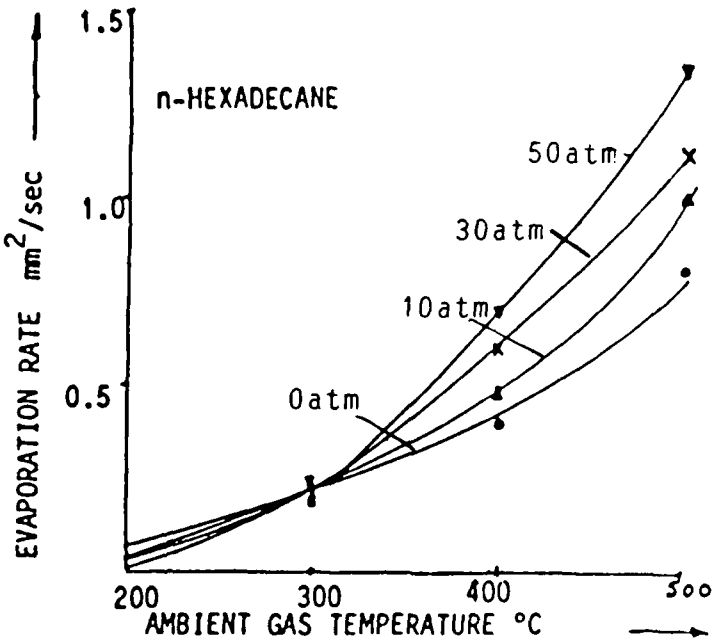

FIG. 3 EVAPORATION RATE----EXPERIMENTAL STUDY OF HIROYASU IN 1977 (FROM REF. 5)

4. MODEL DEVELOPMENT

4.1 MODEL ASSUMPTIONS

The following assumptions were made while developing the computer model to predict the spray geometry, the fuel-air distribution, the time of ignition delay and the subsequent pressure rise during combustion:

(1) The diesel fuel spray has been assumed to be heterogeneous in character, with spray disintegration and droplet formation occurring at the nozzle exit. This assumption is consistent with the findings of Bracco [27] for high speed diesel engines.

(2) The mean value of the Sauter Mean Diameter of droplets emerging from the nozzle during the course of the injection has been evaluated using equation (3.1) in the form

$$ds = A(\Delta P)^{-0.135}(\rho_a)_m^{0.121}\ (Q)^{0.131} \qquad (4.1)$$

where,

A = 23.9 for a hole nozzle

and Q, the liquid fuel injected, is found using

$$Q = \pi/4\ (d)^2\ (V_{lo})_m\ T_{inj}\ C_d \qquad (4.2)$$

where,

d = nozzle diameter

V_{lo} = Liquid fuel velocity at the start of injection

T_{inj} = Duration of injection

C_d = Coefficient of discharge for the nozzle.

The subscript m in the above equations implies the use of the mean value of the variable enclosed in the brackets during the course of injection. The variation in the value of SMD about its mean value across the spray axes is taken to be linear. While bigger droplets are assumed to

remain in the core of the spray, the smaller ones are considered to adhere to the outer fringes of the spray.

(3) For the no-swirl case, the spray is considered to be a right circular cone subtending a constant angle at the apex. This is a fairly safe assumption for L/d ratios of 4 or slightly less. Varde, et al [15] have shown (Fig 2) that nozzles with L/d ratios of 4 do not exhibit any change in spray cone angle with change in pressure differential across the nozzle. For nozzles with L/d ratio less than 4, an increase in gas density or ΔP across the nozzle tends to increase the spray cone angle. Therefore, in actual engines with the piston moving up, the effect of a decrease in pressure differential on the spray cone angle is nullified by the reverse effect due to a simultaneous increase in gas density. The value of the constant spray angle has been computed using the expression given by Reitz and Bracco [32].

$$\text{Tan } \theta/2 = 0.13 \left(1 + \frac{\rho_a}{\rho_1}\right) \tag{4.3}$$

where,

ρ_a = Chamber gas density

ρ_1 = Liquid fuel density

For purposes of convenience in computations, and to facilitate the study of spatial and temporal distribution of liquid and vaporized fuel within the spray, the spray cone has been subdivided into 4 concentric subcones under conditions of no swirl. The innercone subtends an angle of $\theta/4$ at the apex and is a solid cone while the second, third and fourth cones subtend angles $2\,\theta/4$, $3\,\theta/4$ and θ at the apex respectively and are hollow cones which envelope the inner cones.

(4) The distribution of liquid fuel by mass in each of the subcones is assumed to be Gaussian. As we move away from the inner cone the amount of fuel contained in each of the subcones decreases.

(5) The evaporation rate constant, K_o , for diesel fuel in stagnant air was obtained by interpolating the experimental values given in Reference 5. The rate at which liquid fuel evaporates is assumed to follow the "D^2 law" which relates the final size of a droplet to the initial size by:

$$(\text{final diameter})^2 = (\text{initial diameter})^2 - Kt \qquad (4.4)$$

where,

K is the evaporation rate constant and t is the time in which the change in diameter takes place.

Here, the evaporation rate, K, is different from K_o mentioned earlier as the ambient gas in the engine cylinder is not stagnant. The two constants are related by the following expression

$$K = K_o \, (1 + 0.276 \, Re^{\frac{1}{2}} \, Sc^{0.33}) \qquad (4.5)$$

where,

Re = Reynolds number

Sc = Schmidt number, taken to be unity

(6) Since there is relative motion between droplets and the surrounding air, the droplets experience a drag force which is computed using

$$\text{Drag force} = \pi/8 \, C_D \, (d_l)^2 \, (\rho_a) \, (V_r)^2 \qquad (4.6)$$

where,

C_D = Coefficient of drag

d_l = Mass averaged diameter of droplet

ρ_a = Ambient gas density

V_r = Relative velocity between fuel droplets and surrounding air particles

The drag force is composed of viscous drag and pressure drag which depends primarily on the Reynolds number and the rate of mass efflux from the droplet surface. The coefficient of drag to be used in equation (4.6) can be approximated as a function of the Reynolds number and is given by [28]

$$C_D = (24/Re)\ (1 + 0.15\ Re^{0.687}) \qquad (4.7)$$

Yuen and Chen [31], based on their experimental results, suggested use of the above equation for the coefficient of drag provided the Reynolds number is evaluated using the density of the free stream and the characteristic viscosity coefficient is calculated at a reference temperature given by:

$$T_r = T_l + (T_a - T_l)/3$$

where,

T_a = Ambient gas temperature

T_l = Fuel Temperature

(7) The initial velocity of liquid droplets can be calculated by applying Bernoulli's equation at the nozzle exit for constant injection pressure. This initial velocity is assumed to be the same for all droplets irrespective of their size and may be found from

$$V_{lo} = C_d\ (2g\ (p_{inj} - p_{cyl})/\rho_l)^{\frac{1}{2}} \qquad (4.8)$$

where,

C_d = Coefficient of discharge for the nozzle

P_{inj} = Injection pressure

P_{cyl} = Cylinder pressure

ρ_l = Liquid fuel density

(8) The gravity, bouyancy, and pressure forces are very small compared to the acceleration and drag forces and as such have been neglected. For the same reason, Newton's second law of motion in its simple form can be used to trace the history of motion of fuel droplets [28]

$$d/dt\ (m_l \cdot V_l) = 1/2\ C_D\ A_l\ \rho_a\ V_r^2 \qquad (4.9)$$

and

$$V_r = V_{or} exp(-\tfrac{1}{2}\rho_a A_l C_D)\ (X) \qquad (4.10)$$

where,

m_l = Mass of liquid droplet

V_l = Velocity of liquid droplet

C_D = Coefficient of drag

A_l = Surface area of droplet

ρ_a = Ambient gas density

V_r = Relative velocity of droplet

V_{or} = Initial relative velocity of droplet

(9) Air swirl has been assumed to be a solid body rotation around the cylinder axis [8] whereas the air motion due to piston movement and squish has been neglected.

(1Ø) Pressure equilibrium is maintained throughout the cylinder, i.e. changes in the engine cylinder pressure are assumed to stabilize instantaneously.

(11) Collisions among droplets and the impingement of droplets on the combustion chamber wall have not been analyzed.

(12) Swirl causes the concentric right circular cones to be deformed into non-concentric cones with elliptical bases. The minor axes of these cones being equal to the diameter of the cones without swirl.

(13) Vapors generated from droplets in motion form a homogeneous mixture with the surrounding air and move with the same angular and linear velocity as the surrounding air.

(14) The rapid pressure rise period follows immediately after the end of ignition delay which is given by equation (3.2). The values of the constants have been taken from reference 5 to give equation (3.2) the form

$$\tau = 0.872\ (P_a)^{-1.24}(\Phi)^{-2.10}\exp(4050/T_a) \qquad (4.11)$$

where,

P_a = Pressure of gas in chamber in atm

Φ = Oxygen concentration in ambient gas

T_a = Mean temperature of ambient gas in °K

(15) Combustion begins in a zone after the end of ignition delay only if the equivalence ratio lies within the flammability limits of Ø.3 to 3.Ø.

(16) All the premixed fuel identified to ignite burns in three degrees of crank angle rotation [23].

(17) After the end of the rapid pressure rise period, the fuel is assumed to burn at the rate it is injected with equivalence ratio equal to unity.

4.2 MODEL INPUTS

The following are the necessary inputs to the model:

(1) Spray cone angle

(2) Sauter Mean Diameter of fuel droplets and their distribution

(3) Mass averaged diameter of droplets

(4) Liquid fuel mass distribution across the spray

(5) Fuel properties such as evaporation rate constant, density, and boiling point temperature as functions of pressure and temperature

(6) Fuel injection pressure

(7) Swirl ratio

(8) Engine geometry

(9) Engine speed

(10) Fuel injection timing

(11) Duration of injection

(12) Injector nozzle diameter and its coefficient of discharge.

4.3 SUMMARY OF MODEL

The model requires fuel properties and the engine dimensions as the main input parameters and analyzes the spray as an agglomerate of tiny droplets, forming a heterogeneous mixture and existing under supercritical conditions.

A finite difference numerical approach has been adopted that creates new spray segments with the passage of time between the stations traversed by the fuel droplets in small but equal intervals of time. The sizes of segments vary with time and also differ from cone to cone depending on the distance travelled by different sized droplets in the same time interval. The initial momentum of the spray in each cone at the start of injection is the momentum of the fuel injected in the first time increment. As the droplets move through the air they experience drag and evaporation and at the end of a time interval the total momentum is shared by the remaining liquid fuel, vaporized fuel and the entrained air. An identical pattern is followed by the remaining liquid droplets in the next increment of time and also by the succeeding droplets coming out in the following interval of time. Thus, the basic equations of mass and momentum are repeatedly satisfied to solve for decaying velocity of droplets between stations and the increasing velocity of air in the direction of penetration. The non-isothermal character of the spray is recognized by simultaneously establishing an energy balance in each time step. Such a procedure keeps track of droplet history, the amount of fuel vaporized and the quantity of air entrained in a particular time step at different locations of the spray. This enables the model to specify the temporal and spatial variation of combustible mixture in various regions of space.

Another salient feature of the model is its capacity to take into account the swirling of air and the variations in back pressure, chamber volume and chamber gas temperature with time due to the continuous motion of the piston in the cylinder. The progressive deformation of the concentric cones because of swirl has been followed by determining the

deformed boundaries defined by the locus of the positions of droplets in each cone at the end of each time interval and the corresponding deflection of fuel vapors with swirling air in the same interval of time.

Figure 4 shows the velocity and displacement vector diagram for a fuel droplet in the first three increments of time. 1-2' is the intended line of motion of the droplet in the first increment of time. Point 2 is the actual location of the droplet at the end of the first time interval due to superposition of the swirl velocity. The figure also shows the location of the droplet at points 3 and 4 in the next two time intervals. The penetration of the droplet at the end of the "n th " increment of time is given by PEN (n) and is different from the distance actually travelled by the droplet along a curved path. Vapors generated are assumed to have the same linear and angular velocity as that of the surrounding air which makes the fuel-air distribution at the end of the 3rd interval of time appear as shown in Figure 5. The final configuration of the spray is depicted in Figure 6 with elongation of the circular base taking place in the direction of swirl. Since there is no force considered to be acting perpendicular to the plane of the spray, no deformation takes place in that direction. This is primarily the reason why the minor axes of the elliptical bases of the deformed cones are considered to be equal to the diameter of the base of the undeformed cone without swirl.

Keeping account of the spray geometry at all times makes it possible to detemine the intermixing of fuel vapors and air between overlapping cones when computing the equivalence ratio at various locations within the fuel spray.

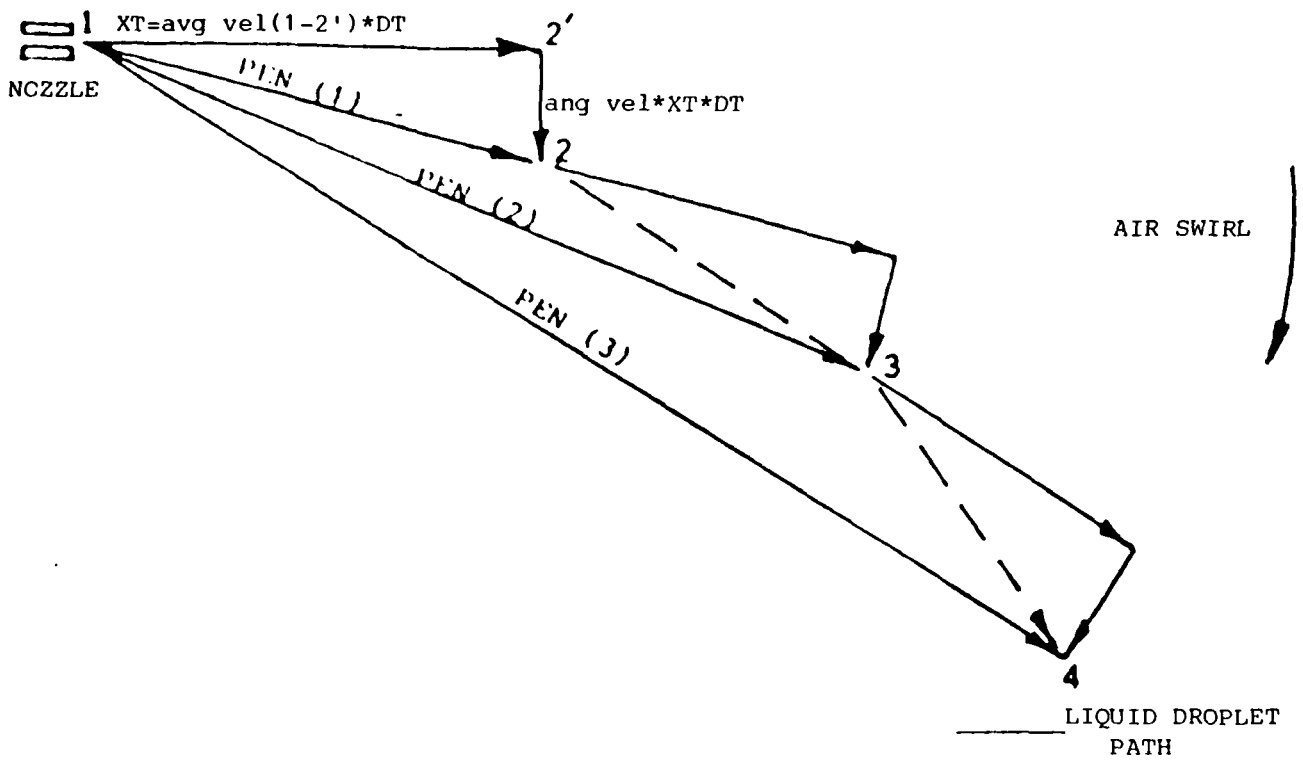

Fig. 4. Velocity and Displacement Diagram

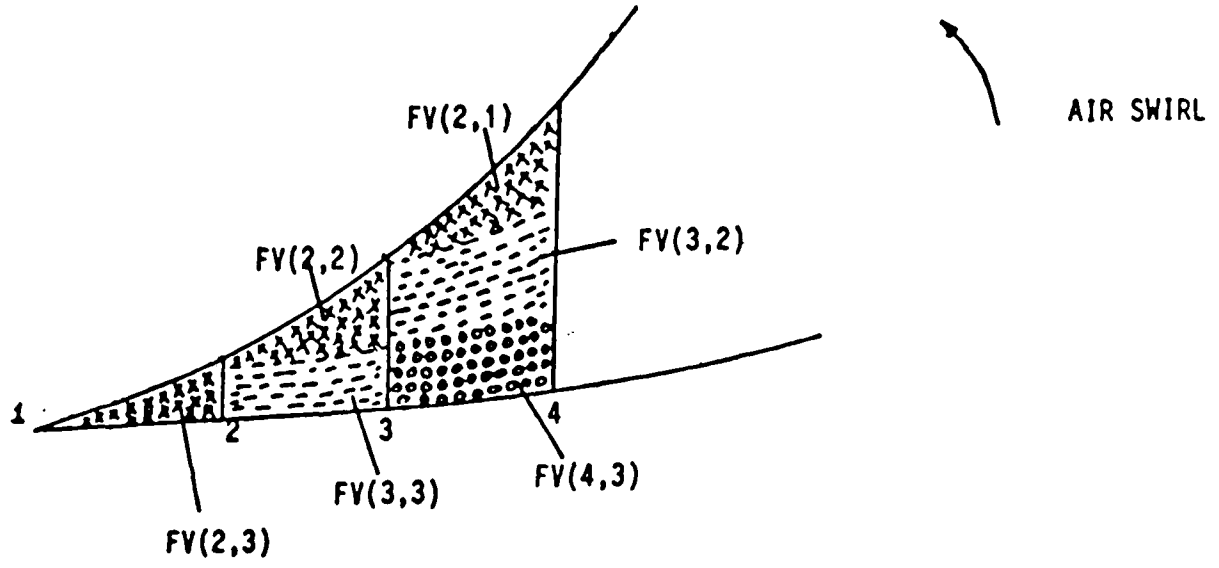

FV(J,I)=VAPOR FORMED BETWEEN STATIONS
J AND J-1 IN Ith INTERVAL
OF TIME

FIG. 5 ASSUMPTION OF VAPOR DISTRIBUTION IN ANY CONE AT THE END OF 3rd INTERVAL OF TIME

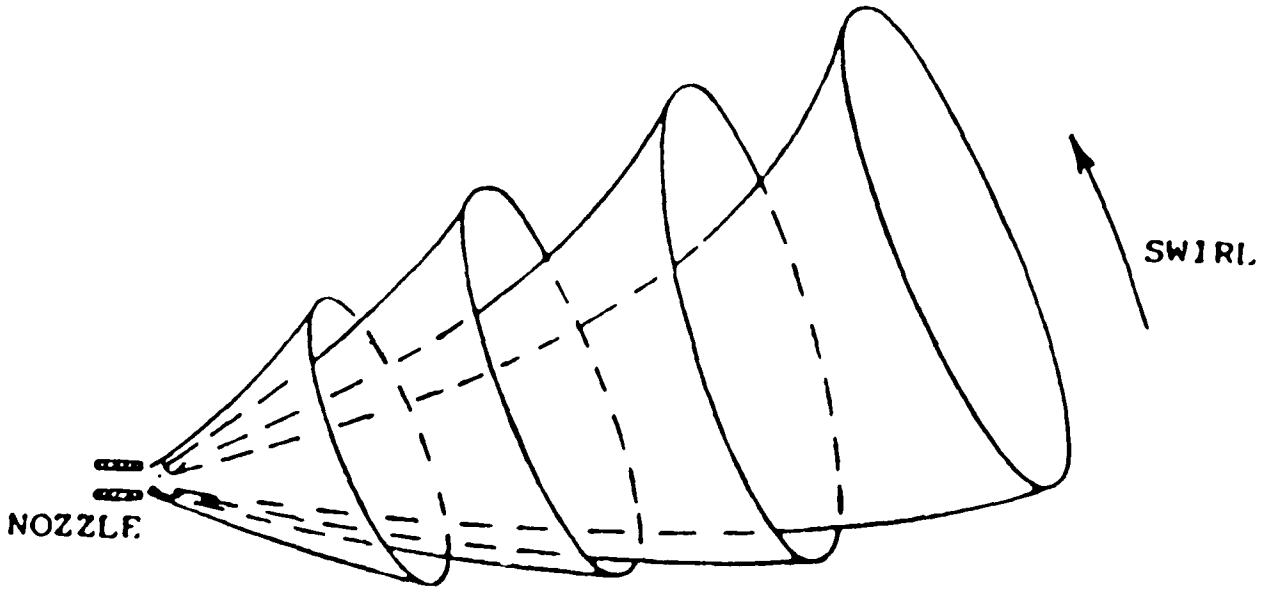

FIG. 6 CONES FORMED BY SWIRL (HAVING ELLIPTICAL BASES)

Figure 7 gives an idea of how the movement of vapors takes place from outer to inner cones. While in the case of no swirl, the vapors generated in a cone may be assumed to be confined to the annular region between the cones, the same assumption cannot be extended to the case with swirl. Since the penetration of droplets in the outer cone is not the same as that of inner cones and the size of the segments varies also, one or more segments of outer cones may contribute vapors to the inner cones. Also, since one or more of these contributing segments may not be formed at the time of observation, the change in equivalence ratio in any segment due to overlapping varies, making equivalence ratio at a particular location a function of time. The mass transfer of vapor from segments of outer cone to that of inner cones is considered proportional to the percentage of overlapping by volume.

Ignition delay for each time dependent segment is calculated individually. Once the ignition delay is over, all segments between the flammability limits of Ø.3 to 3.Ø burn during a period of 3 degrees of crank angle rotation. The remaining fuel burns at the same rate at which it is injected with an equivalence ratio of unity. A program developed at the University of Wisconsin [29] for calculating properties of products of combustion is called as a subroutine to determine the heat released by each segment and the resulting adiabatic flame temperature attained by that segment. Pressure rise is finally determined by equating the product of instantaneous cylinder pressure and volume to the summation of mRT of burned segments, unburned segments and surrounding air at the end of each time step. A listing of the computer program is given in Appendix 1.

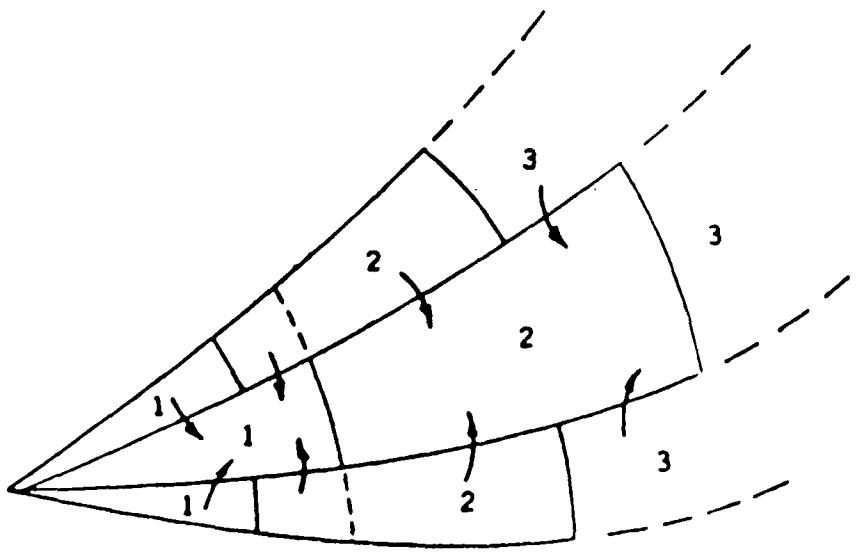

FIG. 7 MOVEMENT OF VAPORS FROM OUTER TO INNER CONE

5. DISCUSSION OF RESULTS

5.1 COMPARISON OF MODEL RESULTS WITH EXISTING DATA

The prediction of the model for spray penetration with zero swirl ratio has been compared in Figures 8 and 9 with data obtained by Takeuchi, et al [16] and Varde and Popa [30] in two seperate experiments conducted in quiescent air. Every care has been taken to extract information concerning inputs to the model from References 16 and 30 in order to make the comparison justifiable. Essential information on inputs known to have substantial bearing on the outcome of results if not available in the above references have had to be assumed. Lack of knowledge on either one or more of the following:

(1) Nozzle coefficient of discharge

(2) Nozzle L/d ratio

(3) Spray cone angle

(4) Properties of fuel used

(5) Chamber gas properties

(6) Breakup time or breakup length of liquid fuel element

appears to be the major factor responsible for small discrepancies noticed.

Not much published data on penetration observed on injecting fuel into air in motion is available. Hiroyasu, et al [13] have recommended the use of a factor which is a function of swirl ratio to evaluate the value of penetration in swirling air provided the value of penetration in stagnant air is known. This factor has been applied to Hiroyasu's experimental data available on penetration without swirl [13] and plotted against the models prediction in Figure 10. Figure 11 shows a similar comparison between

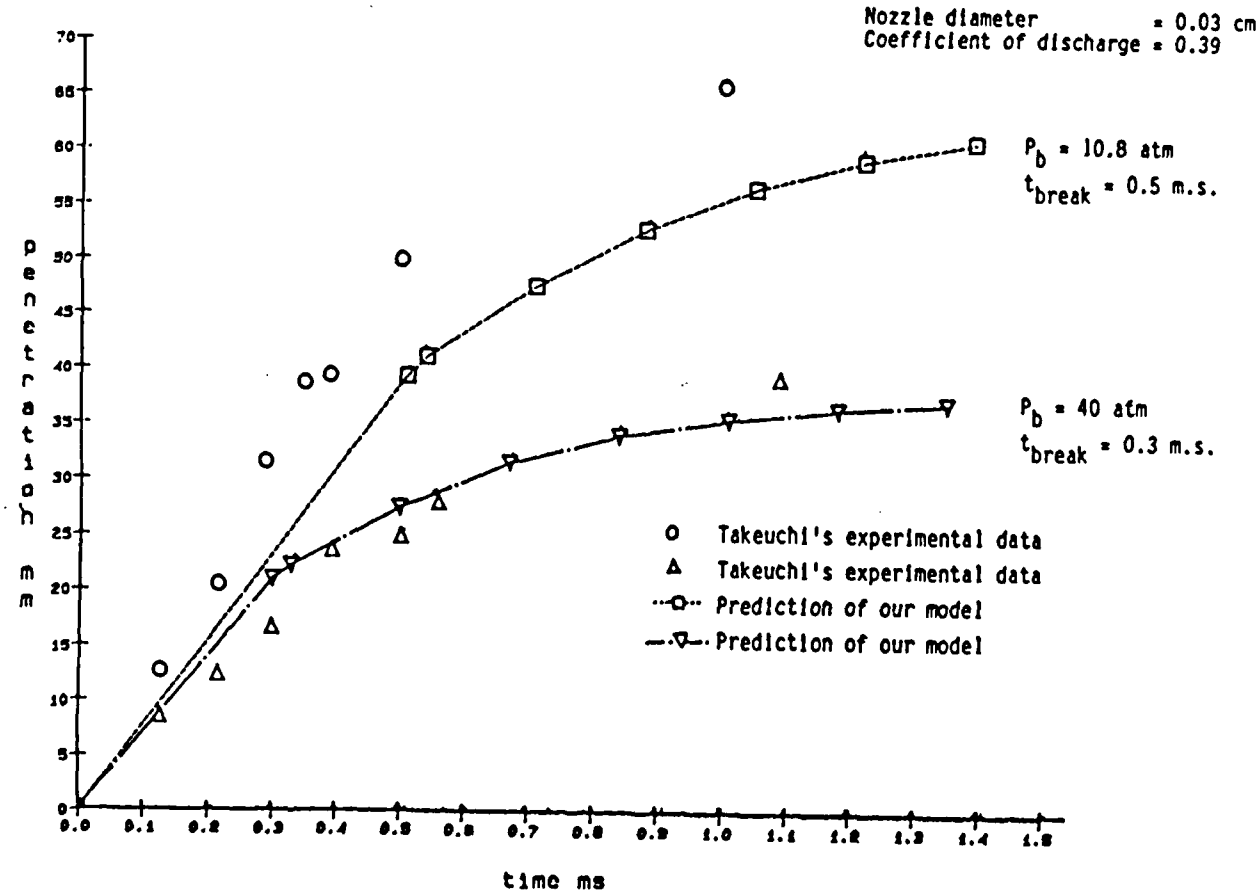

FIG. 8 COMPARISON WITH TAKEUCHI'S MODEL

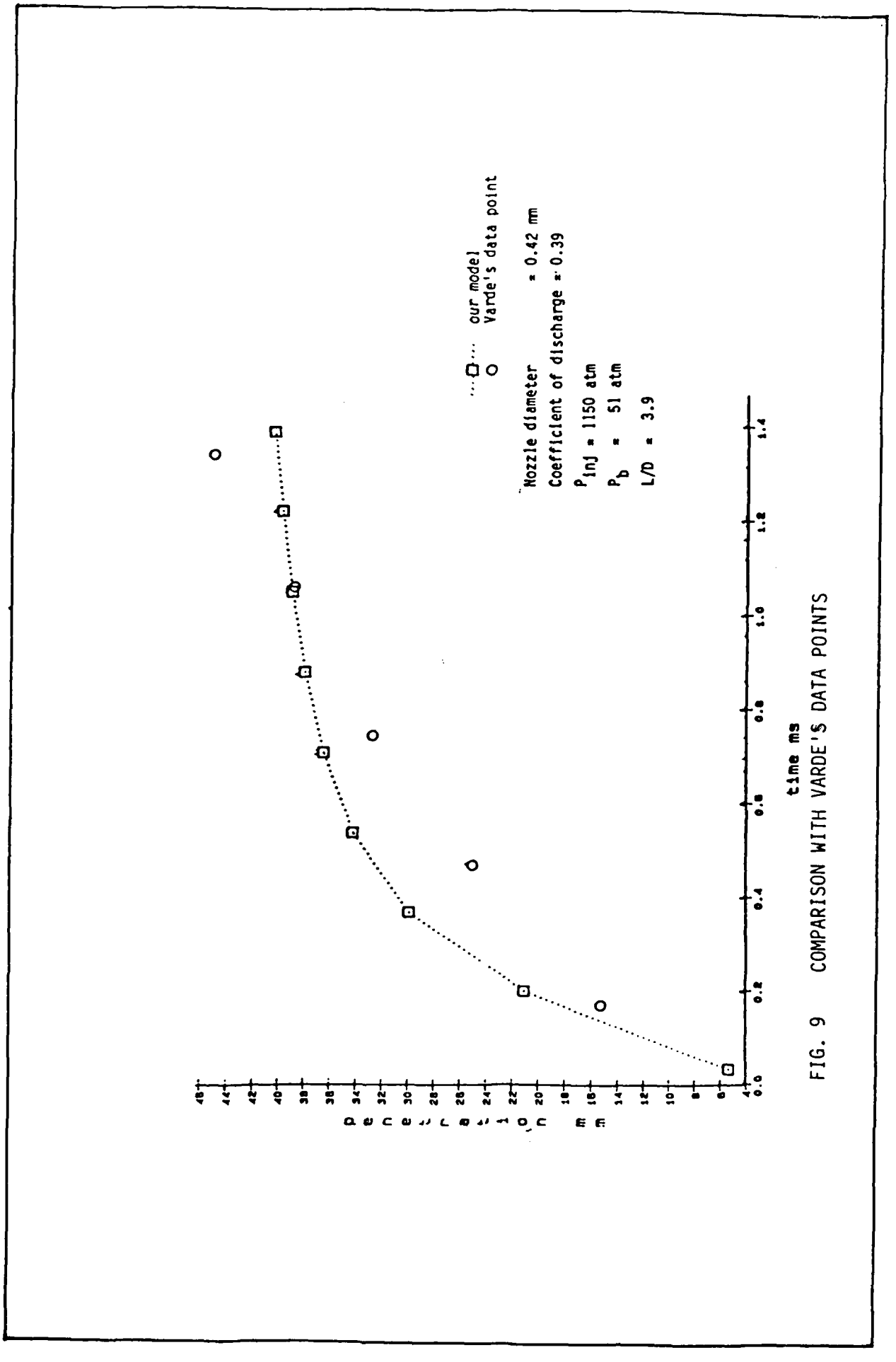

FIG. 9 COMPARISON WITH VARDE'S DATA POINTS

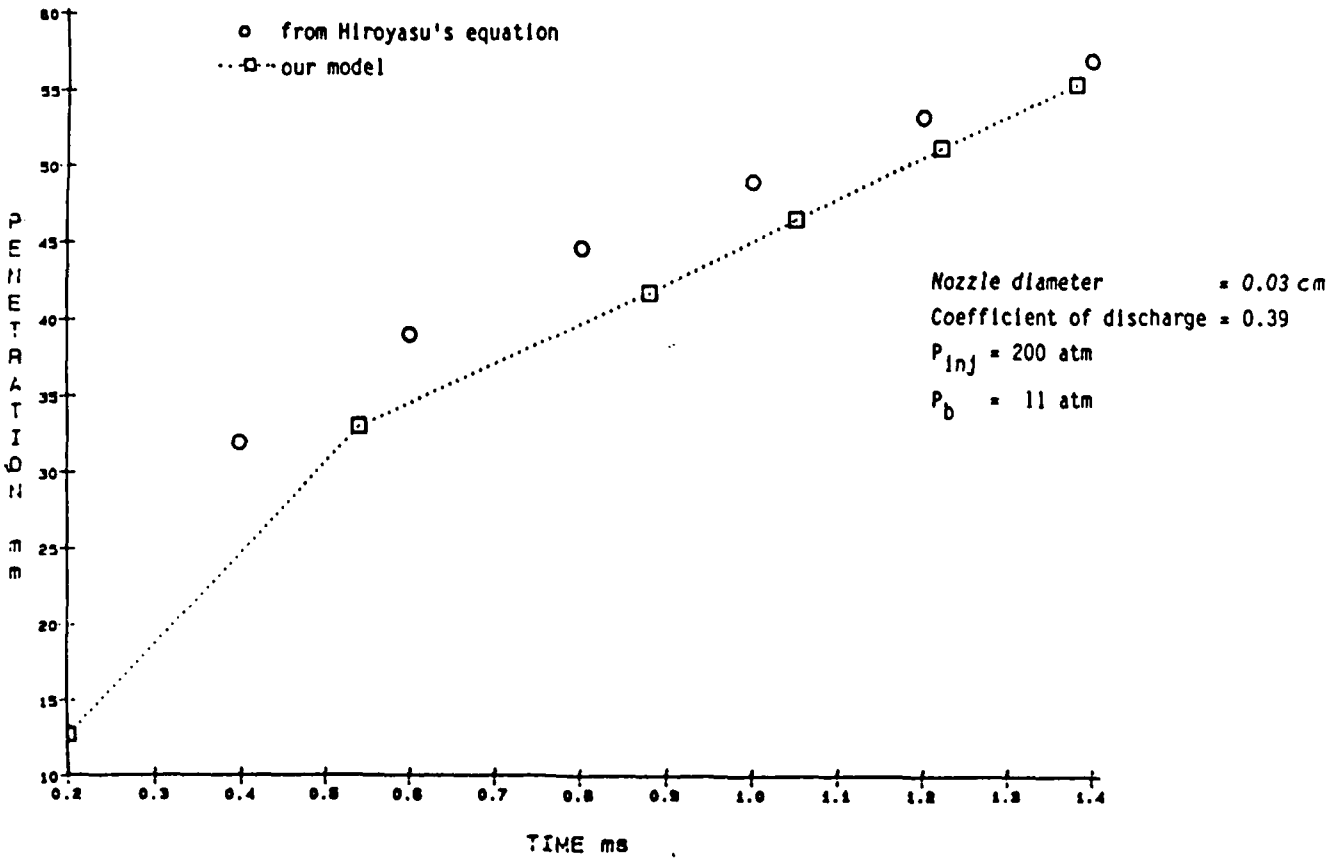

FIG. 10 COMPARISON WITH HIROYASU'S MODEL WITH SWIRL

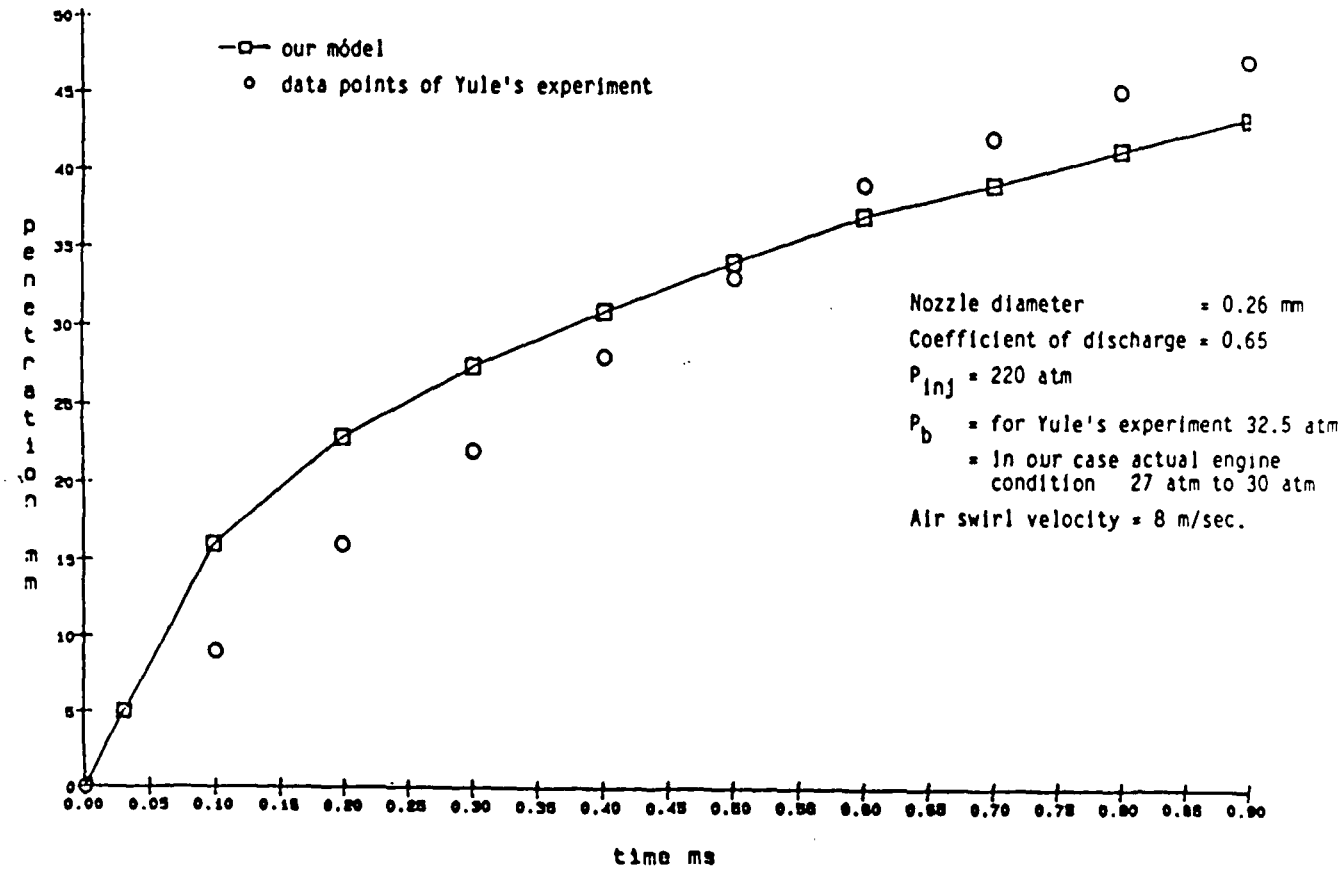

FIG. 11 COMPARISON WITH UNIVERSITY OF MANCHESTER MODEL IN CROSS FLOW

calculated values and the experimental values of Yule, et al [19] obtained in a wind tunnel under constant back pressure. The calculated penetration is slightly higher to begin with but becomes less than the experimental value 1 ms from the start of injection. It may be pointed out again that spray penetration with swirl as given by the model is the distance of the last location of the leading droplet from the nozzle tip. It is different from the actual distance travelled by the droplet along a curved path.

5.2 EFFECT OF SOME ENGINE OPERATING VARIABLES ON PENETRATION AND EQUIVALENCE RATIO

5.2.1 EFFECT OF INJECTION PRESSURE

Figures 12 and 13 show the calculated effect of injection pressure on spray penetration for constant load. Figure 12 has been plotted from results obtained by keeping the back pressure constant at a value corresponding to engine cylinder pressure at the start of injection, viz. 24 atm. Figure 13 shows a similar variation under engine running conditions. The comparison between the two conditions for injection pressures of 22Ø atm and 1ØØ atm has been made in Figure 14. The penetration in both cases increases with an increase in injection pressure but the penetration under engine conditions is less at the same injection pressure due to the increased drag imposed by the denser air. The constant back pressure case has been included for comparison purposes since most of the experimental data available was obtained in constant pressure chambers.

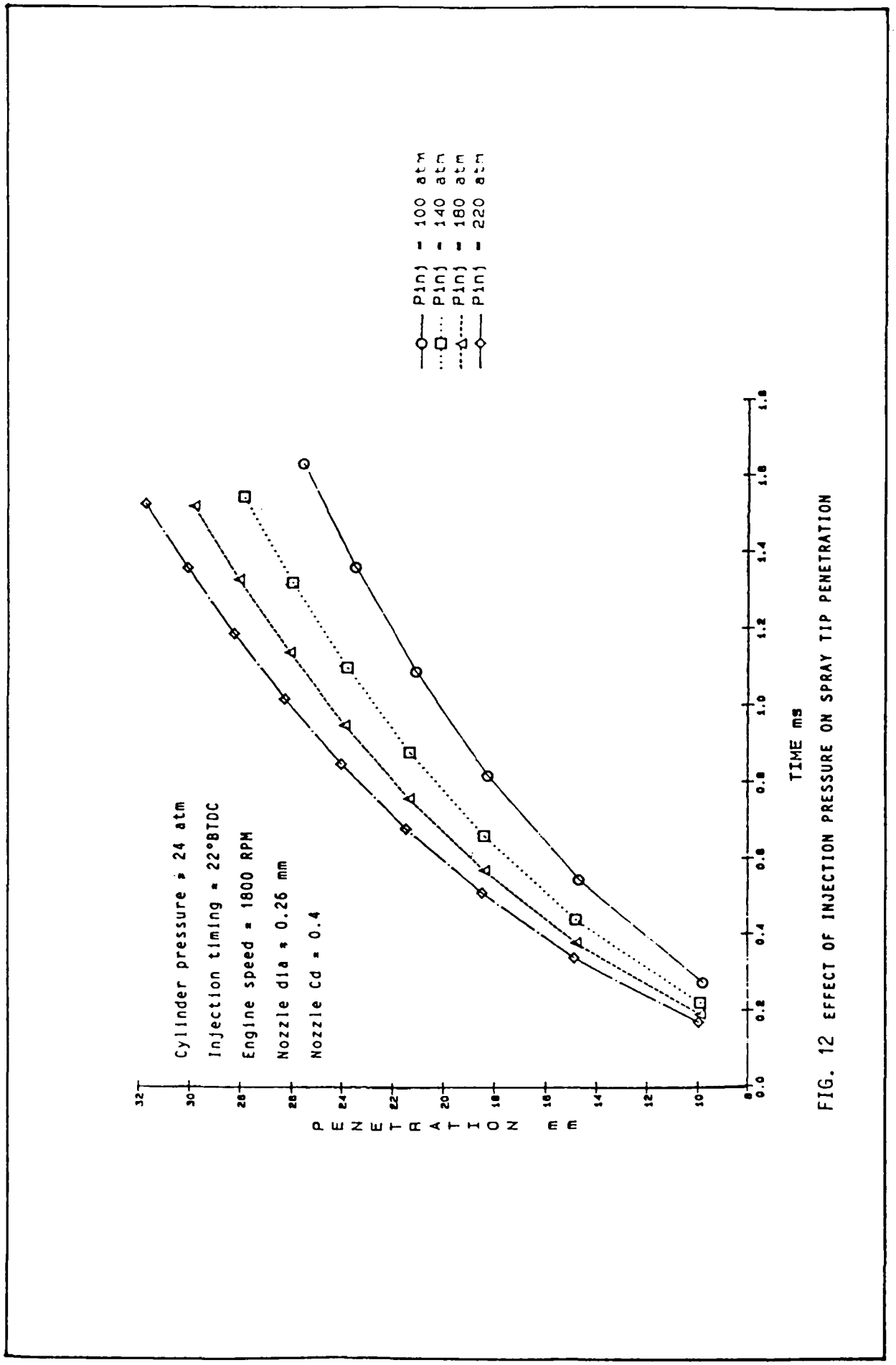

FIG. 12 EFFECT OF INJECTION PRESSURE ON SPRAY TIP PENETRATION

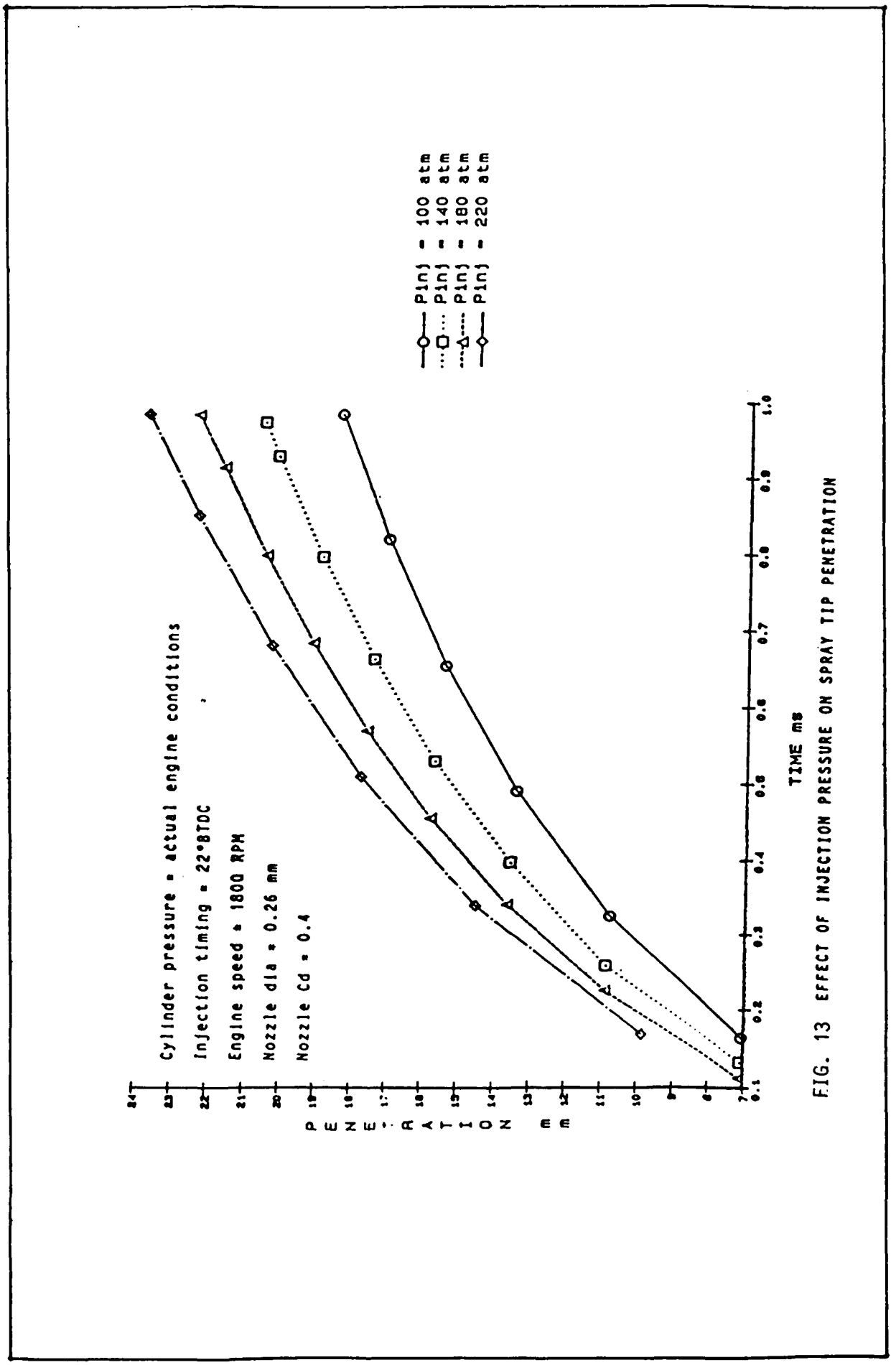

FIG. 13 EFFECT OF INJECTION PRESSURE ON SPRAY TIP PENETRATION

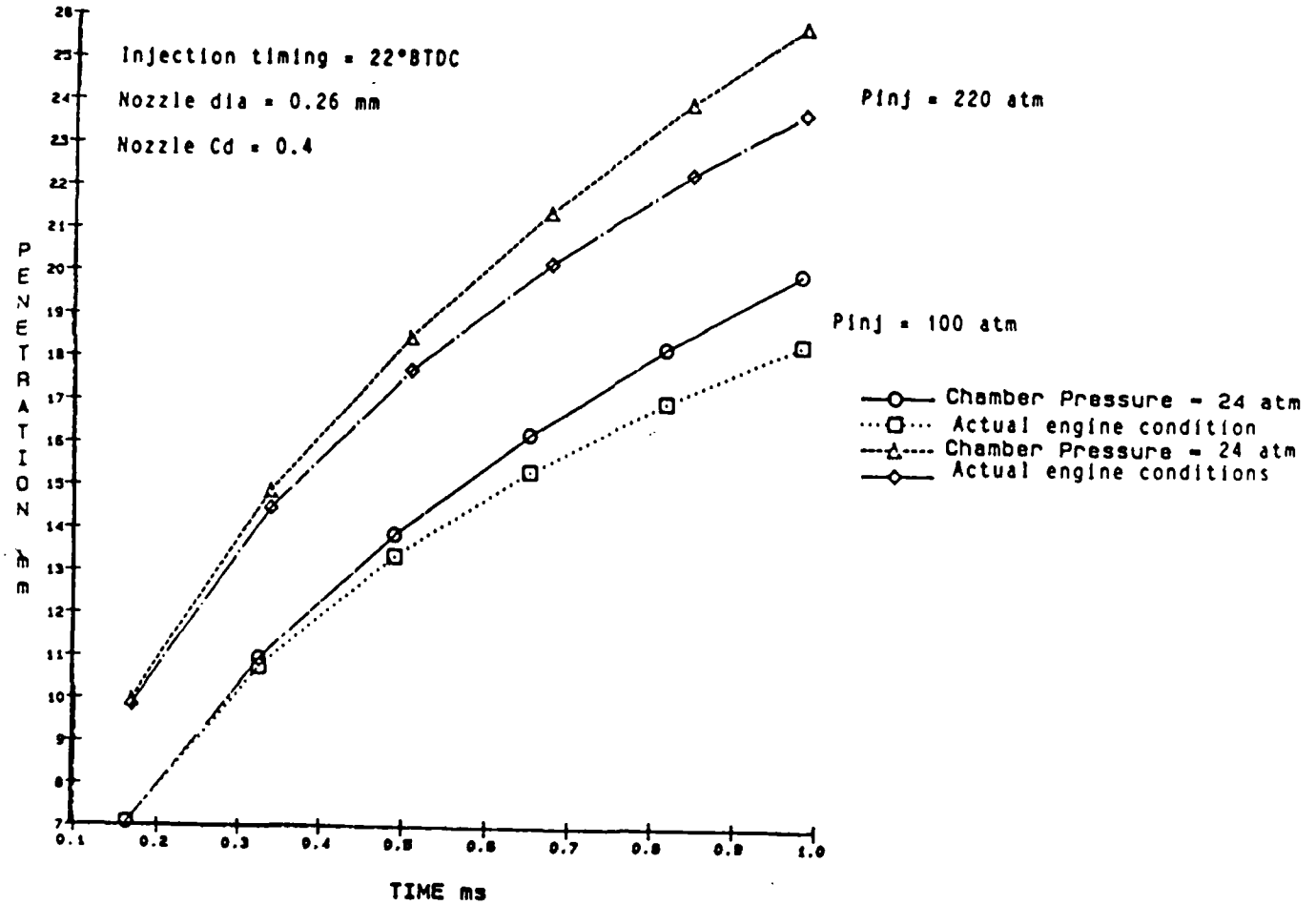

FIG. 14 COMPARISON BETWEEN PENETRATION UNDER CONSTANT BACK PRESSURE AND ACTUAL ENGINE CONDITION

The distribution of air fuel mixture in various subcones after about 1 ms from the start of injection for both the running engine condition and the constant back pressure condition are shown using bargraphs in Figures 15 and 16. The time 1 ms corresponds approximately to the end of ignition delay under typical engine operating conditions. The height of the bar at any time "t" describes the equivalence ratio in a segment of a cone formed at the end of ignition delay from vaporizing droplets that were injected "t" ms before the end of ignition delay. Thus, for example, a group of bars at Ø.22 ms represent equivalence ratio in cone segments close to the nozzle tip at the end of ignition delay while those at time Ø.98 ms represent cone segments near the spray tip at the same instant. With an increase in injection pressure at constant engine load, the duration of injection decreases and a greater mass of fuel is injected in the same time interval. However, this does not result in higher values of equivalence ratio. Indeed, the value decreases due to the fact that penetration is greater at higher injection pressures which allows for more air entrainment. Also, due to higher temperatures and smaller penetrations one would expect richer fuel air mixtures in the case of running engine conditions as compared to constant back pressure conditions. This trend is noticed, but only near the nozzle tip, (Figure 17). Rapid evaporation of droplets in the initial stages leaves less liquid fuel farther away from the nozzle which explains the occurrence of this effect. It is interesting to note that ignition delay is not altered by changing the injection pressure because of the weak influence of equivalence ratio on ignition delay period.

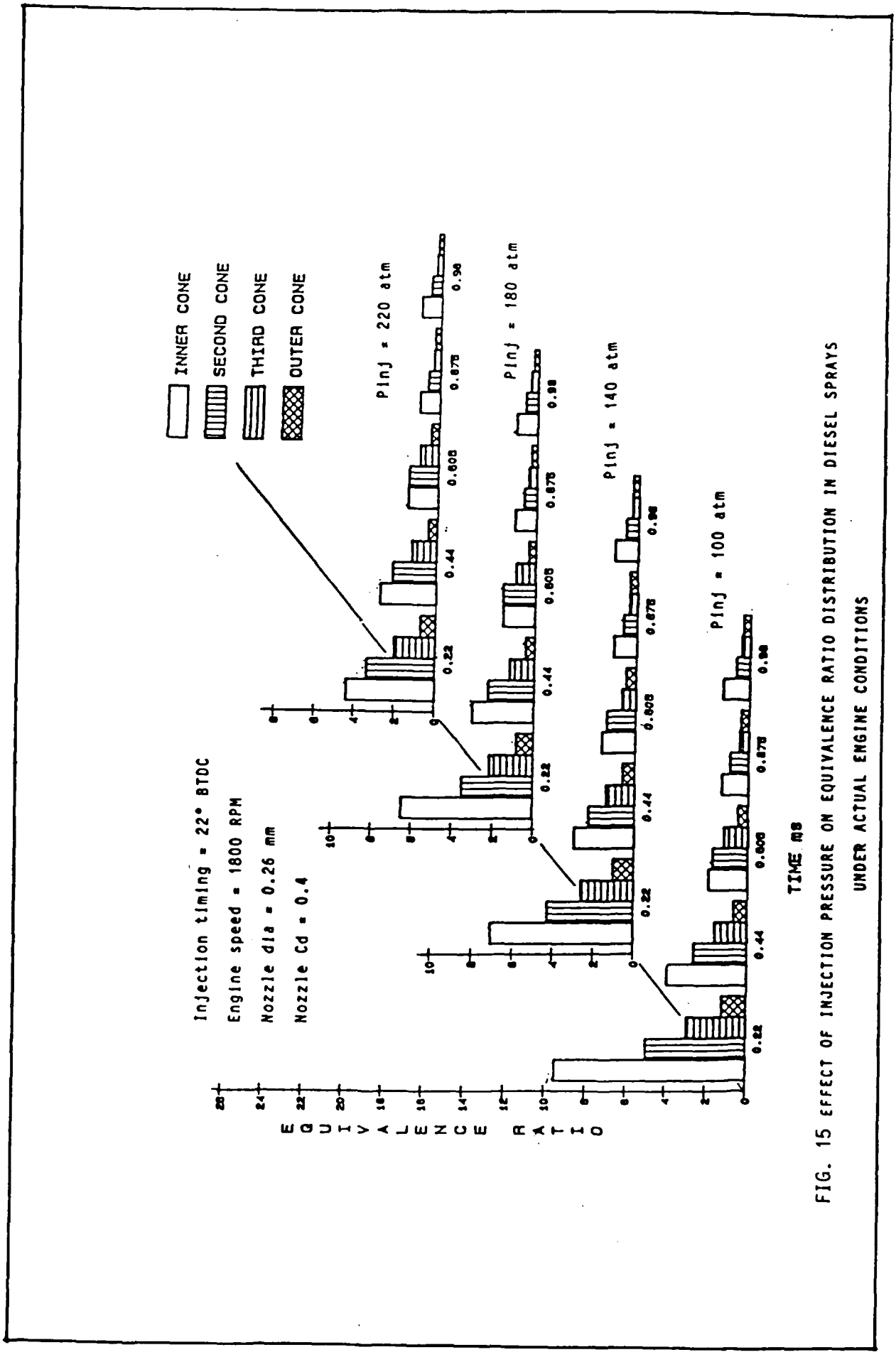

FIG. 15 EFFECT OF INJECTION PRESSURE ON EQUIVALENCE RATIO DISTRIBUTION IN DIESEL SPRAYS UNDER ACTUAL ENGINE CONDITIONS

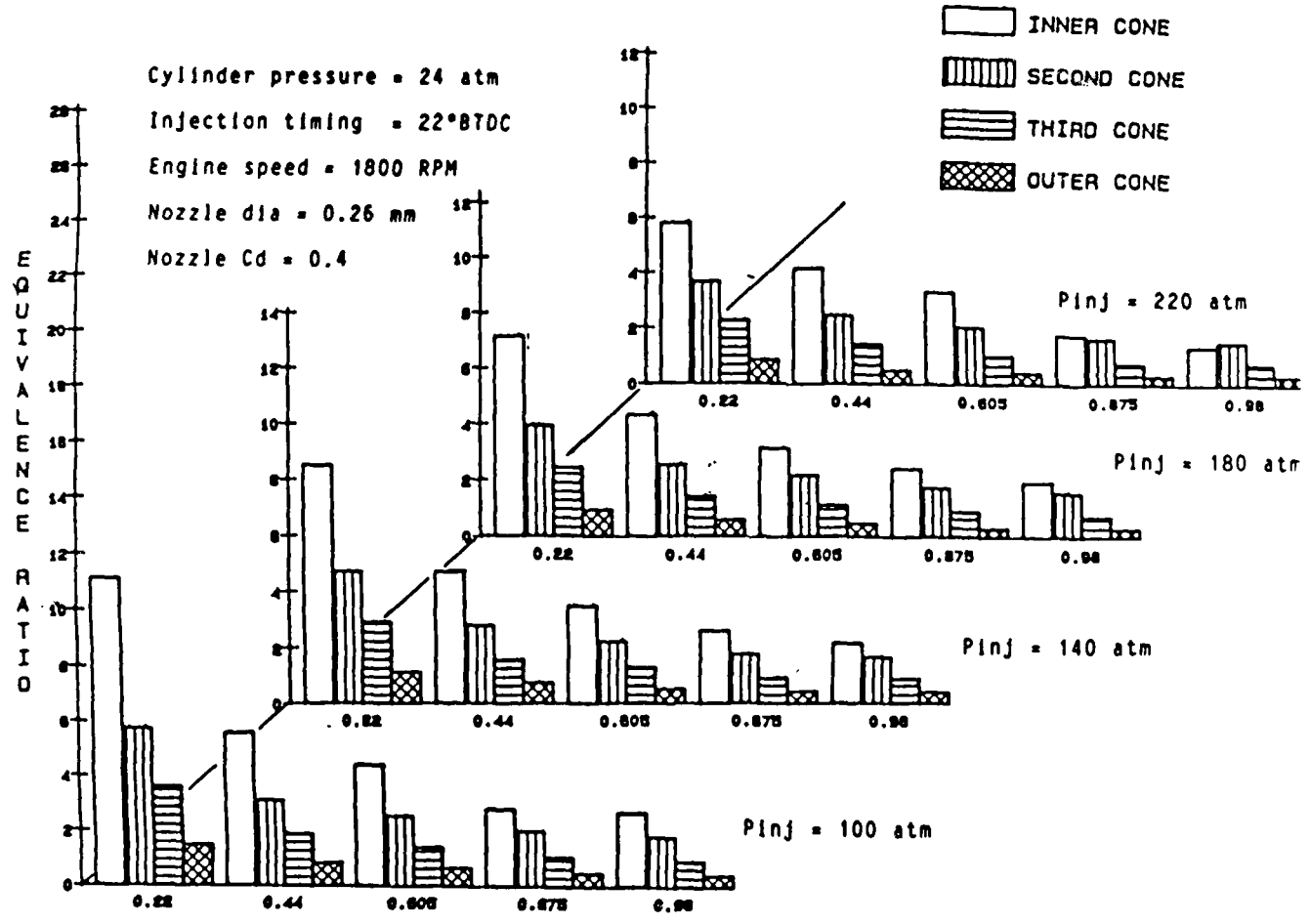

FIG. 16 EFFECT OF INJECTION PRESSURE ON EQUIVALENCE RATIO DISTRIBUTION IN DIESEL SPRAY UNDER CONDITIONS OF SWIRL WITH BACK PRESSURE HELD CONSTANT

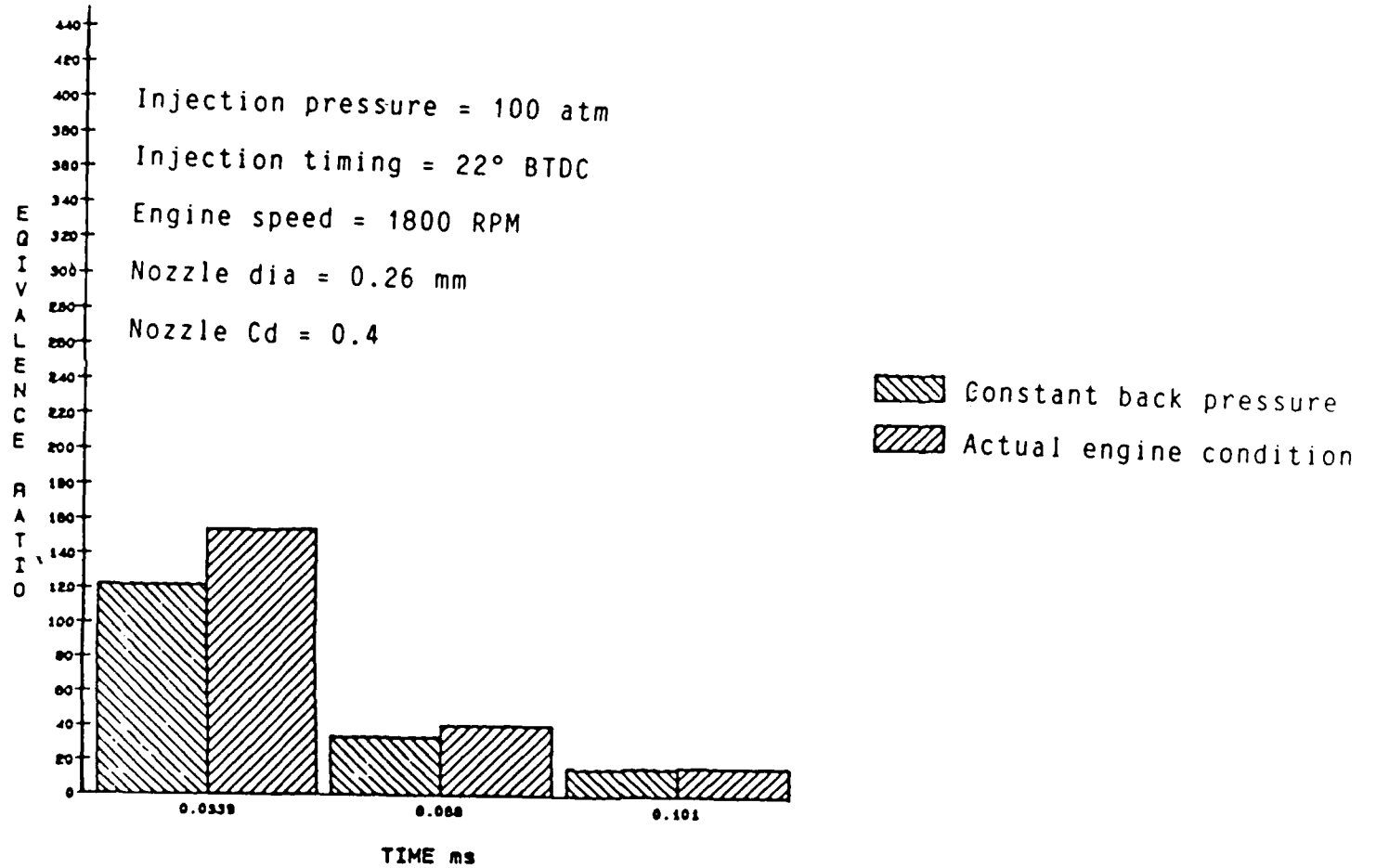

FIG. 17 EQUIVALENCE RATIO DISTRIBUTION NEAR NOZZLE TIP

5.2.2 EFFECT OF INJECTION TIMING

Spray tip penetration decreases as injection timing is retarded due to the increase in chamber gas density as shown in Figures 18 and 19. The reduction in penetration is more in the case of actual engine conditions as compared to constant back pressure conditions for the same change in injection timing as shown in Figure 20.

The variation of equivalence ratio with injection timing is shown in Figures 21 and 22. For a constant duration of injection, the distribution of fuel air mixture is slightly leaner in the case of retarded injection timing. This is probably due to higher back pressures associated with retarded injection which results in smaller droplet velocity and a smaller quantity of fuel injection in the same interval of time, inspite of the fact that penetration and air entrainment is also reduced. In addition, in the case of engine operating conditions, the ignition delay period is also reduced with retarded injection thereby reducing the quantity of total fuel injected during the ignition delay period. This explains why a comparatively leaner distribution is noticed in the case of actual engine conditions.

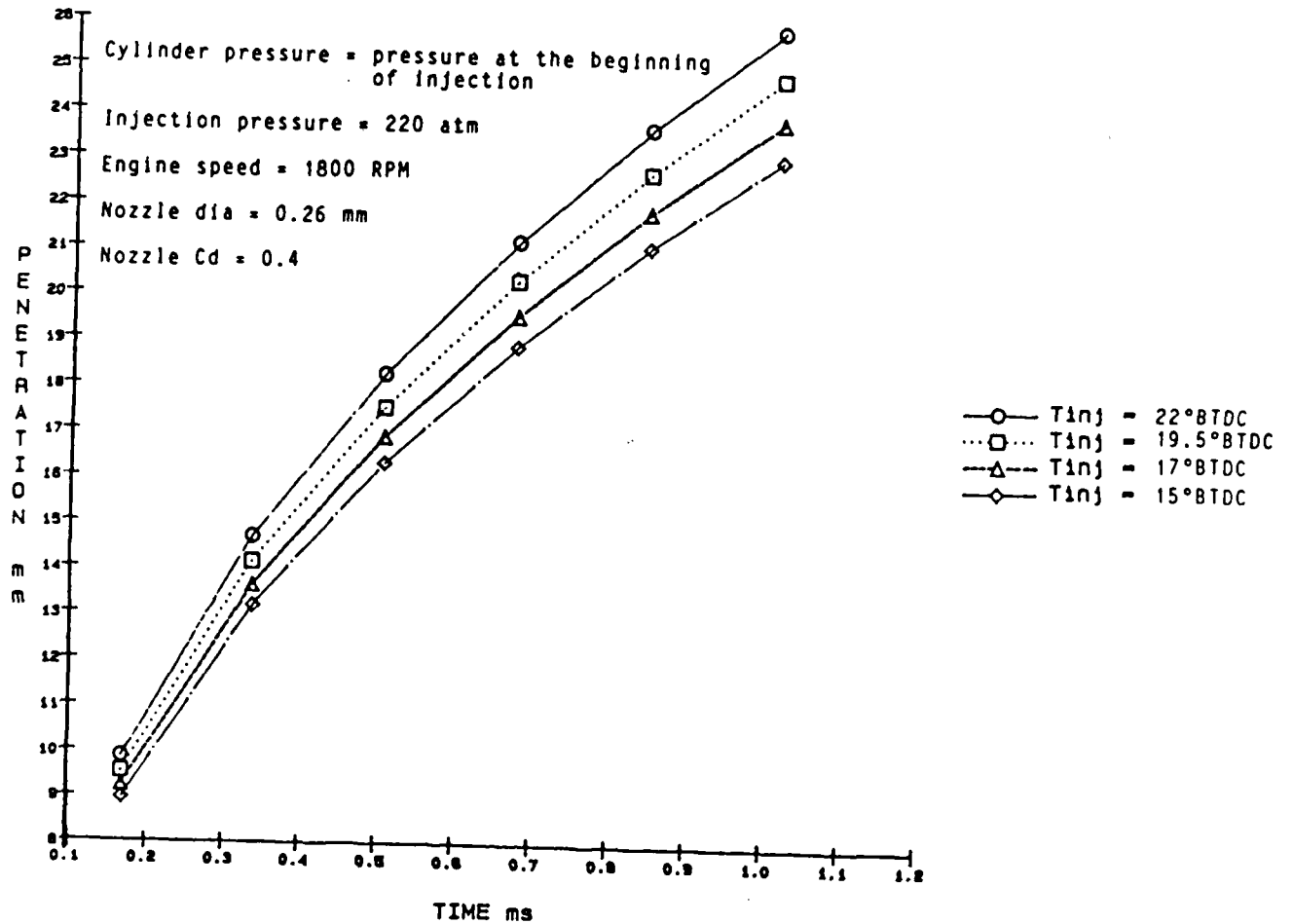

FIG. 18 EFFECT OF INJECTION TIMING ON SPRAY TIP PENETRATION

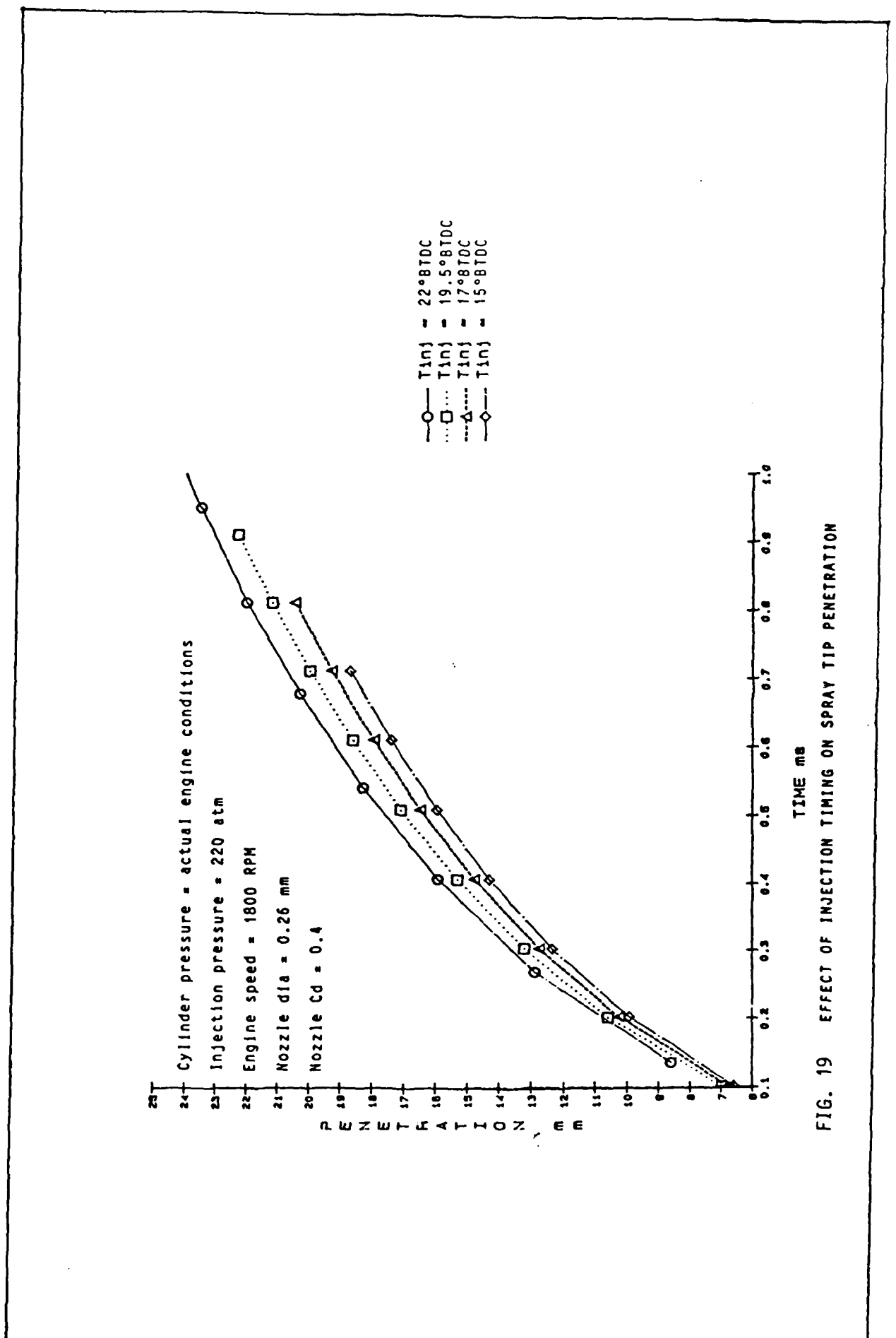

FIG. 19 EFFECT OF INJECTION TIMING ON SPRAY TIP PENETRATION

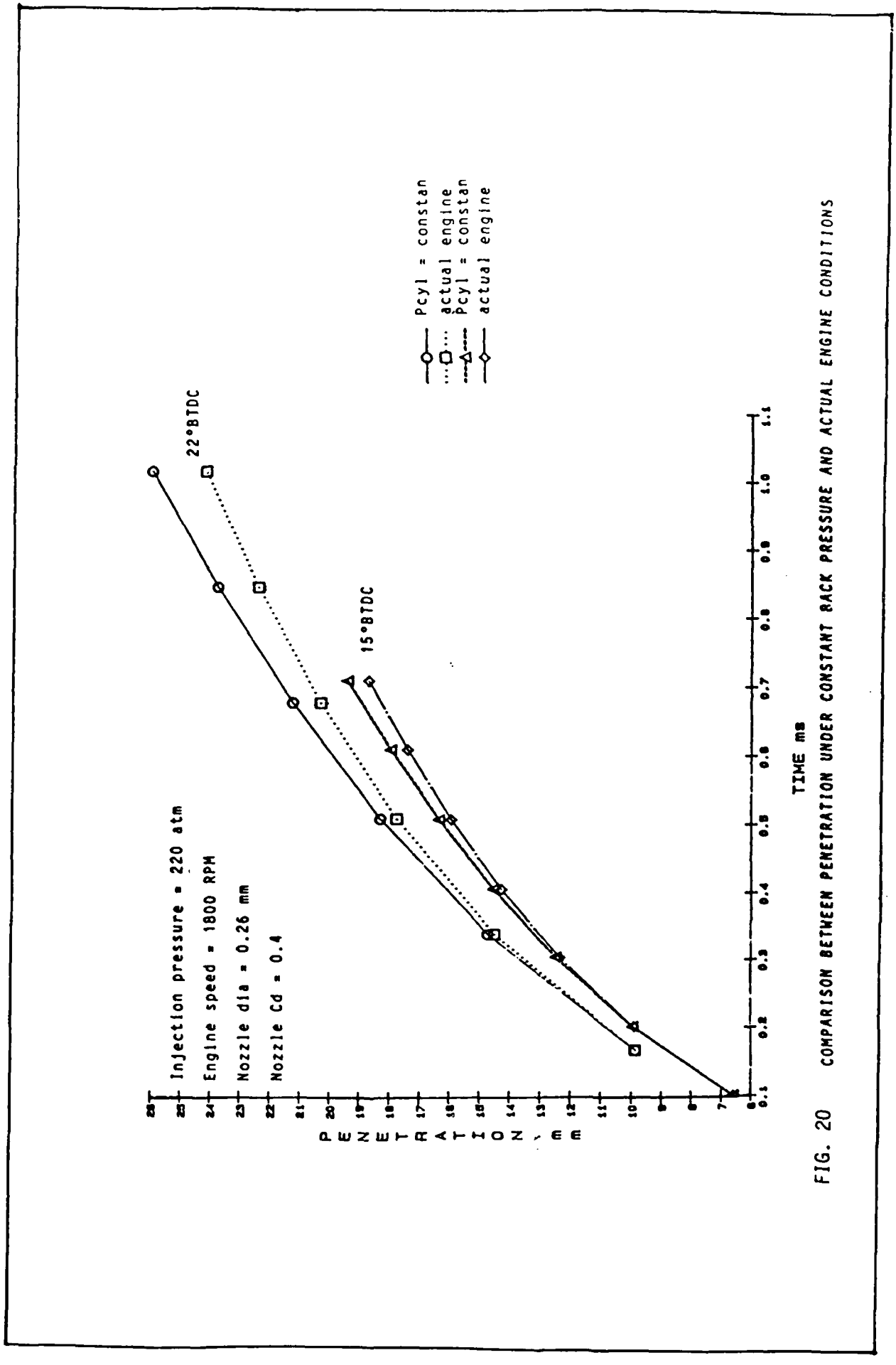

FIG. 20 COMPARISON BETWEEN PENETRATION UNDER CONSTANT RACK PRESSURE AND ACTUAL ENGINE CONDITIONS

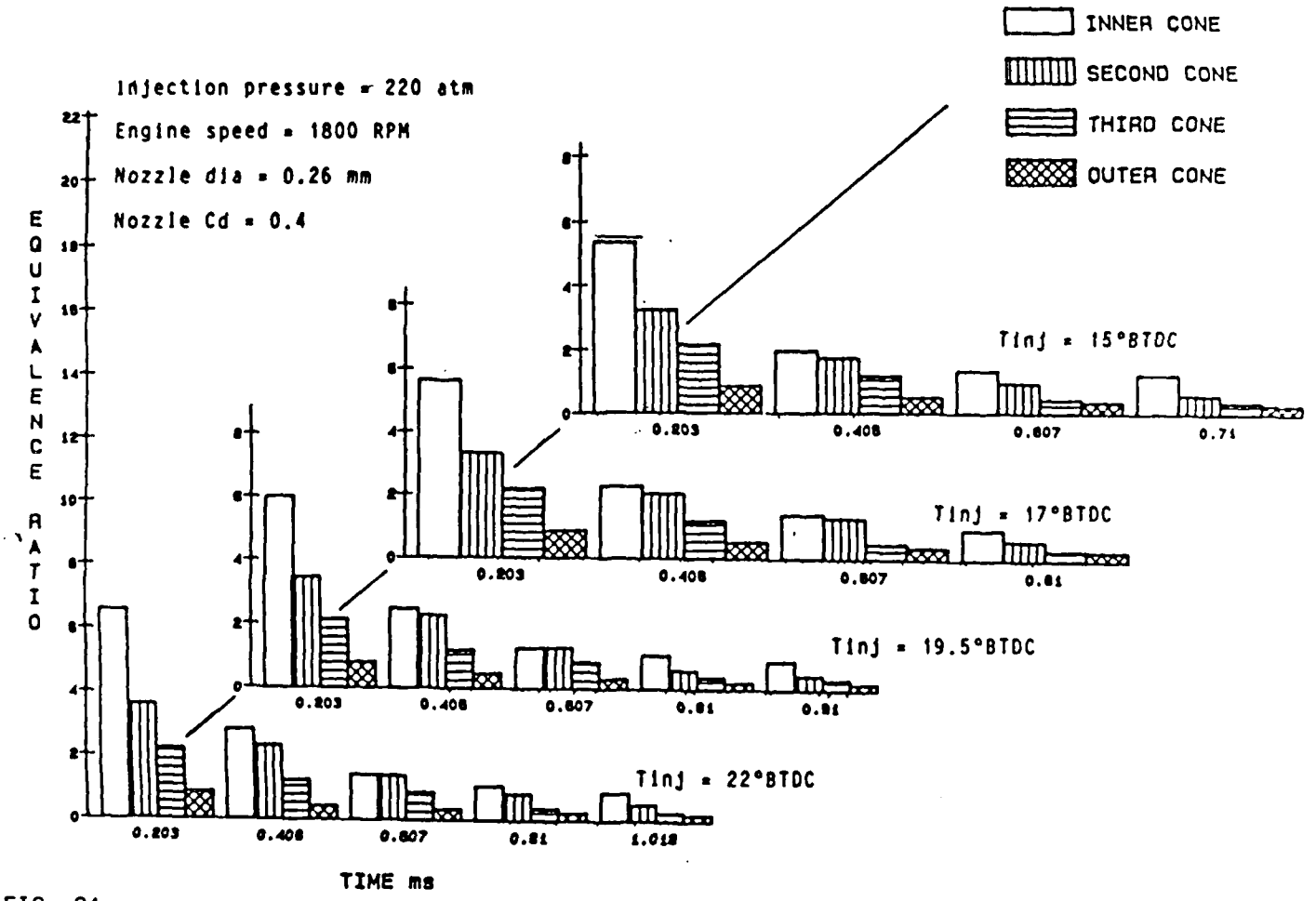

FIG. 21 EFFECT OF INJECTION TIMING ON EQUIVALENCE RATIO DISTRIBUTION IN DIESEL SPRAYS UNDER CONDITIONS OF SWIRL WITH BACK PRESSURE HELD CONSTANT

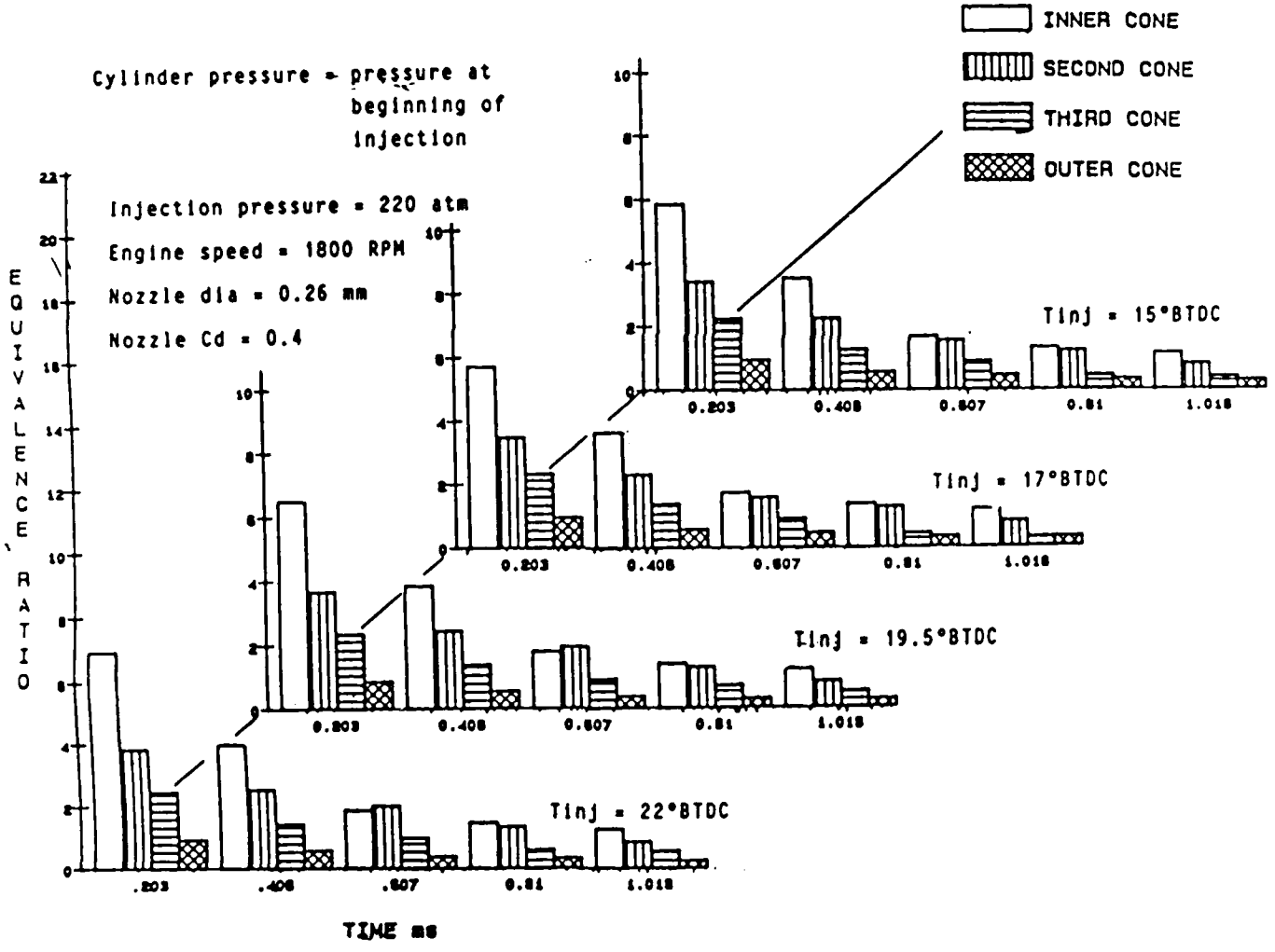

FIG. 22 EFFECT OF INJECTION TIMING ON EQUIVALENCE RATIO DISTRIBUTION IN DIESEL SPRAYS UNDER ACTUAL ENGINE CONDITIONS

5.2.3 EFFECT OF ENGINE SPEED

There is not much change noticed in the spray tip penetration as the engine speed is varied provided the total load on the engine is maintained constant. This was achieved in the model by increasing the total duration of fuel injection and thus allowing for the same quantity of fuel to be injected. The nominal effect of engine speed on penetration is shown in Figure 23.

5.3 PRESSURE RISE DIAGRAM

As mentioned earlier, the pressure rise following ignition delay has been evaluated on the assumption that the "spike" lasts for 3 degrees of crank angle and thereafter, the fuel burns at the rate it is injected with equivalence ratio of 1. A cylinder pressure versus crank angle diagram is shown in Figure 24. The curve a-b-c-d describes the pressure variation during motoring. The curve a-b-c'-d'-e-f-g represents the pressure changes in the cylinder when combustion takes place. In this second curve, b-c' corresponds to the ignition delay period, the premixed fuel burns between c' -d', the remaining fuel is consumed by diffusion flame between d' -e and finally e-f-g is the outcome of compression and expansion due to piston movement.

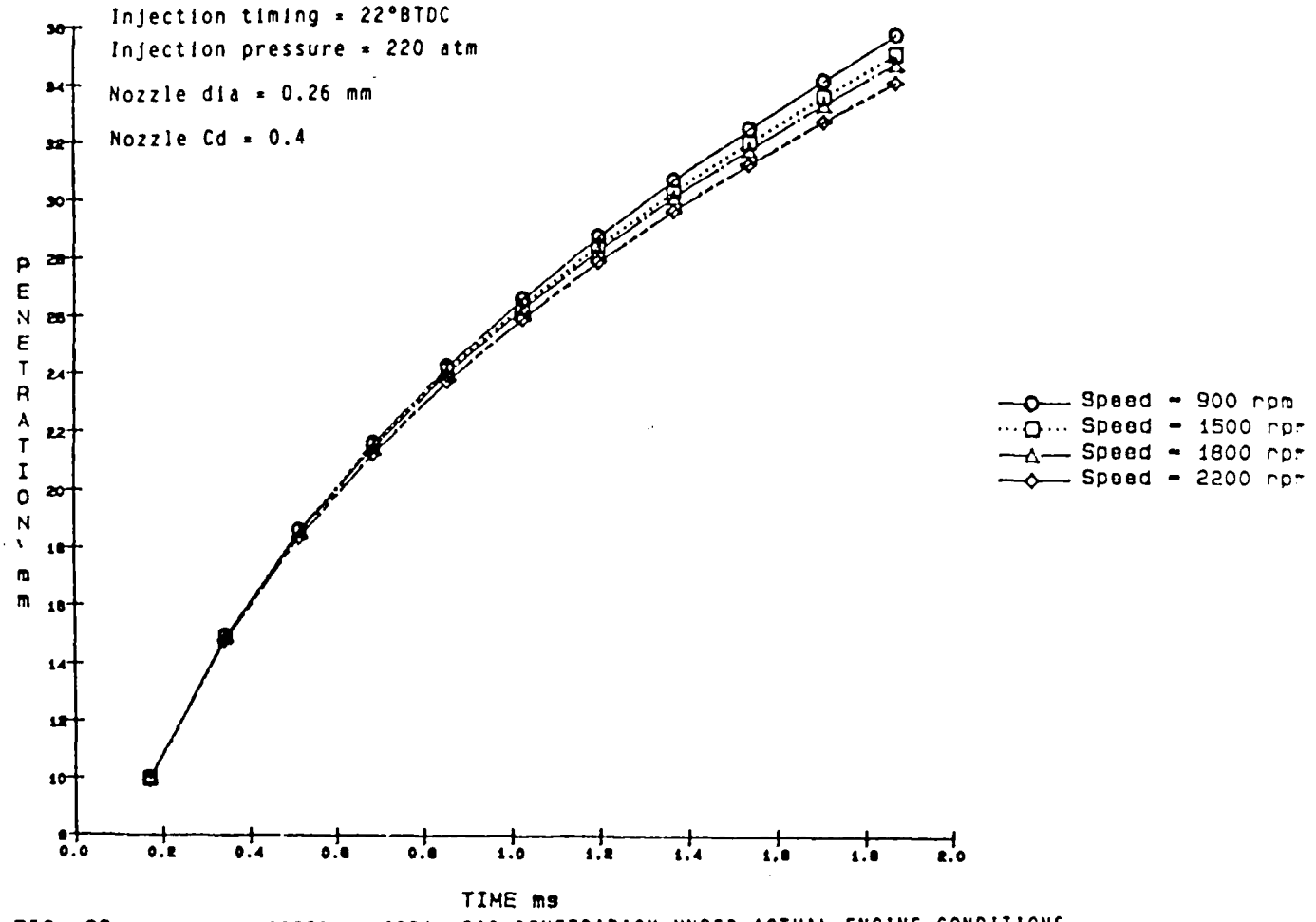

FIG. 23 EFFECT OF SPEED ON SPRAY TIP PENETRATION UNDER ACTUAL ENGINE CONDITIONS

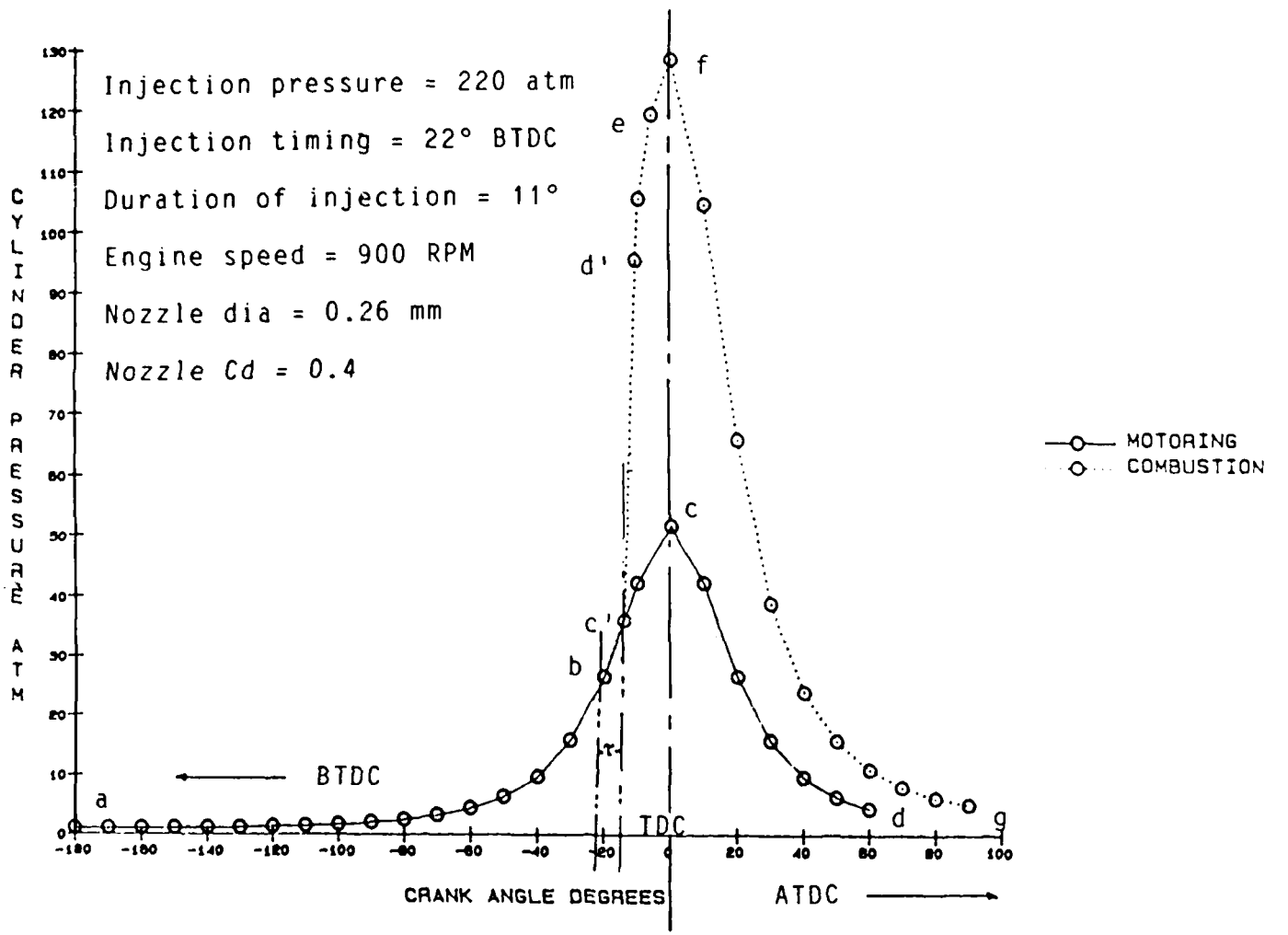

FIG. 24 PRESSURE RISE DURING COMBUSTION

6. EXPERIMENTAL SETUP

6.1 ENGINE DESCRIPTION

A Ricardo Hydra Series Single Cylinder Direct Injection Research Diesel Engine has been installed in the Engine Laboratory. Experiments have been done on this engine to validate the results given by the model. The term "running engine conditions" in the preceding chapters refers to this engine in particular.

Some of the salient features of this engine are:

Engine details:

Bore size	8Ø.26 mm
Stroke length	88.9Ø mm
Rated speed	75 rev/sec
Peak cylinder pressure	12Ø bars
Measured compression ratio	2Ø/1

By changing the crankshaft and connecting rod, the stroke can be varied between 71 mm to 1Ø5 mm.

Fuel injection system:

Nozzle	4 holes, Ø.21 mm diameter
Nozzle Opening Pressure (NOP)	25Ø bars

Instrumentation:

Engine speed	digital display
Engine load	load cell with digital display
Fuel flow	AVL gravimetric flow meter
Air flow	Miriam Laminar flow element
Nozzle needle lift	inductive transducer
Fuel line pressure	strain guage transducer

Cylinder pressure	Kistler piezoelectric transducer
Air inlet temperature	thermocouple
Water outlet temperature	thermocouple
Oil inlet temperature	thermocouple
Fuel temperature	thermocouple
Exhaust outlet temperature	thermocouple

Valve timing :

Inlet opens	1Ø BTDC
Inlet closes	42 ABDC
Exhaust opens	58 BBDC
Exhaust closes	1Ø ATDC

Recommended static injection timing (S.I.T.) under full load:

Speed rev / sec	S.I.T. BTDC
2Ø	13
3Ø	16
4Ø	17
5Ø	19
6Ø	22

Restrictions:

Maximum exhaust temperature	75Ø C
Lube oil inlet temperature	85 C
Water outlet temperature	85 C
Exhaust back pressure	Ø.1 bar
Inlet air temperature	18-22 C
Inlet fuel temperature (to pump)	15-2Ø C

6.1.1 AIR INLET SYSTEM

The inlet system consists of a cast aluminium alloy manifold provided with a 1 KW air heater, a Miriam 5Ø MC2 laminar flow element and an air filter. The temperature of air passing through the heater can be controlled by an air temperature controller at the control console. The signals for this controller are provided by a duplex thermocouple.

6.1.2 FUEL SYSTEM

The system consists of a lift pump which is supplied fuel from the fuel reservoir and delivers it to a Bosch injection pump for injection into the cylinder. The injector is detachable and can be changed to study the effect of injector dimensions on engine performance. There is a provision for recirculating excess fuel from the injector pump back to the flowmeter. The injector unit is provided with a thermocouple to measure the inlet fuel temperature which can be monitored from the control console. Fuel injection pressure is monitored with a strain gauge type pressure transducer. An Inductive Displacement transducer is used to measure the needle lift. Its signal is conditioned by a carrier amplifier for display on an oscilloscope. The quantity of fuel delivered per cycle can be remotely controlled by adjusting the throttle and the injection timing can be set by remote control between Ø and 4Ø BTDC.

An AVL 73Ø gravimetric fuel consumption measuring system is also fitted in the fuel circuit. The change in weight of the vessel containing fuel is determined by the change in its position over a frictionless blade spring. The change is detected by a highly sensitive capacitive displacement transducer. The equipment offers the possibility to compute and indicate:

(a) cumulative consumption over a preset measuring period

(b) Mean consumption rate over a selected measuring period

(c) The instantaneous mass flow rate.

6.1.3 COOLING SYSTEM

The closed circuit pressurized engine coolant system uses water and antifreeze. It is used to cool both the engine block and the cylinder head. A duplex thermocouple at the header tank controls the flow rate of cooling water. The cooling water is also passed through a heat exchanger for cooling the lubricating oil.

6.1.4 OIL SYSTEM

The lubricating system is used both as a lubricating unit and a cooling unit. Oil under pressure is supplied to crankshaft bearings, big end bearings, and camshaft bearings. A safety system gives a warning signal, upon loss of oil pressure or if oil temperature increase beyond 85 C.

6.1.5 PRESSURE MEASUREMENTS AND DATA ACQUISITION

Cylinder pressure is monitored with a Kistler Piezoelectric transducer. This transcucer transmits signals through a charge amplifier to the oscilloscopes. A Data Precision Data 6000 4 channel digital oscilloscope is used to monitor cylinder pressure, needle lift and crankshaft position. The Data 6000 4 channel plug in has a 14 bit 100 KHz A/D converter (25 KHz per channel) and can process and store the data on floppy disks or interface to a computer.

7. CONCLUSIONS AND RECOMMENDATIONS

The outcome of this study has been the development of a mathematical model to represent spray development, heat release and pressure time history in direct injection diesel engines. The model is capable of predicting :

(i) Spray tip penetration

(ii) The local fuel air distribution within the spray

(iii) The ignition delay period

(iv) Locations in spray where autoignition begins

(v) The pressure rise due to fuel combustion

under continuously changing environmental conditions as may be encountered in actual engines.

In addition to predicting the above, the model can effectively be employed to model the effects of varying some of the engine operating variables such as injection pressure, injection timing, engine speed, nozzle dimensions, etc. on each of the above characteristics of a diesel spray.

The commonly available inherent characteristics of an engine and the properties of the fuel serve as the bulk of the essential inputs required by the model. An additional feature of the model is its capability to determine the geometry of the spray under conditions of swirl.

Although experiments have yet to be conducted to validate the efforts of this exercise, the results of the model have been compared to the existing data from experiments performed in constant, volume hot and cold bombs and found to be in good agreement.

When results are available from comparison of model predictions for cylinder pressure history with engine experiments using hexadecane fuel, they will be forwarded as an addendum to this report.

REFERENCES

[1] : Ogasawara, M., and Sami, H., " A Study on the Behavior of a Fuel Droplet Injected into the Combustion Chamber of a Diesel Engine", SAE paper no. 670468, 1967

[2] : Elkotb, M. M. and Rafat, N. M., "Fuel Spray Trajectory in Diesel Engines", ASME paper 77-DGP-1, 1977

[3] : OZ, I. Z., " Calculation of Spray Penetration in Diesel Engines", SAE paper 690254, 1969

[4] : Melton, R. B., "Diesel Fuel Injection Viewed as a Jet Phenomenon", SAE paper 710132, 1971

[5] : Hiroyasu, H. and Kadota, T., " Evaporation and Spontaneous Ignition Delay of a Fuel Droplet and Spray in High Pressure Gaseous Environments", Report by Mechanical Engineering Department Hiroshima University, Japan, for Automobile Exhaust Clarification Study Group, Feb 1977.

[6] : Chiu, W. S., Shahed, S. M., and Lyn, W. T., " A Transient Spray Mixing Model for Diesel Combustion", SAE paper 760138, 1976

[7] : Hiroyasu, H., and Kadota, T.," Models for Combustion and Formation of Nitric oxide and Soot in Direct Injection Diesel Engines", SAE paper 760129, 1976

[8] : Dent, J. C., and Derham, J. A., " Air Motion in a Four Stroke Direct Injection Diesel Engine", Proceedings of Institution of Mechanical Engineers, Vol 188, 21/74, pp269-280

[9] : Schweitzer, P. H., " Oil Sprays - An Investigation of Velocities and Penetrations." The Automobile Engineer, pp 61-64, Feb 1938

[10]: Parks, M. V., Polonski, C., and Toye, R., " Penetration of Diesel Fuel Sprays in Gases", SAE paper 660747, 1966

[11]: Dent, J. C., " A Basis for the Comparison of Various Experimental Methods for Studying Spray Penetration", SAE paper 710571, 1971

[12]: Hay, N., and Jones, P. C., "Comparison of Various Correlations for Spray Penetration", SAE paper 720776, 1972

[13]: Hiroyasu, H., Kadota, T., and Arai, M., " Fuel Spray Characterization in Diesel Engines - Informative Data for the Computation of Diesel Engine Combustion", A Report from Mechanical Engineering Department, University of Hiroshima, Japan, 1978

[14]: Kuniyoshi, H., Tanabe, H., Sato, G. T., and Fujimoto, H., "Investigation on the Characteristics of Diesel Fuel Spray", SAE paper 800968, 1980

[15]: Varde, K. S., Popa, D. M., and Varde, L. K., " Spray Angle and Atomization in Diesel Sprays", SAE paper 841055, 1984

[16]: Takeuchi, K., Senda, J., and Shikayu, M.,"Transient Characteristic of Fuel Atomization and Droplet Size Distribution in Diesel Fuel Spray", SAE paper 830449, 1983

[17]: Kuo, T. W., Yu, R. C., and Shahed, S. M., " A Numerical Study of the Transient Evaporating Spray Mixing Process in the Diesel Environment", SAE paper 831735, 1983

[18]: Fragoulis, A., and Henein, N. A., " Penetration Mean Diameter for Liquid Sprays", ASME Publication, Flows in Internal Combustion Engines - II, Vol 20 pp 99-111

[19]: Yule, A. J., Mo, S. L., Tham, S. Y. and Aval, S. M., " Diesel Spray Structure", Proceedings of ICLASS-85, Third International Conference on Liquid Atomization and Spraying Systems, Imperial College , London, England, July 1985

[20]: Henein, N. A., and Bolt, J. A., " Ignition Delay in Diesel Engines" SAE paper 670007, 1967

[21]: Henein, N. A., and Bolt, J. A., " Correlation of Air Charge Temperature and Ignition Delay of Several Fuels in a Diesel Engine", SAE paper 690252, 1969

[22]: Wong, C. L., and Steere, D. E., " The Effect of Diesel Fuel Properties and Engine Operating Conditions on Ignition Delay", SAE paper 821231, 1982

[23]: Lyn, W. T., " Study of Burning Rate and Nature of Combustion in Diesel Engines", Ninth Symposium (International) on Combustion, (New York : Academic Press) pp 1069-1082, 1963

[24]: Meguerdichian, M., and Watson, N., " Prediction of Mixture Formation and Heat Release in Diesel Engines", SAE paper 780225, 1978

[25]: Primus, R. J., and Wong, V. W., " Performance and Combustion Modelling of Heterogeneous Charge Engines", Engine Combustion Analysis : New Approaches, SAE publication P-156, pp 15-25, March 1985

[26]: Hiroyasu, H., and Kadota, T., " Fuel Droplet Size Distribution in Diesel Combustion Chamber", SAE paper 740715, 1974

[27]: Bracco, F. V., " Structure of High Speed Full Cone Sprays", from Recent Advances in Gas Dynamics, Plenum Publishing Corp., N.Y. 1983.

[28]: Singh, H., Singh, T., and Henein, N. A., " A Mathematical Model for Spray Penetration in Direct Injection Diesel Engines", ASME paper 85-DGP-16, 1985

[29]: Olikara, C., and Borman, G. L., " A Computer Program for Calculating Properties of Equilibrium Combustion Products with Some Applications to I. C. Engines", SAE paper 750468, 1975

[30]: Varde, K. S., and Popa, D. M., " Diesel Fuel Spray Penetration at High Injection Pressures", SAE paper 830448, 1983

[31]: Yuen, M. C. and Chen, L. W., " On Drag of Evaporating Liquid Droplets", Combustion Science and Technology, Vol 14, pp 147-154, 1976

[32]: Reitz, R. D., and Bracco, F. B., " On the Dependence of Spray Angle and Other Spray Parameters on Nozzle Design and Operating Conditions", SAE paper no 790494, 1979

APPENDIX 1

```
C*****************************************************************
C THIS PROGRAM PREDICTS THE SPRAY-TIP PENETRATION AND EQUIVALENCE
C RATIO DISTRIBUTION WITHIN THE GEOMETRY OF SPRAY IN DIRECT
C INJECTION DIESEL ENGINE UNDER CONDITIONS OF SWIRL.
C*****************************************************************
      REAL VX(61,61),SI(60),XTT(60),ATHXV(60),XTPV(60),FTHXV(60)
      REAL VL1(61,61),VR1(61,61),XRE1(61,61),CD1(61,61)
      REAL XMAIR(4,61),FFR(61),XXTP(61),YXTP(61),XXTPV(61),YXTPV(61)
      REAL XK0(5),XK2(61,61),XKK(61),PEN(4,61),XC1(61,61),XK1(61,61)
      REAL FR(5),DSS(5),DM(5),TH(5)
      REAL TFL(61,61),TVOLL(61,61),CV(61),CL(61)
      REAL BCD(61,61)
      REAL YXT(61),XXFV(61),SUMR(61),TSUM(61),FMASS(61)
      REAL D(61,61),AVGD2(61,61),XM1(61),XND(61),VR2(61,61)
      REAL DS(61,61),AVGDS(61,61),XNDS(61),XMS1(61),AVGVR2(61,61)
      REAL XT(61),XRE2(61,61),CD2(61,61),AVGCD2(61,61),XC2(61,61)
      REAL FV(61,61),FL(61,61),XMA(61,61),AVGXC(61,61)
      REAL VR(61),VOLFV(61,61),VOLL(61,61),VOLA(61,61)
      REAL AA(0:61),AM(61,61,61),PHE(4,61)
      REAL V(61),X(61,61)
      REAL X1(61,61)
      REAL TIM(60),DELAY(4,61,61)
      REAL FFVV(61),XXMA(61),DUMMY1(61),VOA(61)
      REAL AVOA(61),FAR(4,61,61),TFV(4,0:61,0:61),TA(4,61,61)
      REAL AVOAI(10),FTA(4,61,61),TAC(4,61,61),TAM(4,61,61)
      COMMON/A/AREA(2)
      DOUBLE PRECISION THXL,ARXL(60),XLAMDA1,XLAMDA2,XXLAMDA,BETA1,BETA2
      DOUBLE PRECISION BETA,SIGMA,VIJ,BTA,SV,AI,RXL,XTP(61),DUMMY2(61)
      DOUBLE PRECISION ARR
C*****************************************************************
C INPUT DATA : THIS NEEDS TO BE CHANGED WITH EVERY TEST RUN TILL SUCH
C TIME THAT WE OBTAIN A GENERAL EXPRESSION FOR EACH ONE OF THEM.
C*****************************************************************
      DATA FR/0.,.60,.25,.10,.05/
      DATA XK0/0.,.009,.011,.012,.015/
      DATA DSS/0.,80.E-4,56.E-4,44.E-4,20.E-4/
      DATA DM/0.,48.E-4,36.E-4,24.E-4,12.E-4/
      DATA TH/0.,.026,.052,.078,.105/
C*****************************************************************
      AVG(X,Y)=(X+Y)/2.
      FVL(PINJ,PA)=.4*SQRT(1962000.*(PINJ-PA)/.74871)
      FXRE(VR,D,CONST)=VR*D*CONST
      FCD(XRE)=24./XRE*(1.+.15*XRE**.687)
      FXK(XK0,XRE,SC)=XK0*(1.+.276*SQRT(XRE)*SC**0.333334)
      FD(DOLD,XK,DT)=(DOLD*DOLD-XK*DT)
      FXC(DNEW,CD,CONST)=4./3.*DNEW/CD*CONST
      FMFL(N,D)=3.1416/6.*N*D**3.
      FVR(V,X1,X2,XC)=V*EXP(-(X2-X1)/XC)
      OPEN (UNIT=1,FILE='SPRAY.DAT',STATUS='NEW')
C*****************************************************************
C CONSTANTS FOR FUEL TO BE USED IN THE EXPRESSION FOR IGNITION DELAY.
C SHOULD BE CHANGED FOR DIFFERENT FUELS.
C*****************************************************************
      A=0.872
```

```
      AN=-1.24
      C=-2.1
      DD=4050.
      PHID=1.
C*********************************************************************
C OTHER KNOWN INPUT PARAMETERS SOME OF WHICH MAY NEED ALTERATIONS WITH
C EACH TEST RUN.
C*********************************************************************
      PI=3.146
      CDD=.4
      DNN=.03
      R=2.8326
      TA0=305.
      TBP=480.
      GC=981.
      TL=480.
      PINJ=220
      THINJ=11
      RAJ=70.
      RPM=900.
      PT0=1.0
      PFL=9.5
      Z=.72
      RHOL=.74871
      SC=1.
      FAS=.066667
C*********************************************************************
C INITIALIZE VALUES
C*********************************************************************
      VAVV=0.
      XVAVV=0.
      XXVAVV=0.0
      XT(1)=0.
      XTF=0.
      XTP(1)=0.
      SI(1)=0.
C*********************************************************************
      RHOA0=PT0/(R*TA0)
      PA0=PT0
      AG=.5
      IM12=60
      DT=THINJ/(IM12*6.*RPM)
C*********************************************************************
C THIS DO LOOP IS RESPONSIBLE FOR THE CREATION OF NEW TIME DEPENDENT
C SEGMENTS
C*********************************************************************
      DO 5000 LK=1,60
C*********************************************************************
C THIS DO LOOP IS FOR ANALYSIS IN EACH SUBCONE TAKEN ONE AT A TIME
C*********************************************************************
      DO 111 IV=2,5
C*********************************************************************
C INITIALIZING FOR EACH SUBCONE
C*********************************************************************
      VOA(1)=0.0
```

```
      AREA(1)=0.0
      TIME=0.
      TMASS=0.
      FVTOT=0.
      VAVV=0.
      XVAVV=0.
      XXVAVV=0.0
      XTV=0.
      ATHXV(1)=0.
      TFV(IV,0,0)=0.
      TFV(IV,0,1)=0.
      TFV(IV,0,2)=0.
      PEN(IV,1)=0.0
C*********************************************************************
C SOME KNOWN ENGINE CHARACTERISTICS- LIQUID FUEL TEMP.,INLET PRESSURE,
C CYLINDER VOLUME, AMBIENT AIR TEMP., AND FUEL INJECTION TIMING
C*********************************************************************
      TL=480.
      P=1.
      V0=246.
      T=300.
      ANG=0.38
C*********************************************************************
      CALL PV(ANG,V0,P,V1,P1)
      T1=TEMP(T,P,P1)
      TR=TL+.3333334*(T1-TL)
      TM=(T1-TL)/ALOG(T1/TL)
      XMEU=10.*(7.13E-6+3.8E-8*TR)
      XK00=XK0(IV)
C*********************************************************************
C THIS DO LOOP ANALYSIS EACH OF THE PREVIOUS SEGMENTS EVERY TIME A NEW
C SEGMENT IS FORMED
C*********************************************************************
      DO 110 I=1,LK
      RHOA=(P1-PFL)/(Z*R*T1)
      IJ1=2
      TL=480.
      D(1,I)=DM(IV)
      AVGD2(1,I)=D(1,I)
      DS(1,I)=DSS(IV)
      AVGDS(1,I)=DS(1,I)
      TIME=TIME+DT
      J=I+1
      VL1(1,I)=FVL(PINJ,P1)
      XMINJ=PI/4.*DNN*DNN*VL1(1,I)*RHOL*DT*FR(IV)
      TMASS=TMASS+XMINJ
      FL(1,I)=XMINJ
      XM1(I)=PI/6.*D(1,I)**3.*RHOL
      XMS1(I)=PI/6.*DS(1,I)**3.*RHOL
      XNDS(I)=XMINJ/XMS1(I)
      XND(I)=XMINJ/XM1(I)
      CONST1=RHOA/XMEU
      CONST2=RHOL/RHOA
      IF(I.GT.1)GO TO 141
      XT(J)=VL1(1,I)*DT+XT(J-1)
```

```
      GO TO 142
141   XT(J)=VL1(I,I-1)*DT+XT(I)
142   CONTINUE
      XTT(J)=XT(J)*COSD(RAJ)
      ANG=ANG-(RPM*2.*PI/60.)*DT
      CALL PV(ANG,V1,P1,V2,P2)
      SM1=0.
      SM2=0.
C*********************************************************************
C INITIAL ESTIMATE OF MASS OF AIR TAKING PART IN MOMENTUM EXCHANGE
C*********************************************************************
      III=IV-1
      HAR=PI/3.*(TAN(TH(IV))*TAN(TH(IV))-TAN(TH(III))*TAN(TH(III)))
      SM1=SM1+HAR*XT(J)**3
      VOLA(J,I)=SM1
      XMA(J,I)=RHOA*SM1
      AIR=SM1*RHOA
      II=I-1
      IF(I.EQ.1)GO TO 52
      XMA(J,I)=XMA(J,I)-XMA(I,II)
52    CONTINUE
      XMAIR(IV,I)=XMA(J,I)
      N=I
      VR1(1,I)=VL1(1,I)-XVAVV
C*********************************************************************
C THIS DO LOOP REPEATS THE ANALYSIS OF NEXT DO LOOP TO APPROACH THE
C EXACT VALUE OF THE QUANTITY OF AIR ENTRAINED IN EACH SEGMENT
C*********************************************************************
      DO 42 KLM=1,3
C*********************************************************************
C THIS DO LOOP SOLVES FOR MOMENTUM AND ENERGY CONSERVATION IN EACH
C OF THE EXISTING SEGMENTS
C*********************************************************************
      DO 100 IJ=IJ1,J,2
C*********************************************************************
C ANALYSIS OF ODD NUMBERED SEGMENTS IS DONE IN THIS SECTION
C*********************************************************************
      N=I
      JJ=IJ-1
      JJJ=IJ+1
      IF(VR1(JJ,I).LT.0.1)VR1(JJ,I)=0.1
      IF(AVGD2(JJ,I).LT.1.E-4)AVGD2(JJ,I)=1.E-4
      IF(IJ.GT.2)GO TO 4000
      XRE1(JJ,I)=FXRE(VR1(JJ,I),AVGD2(JJ,I),CONST1)
      GO TO 4001
4000  XRE1(JJ,I)=FXRE(VR1(JJ,I-1),AVGD2(JJ,I-1),CONST1)
4001  IF(XRE1(JJ,I).LT.12.)XRE1(JJ,I)=12.
      CD1(JJ,I)=FCD(XRE1(JJ,I))
      BCD(I,I)=CD1(JJ,I)
      IF(IJ.GT.2)GO  TO 4007
      XC1(JJ,I)=FXC(AVGD2(JJ,I),CD1(JJ,I),CONST2)
      GO TO 4008
4007  XC1(JJ,I)=FXC(AVGD2(JJ,I-1),CD1(JJ,I),CONST2)
4008  IF(XC1(JJ,I).LE.0.)XC1(JJ,I)=1.E-8
C     WRITE(5,*)VR1(JJ,I)
```

```
      IF(KLM.EQ.1)CALL SWRL(P1,AVGD2(JJ,I),CD1(JJ,I),XTT(IJ),VL1(JJ,I),
     1RXL,THXL,VP)
      IF(IJ.GT.2)GO TO 4002
      VR2(IJ,I)=FVR(VR1(JJ,I),XT(JJ),XT(IJ),XC1(JJ,I))
      VR2(IJ,I)=SQRT(VR2(IJ,I)**2.+VP**2.)
      GO TO 4003
4002  VR2(IJ,I)=FVR(VR1(JJ,I-1),XT(JJ),XT(IJ),XC1(JJ,I))
      VR2(IJ,I)=SQRT(VR2(IJ,I)**2.+VP**2.)
4003  CONTINUE
      IF(I.EQ.1)GO TO 1200
      IF(IJ.EQ.2)GO TO 1201
      TA(IV,IJ-1,I)=(FTA(IV,IJ-2,I-1)+TAC(IV,1,I-1))/2.
      GO TO 1205
1201  TA(IV,1,I)=TAC(IV,1,I-1)
      GO TO 1205
1200  TA(IV,1,1)=T1
      IF(DS(JJ,N).LE.1.E-4)GO TO 61
      GO TO 62
61    DS(JJ,N)=1.E-4
62    CONTINUE
1205  IF(IJ.EQ.2)GO TO 1206
      TL=TBP
1206  IF(IJ.GT.2)GO TO 4004
      CALL EVAP(TBP,P1,TA(IV,IJ-1,I),HLF,SPHV,SHA)
      GO TO 4005
4004  CALL EVAP(TBP,P1,TA(IV,IJ-1,I),HLF,SPHV,SHA)
4005  XK1(JJ,I)=FXK(XK00,XRE1(JJ,I),SC)
      DS(IJ,I)=FD(DS(JJ,N),XK1(JJ,I),DT)
      IF(DS(IJ,I))31,31,20
31    DS(IJ,I)=1.E-8
20    DS(IJ,I)=SQRT(DS(IJ,I))
      AVGDS(IJ,I)=AVG(AVGDS(JJ,N),DS(IJ,I))
      IN=I
      IF(DS(IJ,I).GT.DS(JJ,N))DS(IJ,I)=DS(JJ,N)
      FV(IJ,I)=PI/6.*RHOL*(DS(JJ,N)**3.-DS(IJ,I)**3.)*XNDS(I)
      FL(IJ,I)=FL(JJ,N)-FV(IJ,I)
C*********************************************************************
C ENERGY BALANCE STARTS
C*********************************************************************
      TAC(IV,IJ-1,I)=TEMP(TA(IV,IJ-1,I),P1,P2)
      HLT=FV(IJ,I)*HLF
      TAM(IV,IJ-1,I)=(TA(IV,IJ-1,I)+TAC(IV,IJ-1,I))/2.
      HV=FV(IJ,I)*SPHV*TBP
      HA=XMAIR(IV,IJ-1)*SHA*TAM(IV,IJ-1,I)
      H1=HV+HA-HLT
      H2=XMAIR(IV,IJ-1)*SHA+FV(IJ,I)*SPHV
      FTA(IV,IJ-1,I)=H1/H2
C*********************************************************************
C ENERGY BALANCE IS COMPLETE
C*********************************************************************
      TFV(IV,IJ-1,I)=TFV(IV,IJ-2,I-1)+FV(IJ,I)
      IF(FL(IJ,I).LE.0.)GO TO 100
      VOLL(IJ,I)=FL(IJ,I)/RHOL
      D(IJ,I)=(6./PI/XND(I)*VOLL(IJ,I))**.333334
      IF(D(IJ,I))32,32,33
```

```
32      D(IJ,I)=1.E-4
33      AVGD2(IJ,I)=AVG(AVGD2(JJ,I-1),D(IJ,I))
35      N=I-1
        JHA=(XT(IJ)-XT(JJ))/XC1(JJ,I)
        IF(JHA.LT.Ø.ØØØ1)JHA=.ØØØ1
        VX(IJ,I)=VR2(IJ,I)+XVAVV
        VL1(IJ,I)=VX(IJ,I)
        IF(IJ.EQ.2) AVGVR2(IJ,I)=AVG(VR1(JJ,I),VR2(IJ,I))
        IF(IJ.GT.2) AVGVR2(IJ,I)=AVG(VR1(JJ,I-1),VR2(IJ,I))
        VR1(IJ,I)=VR2(IJ,I)
        IF(AVGVR2(IJ,I).LT.Ø.1)AVGVR2(IJ,I)=Ø.1
        IF(AVGD2(IJ,I).LT.1.E-4)AVGD2(IJ,I)=1.E-4
        XRE2(IJ,I)=FXRE(AVGVR2(IJ,I),AVGD2(IJ,I),CONST1)
        IF(XRE2(IJ,I).LE.12.)XRE2(IJ,I)=12.
        CD2(IJ,I)=FCD(XRE2(IJ,I))
        CD1(IJ,I)=CD2(IJ,I)
        BCD(I,IJ)=CD1(IJ,I)
        IF(IJ.GT.2)GO TO 4Ø15
        AVGCD2(IJ,I)=AVG(CD1(JJ,I),CD2(IJ,I))
        GO TO 4Ø16
4Ø15    AVGCD2(IJ,I)=AVG(CD1(JJ,I-1),CD2(IJ,I))
4Ø16    XC2(IJ,I)=FXC(AVGD2(IJ,I),CD2(IJ,I),CONST2)
        IF(XC2(IJ,I).LE.Ø.)XC2(IJ,I)=1.E-8
        AVGXC(IJ,I)=AVG(XC1(JJ,I),XC2(IJ,I))
        IF(IJ.GT.I)GO TO 22
C*********************************************************************
C EVEN NUMBERED SEGMENTS ARE ANALYSED IN THIS PORTION OF THE PROGRAM
C*********************************************************************
        IF(KLM.EQ.1)CALL SWRL(P1,AVGD2(IJ,I),CD1(IJ,I),XTT(JJJ),VL1(IJ,I),
       1RXL,THXL,VP)
        VR2(JJJ,I)=FVR(VR2(IJ,I-1),XT(IJ),XT(JJJ),XC2(IJ,I-1))
        VR2(JJJ,I)=SQRT(VR2(JJJ,I)**2.+VP**2.)
        IF(DS(IJ,N).LE.1.E-4)GO TO 63
        GO TO 64
63      DS(IJ,N)=1.E-4
64      CONTINUE
        TA(IV,IJ,I)=(FTA(IV,IJ-1,I-1)+TAC(IV,1,I-1))/2.
        CALL EVAP(TBP,P1,TA(IV,IJ,I),HLF,SPHV,SHA)
        XK2(IJ,I)=FXK(XKØØ,XRE2(IJ,I-1),SC)
        DS(JJJ,I)=FD(DS(IJ,N),XK2(IJ,I),DT)
        IF(DS(JJJ,I))34,34,21
34      DS(JJJ,I)=1.E-8
21      DS(JJJ,I)=SQRT(DS(JJJ,I))
        AVGDS(JJJ,I)=AVG(DS(JJJ,I),AVGDS(IJ,N))
        IF(DS(JJJ,I).GT.DS(IJ,N))DS(JJJ,I)=DS(IJ,N)
        FV(JJJ,I)=PI/6.*RHOL*(DS(IJ,N)**3.-DS(JJJ,I)**3.)*XNDS(I)
        FL(JJJ,I)=FL(IJ,N)-FV(JJJ,I)
C*********************************************************************
C ENERGY BALANCE :
C*********************************************************************
        TAC(IV,IJ,I)=TEMP(TA(IV,IJ,I),P1,P2)
        HLT=FV(JJJ,I)*HLF
        TAM(IV,IJ,I)=(TA(IV,IJ,I)+TAC(IV,IJ,I))/2.
        HV=FV(JJJ,I)*SPHV*TBP
        HA=XMAIR(IV,IJ)*SHA*TAM(IV,IJ,I)
```

```
      H1=HV+HA-HLT
      H2=XMAIR(IV,IJ)*SHA+FV(JJJ,I)*SPHV
      FTA(IV,IJ,I)=H1/H2
C*********************************************************************
C ENERGY BALANCE COMPLETE
C*********************************************************************
      TFV(IV,IJ,I)=TFV(IV,IJ-1,I-1)+FV(JJJ,I)
      IF(FL(JJJ,I).LE.0.)GO TO 100
      VOLL(JJJ,I)=FL(JJJ,I)/RHOL
      D(JJJ,I)=(6./PI/XND(I)*VOLL(JJJ,I))**.333334
      IF(D(JJJ,I))38,38,39
38    D(JJJ,I)=1.E-4
39    AVGD2(JJJ,I)=AVG(D(JJJ,I),AVGD2(IJ,N))
      JHA1=(XT(JJJ)-XT(IJ))/XC2(IJ,I)
      IF(JHA1.LT.0.000001)JHA1=.000001
      AVGVR2(JJJ,I)=AVG(VR2(IJ,I-1),VR2(JJJ,I))
      IF(AVGVR2(JJJ,I).LT.0.1)AVGVR2(JJJ,I)=0.1
      IF(AVGD2(JJJ,I).LT.1.E-4)AVGD2(JJJ,I)=1.E-4
      XRE2(JJJ,I)=FXRE(AVGVR2(JJJ,I),AVGD2(JJJ,I),CONST1)
      IF(XRE2(JJJ,I).LE.12.)XRE2(JJJ,I)=12.
      CD2(JJJ,I)=FCD(XRE2(JJJ,I))
      AVGCD2(JJJ,I)=AVG(CD2(IJ,I-1),CD2(JJJ,I))
      VR1(JJJ,I)=VR2(JJJ,I)
      VX(JJJ,I)=VR2(JJJ,I)+XVAVV
      VL1(JJJ,I)=VX(JJJ,I)
22    CONTINUE
100   CONTINUE
      XFV=0.
      DO 80 JKK=2,J
      XFV=XFV+ (FV(JKK,I))
80    CONTINUE
      FVTOT=FVTOT+XFV
      SL=FL(1,I)
      IF(I.EQ.1)GO TO 37
      DO 36 IDD=2,I
      IKK=I-1
36    SL=SL+FL(IDD,IKK)
37    TFL(J,I)=SL-XFV
      TVOLL(J,I)=TFL(J,I)/RHOL
C*********************************************************************
C CONSERVATION OF MOMENTUM:TO SOLVE FOR THE VELOCITY OF LEADING DROPLET
C*********************************************************************
      XM=0.
      XN1=FL(1,I)*VL1(1,I)
      XFL=FL(1,1)
      XN2=0.
      XN4=0.
      IF(I.EQ.1)GO TO 50
      DO 25 ID=2,I
      IK=ID-1
      IA=I+2-ID
      IC=I+3-ID
      XN1=XN1+FL(ID,II)*VL1(ID,II)
      XN2=XN2+FL(ID,I)*VL1(ID,I)
      XN4=XN4+(FV(ID,IK)+XMAIR(IV,IK))*XVAVV
```

```
25    XFL=XFL+FL(1,ID)
50    CONTINUE
      XN3=FL(J,I)*VR2(J,I)
      XN=XN1-XN2-XN3+XN4
      DN1=FL(J,I)
      DN2=0.
      DO 26IM=2,J
      IKK=IM-1
26    DN2=DN2+FV(IM,IKK)+XMAIR(IV,IKK)
      DN=DN1+AG*DN2
      VAVV=0.
      VA=XN/DN
      VAVV=AG*VA+VAVV
C     WRITE(5,*)VAVV
      IF(KLM.LE.3)XXVAVV=VAVV
      VL1(J,I)=VR2(J,I)+XXVAVV
      RAJU=RAJ
      RAJU=RAJU*PI/180.
      IF(I.EQ.1)GO TO 952
      GO TO 953
952   AVGVL=0.5*(VL1(1,1)+VL1(2,1))
      GO TO 954
953   AVGVL=0.5*(VL1(I,I-1)+VL1(J,I))
954   XT(J)=(XTP(I)+AVGVL*DT)
      XTT(J)=XT(J)*COS(RAJU)
      CALL SWRL(P1,AVGD2(J,I),AVGCD2(J,I),XTT(J),AVGVL,RXL,THXL,VP)
C*************************************************************************
C TO DETERMINE THE GEOMETRY OF SPRAY AND EVALUATE SPRAY TIP PENETRATION
C*************************************************************************
      ARXL(J)=RXL
      IF(I-2)7,8,9
7     XTP(J)=ARXL(J)
      SI(J)=THXL*180./PI
      GO TO 1007
C     IF(IV.GT.2)GO TO 1007
C     XXTP(J)=XTP(J)*COSD(SI(J))
C     YXTP(J)=XTP(J)*SIND(SI(J))
C     GO TO 6
8     SIGMA=PI-THXL
      VIJ=COS(SIGMA)
      XTP(J)=((XTP(J-1))**2.+(ARXL(J))**2.-2.*XTP(J-1)*ARXL(J)*VIJ)**.5
      GO TO 10
9     BETA1=-(XTP(J-2))**2.+(ARXL(J-1))**2.+(XTP(J-1))**2.
      BETA2=2.*ARXL(J-1)*XTP(J-1)
      BBETA=BETA1/BETA2
      IF(BBETA.EQ.1.)BBETA=0.9999999
      BETA=ACOS(BBETA)
      BTA=BETA+THXL
      SV=PI-BTA
      AI=COS(SV)
      XTP(J)=((XTP(J-1))**2.+(ARXL(J))**2.-2.*XTP(J-1)*ARXL(J)*AI)**0.5
10    XLAMDA1=-(ARXL(J))**2.+(XTP(J-1))**2.+(XTP(J))**2.
      XLAMDA2=2.*XTP(J-1)*XTP(J)
      XXLAMDA=XLAMDA1/XLAMDA2
      IF(XXLAMDA.EQ.1.)XXLAMDA=0.9999999
```

```
      XLAMDA=ACOS(XXLAMDA)
      SI(J)=SI(J-1)+XLAMDA*180./PI
C     IF(IV.GT.2)GO TO 1007
C     XXTP(J)=XTP(J)*COSD(SI(J))
C     YXTP(J)=XTP(J)*SIND(SI(J))
C     GO TO 6
1007  XXTP(J)=XTP(J)*COSD((TH(IV)*180./PI)-SI(J))
      YXTP(J)=XTP(J)*SIND(-(TH(IV)*180./PI)+SI(J))
6     WA=820.
      XTV=XXVAVV*DT+XTV
      XLV=WA*XTV*DT
      THXV=ATAN(XLV/XTV)
      XTV=SQRT(XTV**2.+XLV**2)
      ATHXV(J)=ATHXV(I)+THXV
      FTHXV(J)=ATHXV(J)*180./PI
      XTPV(J)=XTV
      XXTPV(J)=XTPV(J)*COSD(FTHXV(J)+(TH(IV)*180./PI))
      YXTPV(J)=XTPV(J)*SIND(FTHXV(J)+(TH(IV)*180./PI))
      IF(KLM.GE.3)GO TO 42
C*********************************************************************
C TO CALCULATE ACTUAL MASS OF AIR ENTRAINED IN DEFORMED CONE
C*********************************************************************
      CALL CONEV(XTP(J),TH(IV),XXTP(J),YXTP(J),XXTPV(J),YXTPV(J),
     1XTP(J-1),DVOL)
      IF(I.EQ.1)GO TO 1000
      VOA(J)=VOA(I)+DVOL
      GO TO 1001
1000  VOA(J)=VOA(I)+DVOL*2./3.
1001  IF(IV.EQ.2)GO TO 1004
C*********************************************************************
C TO CALCULATE MASS OF AIR IN THE ANNULAR SECTION OF OUTER CONES BY
C INTERPOLATING THE VOLUME OF INNER CONE TO BE SUBTRACTED
C*********************************************************************
      CALL CRAFT1(LK+1,DUMMY2,DUMMY1,XTP(J),FCOVOLI)
      GO TO 1003
1004  FCOVOLI=0.0
1003  TCOVOL=VOA(J)-FCOVOLI
      IF(TCOVOL.LE.0.)TCOVOL=.001
      AVOA(J)=TCOVOL-TVOLL(J,I)
      XMAIR(IV,I)=(AVOA(J)-AVOA(I))*RHOA
42    CONTINUE
      AREA(1)=AREA(2)
      AA(I)=AREA(2)
      XVAVV=VAVV
      XXVAVV=VAVV
30    CONTINUE
      V(I)=VAVV
      X(I,I)=0.
      J=I+1
      X1(I,I)=X(I,I)+XT(J)
      LLL=I
      XXFV(LLL)=XFV/XT(J)
      YXT(LLL)=XT(J)-XT(J-1)
      TIM(I)=TIME
      P1=P2
```

```
      V1=V2
110   CONTINUE
      DO 1100 I=1,LK
      J=I+1
C     WRITE(5,*)XTP(J)
C     WRITE(1,*)XTP(J),XXTP(J),YXTP(J),XXTPV(J),YXTPV(J)
1100  CONTINUE
      DO 1008 J=2,LK+1
      DUMMY1(J)=VOA(J)
      DUMMY2(J)=XTP(J)
      PEN(IV,J)=XTP(J)
      IF(IV.EQ.2)WRITE(5,*)PEN(IV,J)
1008  CONTINUE
      DO 172 J=2,81,5
C     WRITE(5,*)XXTP(J),YXTP(J),XXTPV(J),YXTPV(J)
172   CONTINUE
111   CONTINUE
C*********************************************************************
C EVALUATION OF EQUIVALENCE RATIO WITHOUT CONSIDERING OVERLAP
C*********************************************************************
      DO 4020 MN=2,5
      DO 4022 LN=1,LK
      DO 4021 NM=1,LN
      PHE(MN,NM)=TFV(MN,NM,LN)/(XMAIR(MN,NM)*0.06667)
C     WRITE(5,*)PEN(MN,NM+1),XMAIR(MN,NM),TFV(MN,NM,LN),PHE(MN,NM)
4021  CONTINUE
4022  CONTINUE
4020  CONTINUE
C*********************************************************************
C NOW CONSIDERING OVERLAP
C*********************************************************************
      DO 3000 J=1,LK+1
      DO 3001 L=2,5
      DO 3002 IV=L+1,5
      ADD3=0.0
      ADD5=0.0
      K=J
3003  IF(PEN(L,J)-PEN(IV,K))3004,3005,3005
3005  IF(K.GE.LK+1)GO TO 3015
      K=K+1
      GO TO 3003
3004  M=K-1
      N=K+1
3006  IF(PEN(L,J+1)-PEN(IV,N))3007,3008,3008
3008  IF(N.GE.LK+1)GO TO 3007
      N=N+1
      GO TO 3006
3007  IJ=N-1
      D1=(PEN(L,J)-PEN(IV,M+1))/(PEN(IV,M+1)-PEN(IV,M))*TFV(IV,M,LK)
      ADD1=ABS(D1)
      D2=(PEN(L,J+1)-PEN(IV,IJ))/(PEN(IV,IJ+1)-PEN(IV,IJ))*TFV(IV,IJ,LK)
      ADD2=ABS(D2)
      IF(N.GE.LK+1)ADD2=0.0
      IF(IJ.GE.M+2)GO TO 3009
      IF(IJ.EQ.60.AND.M.EQ.59)ADD5=TFV(IV,IJ,LK)
```

```
      GO TO 3010
3009  DO 3011 LM=M+2,IJ
      ADD3=TFV(IV,LM-1,LK)
3011  CONTINUE
3010  ADD4=ADD1+ADD2+ADD3+ADD5
      XNV=(IJ+M)/2.*0.31+(TH(IV)*180./PI)
      XDE=J*0.31+(TH(L)*180./PI)
      RATIO=(TAND(XDE))**2./(TAND(XNV))**2.
      ADD=RATIO*ADD4
      TFV(L,J,LK)=TFV(L,J,LK)+ADD
      TFV(IV,M,LK)=TFV(IV,M,LK)-RATIO*ADD1
      TFV(IV,IJ,LK)=TFV(IV,IJ,LK)-RATIO*ADD2
      IF(IJ.LT.M+2)GO TO 3002
      DO 3013 KL=M+2,IJ
      TFV(IV,KL-1,LK)=TFV(IV,KL-1,LK)-RATIO*(ADD3/(IJ-M-1))
3013  CONTINUE
3002  CONTINUE
3015  IF(XMAIR(L,J).EQ.0.0)GO TO 3001
      PHE(L,J)=TFV(L,J,LK)/(XMAIR(L,J)*0.06667)
      DELAY(L,J,LK)=A*(P1**AN)*(PHID**C)*(EXP(DD/FTA(L,J,LK)))
      WRITE(5,*)'PHE',PHE(L,J),'DELAY',DELAY(L,J,LK),'J',J
      IF(DELAY(L,J,LK).GT.(J*DT*1000.))GO TO 3001
      I=LK
      GO TO 5001
3001  CONTINUE
3000  CONTINUE
5000  CONTINUE
5001  NO=0
C*********************************************************************
C TO CALCULATE THE PRESSURE RISE
C*********************************************************************
      SMRT=0
      SMRT1=0
      DO 5002 K=2,5
      DO 5003 L=1,I
      IF((PHE(K,L).GT.0.3).AND.(PHE(K,L).LT.3.))GO TO 5004
      SMRT1=SMRT1+(TFV(K,L,I)+XMAIR(K,L))*2.83*FTA(K,L,I)
      SAIR=SAIR+XMAIR(K,L)
      GO TO 5003
5004  CALL AFT(PHE(K,L),FTA(K,L,I),P1,AT,ARR)
      SMRT=SMRT+(TFV(K,L,I)+XMAIR(K,L))*ARR*AT
      SAIR=SAIR+XMAIR(K,L)
      NO=NO+1
5003  CONTINUE
5002  CONTINUE
C     SINCE THERE ARE 4 NOZZLES
      SMRT1=4*SMRT1
      SMRT=4*SMRT*2.2*778*12*2.54**3/14700
C     IF SPIKE IS ASSUMED TO BE 3 DEGREES CRANK ANGLE
C     THE VOLUME AND TEMPERATURE DUE TO COMPRESSION ALONE WOULD BE:
      ANG=ANG-3*PI/180.
      CALL PV(ANG,V1,P1,V2,P2)
      TAIR=TEMP(TA(2,1,I),P1,P2)
      E11=V1*RHOA-4*SAIR
      E1=E11*2.83*TAIR
```

```
      P1=(SMRT1+SMRT+E1)/V2
C     WRITE(1,*)ANG*180/PI,P1
      V1=V2
C     MASS OF FUEL COMING OUT IN THE REMAINING TIME FROM ALL 4 NOZZLES
      RM=4*(PI/4.*DNN*DNN*VL1(1,I)*RHOL*3/(6*RPM))
C     ASSUMING THIS FUEL TO BURN AT PHI=1 IN NEXT 1 DEGREE OF ROTATION
      TT=TAIR
      CALL AFT(1.,TAIR,P1,AT,ARR)
      SMRT=SMRT+(RM+RM)*ARR*AT*2.2*778*12*2.54**3/14700
C     BECAUSE PHI=1 MASS OF AIR WILL ALSO BE RM
      ANG=ANG-PI/180.
      CALL PV(ANG,V1,P1,V2,P2)
      TAIR1=TEMP(TT,P1,P2)
      E1=(E11-RM)*2.83*TAIR1
      P2=(SMRT1+SMRT+E1)/V2
C     WRITE(1,*)ANG*180/PI,P2
C*************************************************************************
C THIS IS A PARTICULAR SOLUTION AND WILL REQUIRE CHANGES FOR EACH TEST
C RUN. IT IS POSSIBLE TO SUBSTITUTE IT WITH A GENERAL SOLUTION
C*************************************************************************
5010  P1=P2
      V1=V2
      ANG=ANG-PI/180.
      CALL PV(ANG,V1,P1,V2,P2)
C     WRITE(1,*)ANG*180/PI,P2
      IF (P2.LT.5)GO TO 5011
      GO TO 5010
5011  CLOSE (UNIT=1)
      STOP
      END
C*************************************************************************
      SUBROUTINE SWRL(PT,D,CD,XT,AVGVL,RXL,THXL,VP)
      DOUBLE PRECISION RXL,THXL,WA1,WA2,WL,XL
      PI=3.1416
      GC=981.
      TAO=305.
      PTO=1.
      R=2.8326
      RHOAO=PTO/(R*TAO)
      THINJ=11
      IM12=60
      DELAY=8.
      RPM=900.
      DT=THINJ/(IM12*6.*RPM)
      RHOA=(PT/PTO)**(1./1.256)*RHOAO
      RHOL=.74871
      CONST2=RHOL/RHOA
      WA=820.
      IF(XT.LT.0.01)XT=0.01
      WA1=4.*CONST2*GC*D/(3.*CD*XT*DT)
      WA2=SQRT((WA1+2.*WA)**2.-4.*WA*WA)
      WL=(WA1+2.*WA-WA2)/2.
      IF(AVGVL.EQ.0.)AVGVL=0.00001
      VP=AVGVL*DT*WL
      XL=VP*DT
```

```
      RXL=SQRT((AVGVL*DT)**2.+XL*XL)
      THXL=ATAN(XL/(AVGVL*DT))
      RETURN
      END
C*****************************************************************************
      SUBROUTINE CONEV(X2,ANGLE,XL,YL,XV,YV,X1,DV)
      COMMON/A/AREA(2)
      PI=3.1415
      AMINOR=2*X2*TAN(ANGLE)
      AMAJOR=((XL-XV)**2.+(YL-YV)**2.)**0.5
      AREA(2)=PI*AMINOR*AMAJOR
      BASE=(AREA(2)+AREA(1))/2.
      HT=X2-X1
      DV=BASE*HT
      RETURN
      END
C*****************************************************************************
      SUBROUTINE CRAFT1(MM,A,F,X,VRS)
      DIMENSION F(61),D(61),B(61),DD(62),XF(0:61,61)
      DOUBLE PRECISION A(61),X
      DO 20 J=1,MM
      D(J)=A(J)-X
      IF (J.EQ.1)GO TO 40
      IF(ABS(D(J)).LT.ABS(D(J-1)).AND.D(J).LT.0.0)GO TO 40
      GO TO 20
40    K=J
20    CONTINUE
      IF(K.EQ.1)GO TO 60
      DO 50 L=1,MM+1-K
      B(L)=A(K-1+L)
      XF(0,L)=F(K-1+L)
50    CONTINUE
      DO 70 M=MM+2-K,MM
      DO 70 N=1,K-1
      B(M)=A(K-N)
      XF(0,M)=F(K-N)
70    CONTINUE
      GO TO 90
60    DO 80 N=1,MM
      B(N)=A(N)
      XF(0,N)=F(N)
80    CONTINUE
90    DO 100 JJ=1,MM
      DD(JJ)=B(JJ)-X
100   CONTINUE
      DO 120 L=1,1
      DO 110 N=L+1,2
      XF(L,N)=(XF(L-1,L)*DD(N)-XF(L-1,N)*DD(L))/(B(N)-B(L))
110   CONTINUE
120   CONTINUE
      VRS=XF(1,2)
      RETURN
      END
C*****************************************************************************
      SUBROUTINE EVAP(TL,P,T,HLF,SPHV,SHA)
```

```
C     TC IS CRITICAL TEMP
C     PC IS CRITICAL PRESSURE
C     XMW IS MOL. WT.OF FUEL
      PC=18.
      TC=660.
      R=1.987
      XMW=226.
      TM=(T-TL)/ALOG(T/TL)
      HLF=(2.303*R*TL*TC*ALOG10(PC))/((TC-TL)*XMW)
      X=-9.68+0.27045*TM-1.0133E-8*TM*TM
      SPHV=(X+(5.03*P/PC*(TC/TM)**3.))/XMW
      SHA=0.24332+0.00004593*TM
      RETURN
      END
C*********************************************************************
      SUBROUTINE PV(THETA,VOL1,PR1,VOL2,PR2)
C     THIS SUBROUTINE CALCULATES VOLUME OF CYLINDER FROM
C     ENGINE GEOMETRY.
      PI=3.142
C*********************************************************************
C     CL=CLEARANCE,D=DIA OF CYLINDER,CRR=CRANK RADIUS,CR=LENGHT
C     OF CONNECTING ROD,DRP=DIFF BETWEEN CENTERS OF CYLINDER
C     AND PISTON. ALL DIMENSIONS ARE IN CM
C*********************************************************************
      CL=0.2841
      D=8.026
      CR=8.89
C     CRR IS APPROXMATE VALUE
      CRR=2.29
      ANC=1.39
C     DRP IS APPROXIMATE VALUE
      DRP=0.006
C*********************************************************************
C     PR IS PRESSURE VOL IS VOLUME OF CYLINDER
C*********************************************************************
      VOL11=SQRT(CR**2-(DRP+CRR*SIN(THETA))**2)
      VOL2=PI/4.*(D**2)*(CL+CR+CRR*(1.-COS(THETA))-VOL11)
      PR2=PR1*(VOL1/VOL2)**ANC
C     WRITE(5,*)VOL2,PR2
      RETURN
      END
      FUNCTION TEMP(T1,P1,P2)
      TEMP=T1*(P2/P1)**0.286
C     WRITE(5,*)TEMP
      RETURN
      END
C*********************************************************************
        SUBROUTINE AFT(FF,TT,PP,AT,ARR)
        IMPLICIT DOUBLE PRECISION (A-H,O-Z)
        COMMON/BLOCK/AN,AM,AL,AK,F,T,P,KL0,IERR,XPA
        COMMON/TAB/DXT(12),DXP(12),DXF(12)
        COMMON/PROP/AVM,R,H,U,DRT,DHT,DUT,DRP,DHP,DUP,DRF,DHF,DUF
        F=FF
        AN=16.
        AM=34.
```

```
      AL=0.
      AK=0.
      P=14.7*PP
      TM=TT*1.8
      TH1=537.0/1.8
      HRF=(3.55E-5*TT**2-0.076997*TT-69.95)*1000.*453.59/252.
      HAIR=(1.286E-5*TM**2+0.274675*TM+3.33)*29.8
      XAIR=24.5*4.607/F
      HMR=226.+XAIR*29.8
      HR=(HRF+XAIR*29.8)/HMR
      KL0=1
      T=6000.
      IND=0
10    IND=IND+1
      CALL PER(1,RR)
      ARR=RR
C     WRITE(1,*)'RR',RR,'NO. OF ITERATIONS',IND
      IF(IERR.NE.0) GO TO 20
889   FORMAT(1X,'H  HR  DELT DHT',4F15.5)
C888  FORMAT(1X,'H  HR  DHT',3F10.2)
      DELT=(H-HR)/DHT
      T=T-DELT
      AT=T
C     WRITE(1,889)H,HR,DELT,DHT
      IF(DABS(DELT).LE.1.) GO TO 30
      IF(IND.LT.100) GO TO 10
C     WRITE(1,40)
40    FORMAT(10X,'ITERATION DID NOT CONVERGE IN 25 ATTEMPTS')
      GO TO 5
30    WRITE(5,60)AT
60    FORMAT(10X,'FLAME TEMPERATURE (DEG. R) =',F8.1)
      GO TO 5
20    WRITE(5,70)IERR,AN,AM,AL,AK,F,T,P,KL0
70    FORMAT(10X,'SUBROUTINE PER FAILED. ERROR CODE IS',I2/10X
     C,'CONDITIONS OF FAILURE (AN,AM,AL,AK,F,T,P,KL0)ARE',7F10.2
     D,I5)
5     WRITE(5,*)'ARR',ARR
      RETURN
      END
      SUBROUTINE EQMD(JDR,RR)
      IMPLICIT DOUBLE PRECISION (A-H,O-Z)
      COMMON/BLOCK/AN,AM,AL,AK,PHI,T,P,KL0,IERR,X1,X2,X3,X4,X5,
     E X6,X7,X8,X9,X10,X11,X12,X13
      COMMON/TAB/DX1T,DX2T,DX3T,DX4T,DX5T,DX6T,DX7T,DX8T,DX9T,
     FDX10T,DX11T,DX12T,DX1P,DX2P,DX3P,DX4P,DX5P,DX6P,DX7P,DX8P,
     GDX9P,DX10P,DX11P,DX12P,DX1F,DX2F,DX3F,DX4F,DX5F,DX6F,DX7F,
     HDX8F,DX9F,DX10F,DX11F,DX12F
C     COMMON/TAB/DXT(12),DXP(12),DXF(12)
      DIMENSION A(4,4),B(4),C(4,3)
      DATA JF,PREC/0,1.0E-03/
      IF((T-1080.)*(7200.-T))102,105,105
102   IERR=1
      GO TO 710
105   R0=(AN+0.25*AM-0.5*AL)/PHI
      R=R0+0.5*AL
```

```
      R1=R0*3.7274+0.5*AK
      R2=R0*0.0444
      GG=R+R1+R2
C      WRITE(6,*)' GG=',GG
999   FORMAT(1X,'PHI  R  R0  R1  R2',5F10.5)
8     FORMAT(3F8.4)
      IF(R.GT..5*AN)GO TO 110
      IERR=2
      GO TO 710
110   D1=AM/AN
      D2=2.0*R/AN
      D3=2.0*R1/AN
      D4=R2/AN
115   SQP=DSQRT(P/14.696)
      TA=0.005*T/9.0
      ALTA=DLOG(TA)
      TAIN=1.0/TA
      TASQ=TA*TA
 998  FORMAT(1X,'I AM O.K.')
      C1=(10.0**(0.432168*ALTA-11.2464*TAIN+2.67269-0.745744E-01*TA
     A+0.242484E-02*TASQ))/SQP
      C2=(10.0**(0.310805*ALTA-12.9540*TAIN+3.21779-0.738336E-01*TA
     B+0.344645E-02*TASQ))/SQP
      C3=(10.0**(0.389716*ALTA-24.5828*TAIN+3.14505-0.963730E-01*TA
     C+0.585643E-02*TASQ))/SQP
      C5=10.0**(-0.141784*ALTA-2.13308*TAIN+0.853461+0.355015E-01*TA
     D-0.310227E-02*TASQ)
      C7=10.0**(0.150879E-01*ALTA-4.70959*TAIN+0.646096+0.272805E-02*T
     EA-0.154444E-02*TASQ)
      C9=(10.0**(-0.752364*ALTA+12.4210*TAIN-2.60286+0.259556*TA
     F-0.162687E-01*TASQ))*SQP
      C10=(10.0**(-0.415302E-02*ALTA+14.8627*TAIN-4.75746+0.124699*TA
     G-0.900227E-02*TASQ))*SQP
C
C     SECTION DECIDES WHETHER TO MAKE A NEW ESTIMATE OF X4,X6,X8,X11
C
      IF(KL0-1)305,205,410
205   IF(JF.EQ.0)GO TO 305
      IF(DABS(PHI-PHIPR).GT.1.0E-6)GO TO 305
      IF(DABS(T/TPR-1.0).GT.0.02) GO TO 305
      IF(DABS(P/PPR-1.0).GT.0.05)GO TO 305
      X4=X4PR
      X6=X6PR
      IF(X6.LE.0.0)X6=0.0000001
      X8=X8PR
      X11=X11PR
      GO TO 410
C
C     SECTION 300 CAN MAKE AN INITIAL ESTIMATE OF X4,X6,X8,_X11
C
305   IF(PHI.GE.1.0)GO TO 310
      PAR=1.0/(R1+R2+R+0.25*AM)
      GO TO 315
310   PAR=1.0/(R1+R2+A..+0.5*AM)
315   FUN1=2.0*AN*C10
```

```
      FUN2=0.5*AM*C9
      FUN3=2.0/PAR
      FUN4=2.0*R
      OX=1.0
320   SQOX=DSQRT(OX)
      FOX=(FUN1*SQOX+AN)/(1.0+C10*SQOX)+FUN2*SQOX/(1.0+C9*SQOX)
     A+FUN3*OX-FUN4
      IF(FOX)325,330,335
335   OX=0.1*OX
      IF(OX.GE.1.0E-30)GO TO 320
      IERR=3
      GO TO 710
325   IND=1
327   FOX=(FUN1*SQOX+AN)/(1.0+C10*SQOX)+FUN2*SQOX/
     1  (1.0+C9*SQOX)+FUN3*OX-FUN4
      DOX=0.25*FUN1/(SQOX*(1.0+C10*SQOX)**2)+0.5*FUN2/(SQOX*
     2  (1.0+C9*SQOX)**2)+FUN3
      RAT=FOX/DOX
      OX=OX-RAT
      SQOX=DSQRT(OX)
      IF(DABS(RAT/OX).LE.1.0E-2)GO TO 330
      IND=IND+1
      IF(IND.LE.100)GO TO 327
330   X4=0.5*AM*PAR/(1.0+C9*SQOX)
      X6=AN*PAR/(1.0+C10*SQOX)
      IF (X6.LE.0.0)X6=0.0000001
      X8=OX
      X11=R1*PAR
C
C     SECTION 400 CALCULATES THE ELEMENTS OF THE MATRIX(LINEARISED EQ)
410   IND=1
      NCALL=0
455   IF(X4.LE.0.0) X4=0.0000001
      SQX4=DSQRT(X4)
      IF (X8.LE.0.0) X8=0.0000001
      SQX8=DSQRT(X8)
      SQX11=DSQRT(X11)
      X1=C1*SQX4
      X2=C2*SQX8
      X3=C3*SQX11
      X5=C5*SQX4*SQX8
      X7=C7*SQX11*SQX8
      X9=C9*X4*SQX8
      X10=C10*X6*SQX8
460   T14=0.5*C1/SQX4
      T28=0.5*C2/SQX8
      T311=0.5*C3/SQX11
      T54=0.5*C5*SQX8/SQX4
      T58=0.5*C5*SQX4/SQX8
      T78=0.5*C7*SQX11/SQX8
      T711=0.5*C7*SQX8/SQX11
      T94=C9*SQX8
      T98=0.5*C9*X4/SQX8
      T106=C10*SQX8
      T108=0.5*C10*X6/SQX8
```

```
      A(1,1)=T14+2.+T54+2.*T94
      A(1,2)=-D1*(1.+T106)
      A(1,3)=(T58+2.0*T98)-D1*T108
      A(1,4)=0.0
      A(2,1)=T54+T94
      A(2,2)=(1.+2.*T106)-D2*(1.+T106)
      A(2,3)=(T28+T58+T78+2.+T98+2.*T108)-D2*T108
      A(2,4)=T711
      A(3,1)=0.
      A(3,2)=-D3*(1.+T106)
      A(3,3)=T78-D3*T108
      A(3,4)=T311+T711+2.
      A(4,1)=T14+1.+T54+T94
      A(4,2)=1.+T106+D4*(1.+T106)
      A(4,3)=T28+T58+T78+1.0+T98+T108+D4*T108
      A(4,4)=T311+T711+1.
      IF(NCALL.EQ.1)GO TO 810
      B(1)=-(X1+2.0*X4+X5+2.0*X9)+D1*(X6+X10)
      B(2)=-(X2+X5+X6+X7+2.*X8+X9+2.*X10)+D2*(X6+X10)
      B(3)=-(X3+X7+2.*X11)+D3*(X6+X10)
      B(4)=-(X1+X2+X3+X4+X5+X6+X7+X8+X9+X10+X11+D4*(X6+X10))+1.
C
C     SECTION 500:MATRIX IS SOLVED BY GAUSSIAN ELIMINATION
C
      DO 505 K=1,3
      KP1=K+1
      BIG=DABS(A(K,K))
      IF(BIG.GE.1.0E-05) GO TO 520
      IBIG=K
      DO 510 I=KP1,4
      IF(DABS(A(I,K)).LE.BIG) GO TO 510
      BIG=DABS(A(I,K))
      IBIG=I
510   CONTINUE
      IF(BIG.GT.0.) GO TO 512
      IERR=4
      GO TO 710
512   IF(IBIG.EQ.K) GO TO 520
      DO 515 J=K,4
      TERM=A(K,J)
      A(K,J)=A(IBIG,J)
      A(IBIG,J)=TERM
515   CONTINUE
      TERM=B(K)
      B(K)=B(IBIG)
      B(IBIG)=TERM
520   DO 525 I=KP1,4
      TERM=A(I,K)/A(K,K)
      DO 530 J=KP1,4
      A(I,J)=A(I,J)-A(K,J)*TERM
530   CONTINUE
      B(I)=B(I)-B(K)*TERM
525   CONTINUE
505   CONTINUE
      IF(DABS(A(4,4)).GT.0.) GO TO 550
```

AD-A193 787 MODELING OF SPRAY COMBUSTION IN DIRECT INJECTION DIESEL ENGINE(U) NORTH CAROLINA AGRICULTURAL AND TECHNICAL STATE UNIV GREENSBO.. H SINGH ET AL. 30 JAN 88 2/2

UNCLASSIFIED ARO-21329.3-EG-H DAAG29-84-G-0001 F/G 21/2 NL

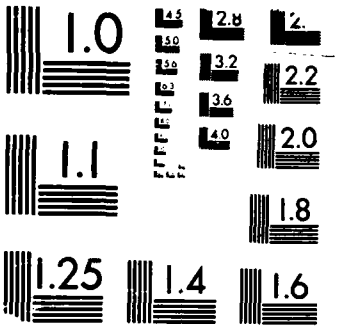

MICROCOPY RESOLUTION TEST CHART

```
      IERR=4
      GO TO 710
550   B(4)=B(4)/A(4,4)
C     WRITE(6,698)B(3),X3,X7,X11,X6,X10,D3
698   FORMAT(1X,'B X3 X7 X11 X6 X10 D3',7F10.3)
      B(3)=(B(3)-A(3,4)*B(4))/A(3,3)
      B(2)=(B(2)-A(2,3)*B(3)-A(2,4)*B(4))/A(2,2)
      B(1)=(B(1)-A(1,2)*B(2)-A(1,3)*B(3)-A(1,4)*B(4))/A(1,1)
C
C     CHECKS PRECISION
C
602   NCK=0
      X4=X4+B(1)
      IF(DABS(B(1)/X4 ).GT.PREC) NCK=1
      X6=X6+B(2)
      IF (X6.LE.0.0)X6=0.0000001
      IF(DABS(B(2)/X6 ).GT.PREC) NCK=1
C     WRITE(1,699)X8,B(3),T311,T711
 699  FORMAT(1X,'X8 B(3) T311 T711',4F15.5)
      X8=X8+B(3)
      IF(DABS(B(3)/X8 ).GT.PREC) NCK=1
      X11=X11+B(4)
      IF(DABS(B(4)/X11).GT.PREC) NCK=1
      XABS4=DABS(B(1)/X4)
      XABS6=DABS(B(2)/X6)
      XABS8=DABS(B(3)/X8)
      XABS11=DABS(B(4)/X11)
C     WRITE(5,*)XABS4,XABS6,XABS8,XABS11
C     WRITE(5,*)'B1',B(1),'B2',B(2),'B3',B(3),'B4',B(4),'NCK',NCK
 995  FORMAT(1X,'X4 X6 X8 X11',4F15.5)
C     WRITE(1,995)X4,X6,X8,X11
      IF (X8.LE.0.0) X8=0.0000001
      IF (X4.LE.0.0) X4=0.0000001
      IF((X4.GT.0.).AND.(X8.GT.0.).AND.(X11.GT.0.)) GO TO 620
      IERR=5
      GO TO 710
C
C     SECTION 700 CALCULATES THE REMAINING MOLE FRACTIONS
C
 991  FORMAT(1X,'NCK=',I2)
620   IF(NCK.EQ.0) GO TO 625
      IF(IND.LT.100) GO TO 622
      IERR=6
      GO TO 710
622   IND=IND+1
      GO TO 455
625   IF(X6.GE.0.) GO TO 702
      IERR=5
 997  FORMAT(1X,'I AM ALL RIGHT')
      GO TO 710
702   IERR=0
      JF=1
      PHIPR=PHI
      TPR=T
      PPR=P
```

```
      X4PR=X4
      X6PR=X6
      X8PR=X8
      X11PR=X11
      SQX4=DSQRT(X4)
      SQX8=DSQRT(X8)
      SQX11=DSQRT(X11)
      X1=C1*SQX4
      X2=C2*SQX8
      X3=C3*SQX11
      X5=C5*SQX4*SQX8
      X7=C7*SQX11*SQX8
      X9=C9*X4*SQX8
      X10=C10*X6*SQX8
      X13=(X6+X10)/AN
      X12=R2*X13
C     WRITE(1,*)' X1',X1,'X2',X2,'X3',X3,'X4',X4,'X5',X5,'X6',X6,
C    1 'X7',X7,'X8',X8,'X9',X9,'X10',X10,'X11',X11,'X12',X12,'X13',X13
      IF(JDR-1)725,800,800
725   RETURN
710   JF=0
      RETURN
C
C     SECTION 800 CALCULATES THE ELEMENTS OF THE MATRIX OF THE
C     PARTIAL DIFFERNTIAL EQUATIONS
C
800   NCALL=1
      GO TO 460
810   ZZ=ALOG(10.)*0.005/9.
      DC1T=X1*ZZ*(0.432168*TAIN+11.2464/TASQ-0.745744E-1+.484968E-2*TA)
      DC2T=X2*ZZ*(.310805*TAIN+12.9540/TASQ-.738336E-1+.689290E-2*TA)
      DC3T=X3*ZZ*(.389716*TAIN+24.5828/TASQ-.963730E-1+1.171286E-2*TA)
      DC5T=X5*ZZ*(-.141784*TAIN+2.13308/TASQ+.355015E-1-.620454E-2*TA)
      DC7T=X7*ZZ*(.150879E-1*TAIN+4.70959/TASQ+.272805E-2-.308888E-2*TA)
      DC9T=X9*ZZ*(-.752364*TAIN-12.4210/TASQ+.259556-.325374E-1*TA)
      DC10T=X10*ZZ*(-.415302E-2*TAIN-14.8627/TASQ+.124699-.01800454*TA)
      PP2=.5/P
      DC1P=-X1*PP2
      DC2P=-X2*PP2
      DC3P=-X3*PP2
      DC9P=X9*PP2
      DC10P=X10*PP2
      D5AN=-R0*X13/PHI
      DD4F=0.0444*D5AN
      C(1,1)=-(DC1T+DC5T+2.*DC9T-D1*DC10T)
      C(2,1)=-(DC2T+DC5T+DC7T+DC9T+(2.-D2)*DC10T)
      C(3,1)=-(DC3T+DC7T-D3*DC10T)
      C(4,1)=-(DC1T+DC2T+DC3T+DC5T+DC7T+DC9T+(1.+D4)*DC10T)
      C(1,2)=-(DC1P+2.*DC9P-D1*DC10P)
      C(2,2)=-(DC2P+DC9P+(2.-D2)*DC10P)
      C(3,2)=-(DC3P-D3*DC10P)
      C(4,2)=-(DC1P+DC2P+DC3P+DC9P+(1.+D4)*DC10P)
      C(1,3)=0.
      C(2,3)=2.*D5AN
      C(3,3)=7.4548*D5AN
```

```
      C(4,3)=-DD4F
      DO 905 K=1,3
      KP1=K+1
      AMAX=DABS(A(K,K))
      MAX=K
      DO 910 I=KP1,4
      IF(DABS(A(I,K)).LE.AMAX) GO TO 910
      AMAX=DABS(A(I,K))
      MAX=I
910   CONTINUE
      IF(AMAX.GT.0.0) GO TO 912
      IERR=7
      GO TO 710
912   IF(MAX.EQ.K) GO TO 950
      DO 915 J=K,4
      TERM=A(K,J)
      A(K,J)=A(MAX,J)
      A(MAX,J)=TERM
915   CONTINUE
      DO 920 J=1,3
      TERM=C(K,J)
      C(K,J)=C(MAX,J)
      C(MAX,J)=TERM
920   CONTINUE
950   DO 925 I=KP1,4
      TERM=A(I,K)/A(K,K)
      DO 930 J=KP1,4
      A(I,J)=A(I,J)-A(K,J)*TERM
930   CONTINUE
      DO 935 J=1,3
      C(I,J)=C(I,J)-C(K,J)*TERM
935   CONTINUE
925   CONTINUE
905   CONTINUE
      IF(DABS(A(4,4)).GT.0.0)GO TO 938
      IERR=7
      GO TO 710
938   DO 940 J=1,3
      C(4,J)=C(4,J)/A(4,4)
      C(3,J)=(C(3,J)-A(3,4)*C(4,J))/A(3,3)
      C(2,J)=(C(2,J)-A(2,3)*C(3,J)-A(2,4)*C(4,J))/A(2,2)
      C(1,J)=(C(1,J)-A(1,2)*C(2,J)-A(1,3)*C(3,J)-A(1,4)*C(4,J))/A(1,1)
940   CONTINUE
      DX4T=C(1,1)
      DX6T=C(2,1)
      DX8T=C(3,1)
      DX11T=C(4,1)
      DX4P=C(1,2)
      DX6P=C(2,2)
      DX8P=C(3,2)
      DX11P=C(4,2)
      DX4F=C(1,3)
      DX6F=C(2,3)
      DX8F=C(3,3)
      DX11F=C(4,3)
```

```
      DX1T=T14*DX4T+DC1T
      DX2T=T28*DX8T+DC2T
      DX3T=T311*DX11T+DC3T
      DX5T=T54*DX4T+T58*DX8T+DC5T
      DX7T=T78*DX8T+T711*DX11T+DC7T
      DX9T=T94*DX4T+T98*DX8T+DC9T
      DX10T=T106*DX6T+T108*DX8T+DC10T
      DX12T=D4*(DX6T+DX10T)
      DX1P=T14*DX4P+DC1P
      DX2P=T28*DX8P+DC2P
      DX3P=T311*DX11P+DC3P
      DX5P=T54*DX4P+T58*DX8P
      DX7P=T78*DX8P+T711*DX11P
      DX9P=T94*DX4P+T98*DX8P+DC9P
      DX10P=T106*DX6P+T108*DX8P+DC10P
      DX12P=D4*(DX6P+DX10P)
      DX1F=T14*DX4F
      DX2F=T28*DX8F
      DX3F=T311*DX11F
      DX5F=T54*DX4F+T58*DX8F
      DX7F=T78*DX8F+T711*DX11F
      DX9F=T94*DX4F+T98*DX8F
      DX10F=T106*DX6F+T108*DX8F
      DX12F=D4*(DX6F+DX10F)+DD4F
      RETURN
      END
      SUBROUTINE PER(JDR,RR)
      IMPLICIT DOUBLE PRECISION (A-H,O-Z)
      COMMON/BLOCK/AN,AM,AL,AK,PHI,T,P,KL0,IERR,X(13)
      COMMON/TAB/DXT(12),DXP(12),DXF(12)
      COMMON/PROP/AVM,R,H,U,DRT,DHT,DUT,DRP,DHP,DUP,DRF,DHF,DUF
      DIMENSION SH(12),SM(12),HT(351),CT(351)
C     DIMENSION HT1(135),HT2(135),CT1(135),CT2(96)
      DATA SM/1.008,16.00,14.008,2.016,17.007,28.011,30.008,31.999,
     A 18.016,44.010,28.013,39.944/
      DATA HT/62.141, 62.645, 63.147, 63.649, 64.149, 64.648, 65.148,
     B 65.646, 66.145, 66.643, 67.141, 67.639, 68.137, 68.635, 69.133,
     C 69.631, 70.129, 70.626, 71.124, 71.623, 72.121, 72.620, 73.119,
     D 73.619, 74.119, 74.620, 75.121, 75.623, 76.126, 76.630, 77.134,
     E 77.640, 78.146, 78.654, 79.162, 115.501,115.997,116.494,116.991,
     F 117.448,117.985,118.482,118.978,119.475,119.972,120.469,120.996,
     G 121.462,121.959,122.456,122.953,123.450,123.947,124.445,124.942,
     H 125.440,125.939,126.438,126.937,127.438,127.940,128.442,128.947,
     I 129.452,129.960,130.470,130.981,131.496,132.013,132.532, 4.130,
     J   4.832,  5.538,  6.250,  6.968,  7.694,  8.428,  9.172, 9.926,
     K  10.692, 11.470, 12.257, 13.054, 13.860, 14.675, 15.499, 16.331,
     L  17.170, 18.017, 18.872, 19.732, 20.599, 21.472, 22.350, 23.234,
     M  24.112, 25.016, 25.915, 26.818, 27.727, 28.640, 29.559, 30.481,
     N  31.409, 32.341, 13.618, 14.326, 15.037, 15.756, 16.484, 17.223,
     M  17.972, 18.733, 19.504, 20.286, 21.077, 21.878, 22.688, 23.505,
     N  24.330, 25.162, 26.001, 26.845, 27.695, 28.550, 29.410, 30.275,
     A 31.143, 32.016, 32.892, 33.772, 34.655, 35.541, 36.430, 37.322,
     B 38.216, 39.113, 40.013, 40.915, 41.819,-22.991,-22.255,-21.501,
     C -20.731,-19.945,-19.145,-18.334,-17.512,-16.682,-15.843,-14.998,
     D-14.148,-13.292,-12.431,-11.567,-10.698, -9.827, -8.953, -8.076,
```

```
E -7.197, -6.315, -5.432, -4.546, -3.659, -2.771, -1.880, -0.989,
F -0.096,  0.799,  1.694,  2.591,  3.489,  4.388,  5.288,  6.188,
G 25.839, 26.595, 27.369, 28.160, 28.966, 29.784, 30.673, 31.451,
H 33.297, 33.149, 34.007, 34.870, 35.737, 36.608, 37.482, 38.359,
I 39.240, 40.122, 41.007, 41.894, 42.782, 43.673, 44.564, 45.458,
J 46.353, 47.249, 48.146, 49.045, 49.944, 50.845, 51.747, 52.650,
K 53.553, 54.458, 55.363,  4.285,  5.063,  5.861,  6.675,  7.502,
L  8.341,  9.189, 10.046, 10.910, 11.781, 12.658, 13.540, 14.429,
M 15.324, 16.224, 17.129, 18.041, 18.957, 19.879, 20.807, 21.739,
N 22.677, 23.620, 24.568, 25.521, 26.478, 27.440, 28.406, 29.377,
O 30.351, 31.329, 32.311, 33.296, 34.284, 35.276,-52.227,-51.346,
P-50.436,-49.496,-48.527,-47.526,-46.496,-45.438,-44.352,-43.241,
A-42.106,-40.949,-39.772,-38.576,-37.363,-36.134,-34.890,-33.633,
B-32.364,-31.083,-29.791,-28.490,-27.180,-25.861,-24.535,-23.201,
C-21.860,-20.513,-19.159,-17.80,-16.436,-15.067,-13.693,-12.314,
D-10.931,-88.640,-87.482,-86.274,-85.025,-83.743,-82.431,-81.095,
E-79.739,-78.365,-76.977,-75.575,-74.162,-72.740,-71.309,-69.87,
F-68.424,-66.972,-65.515,-64.053,-62.586,-61.114,-59.639,-58.160,
G-56.678,-55.192,-53.703,-52.212,-50.717,-49.220,-47.721,-46.219,
H-44.715,-43.209,-41.700,-40.189,  4.197,  4.925,  5.668,  6.427,
I  7.201,  7.989,  8.790,  9.601, 10.422, 11.251, 12.087, 12.930,
J 13.779, 14.632, 15.490, 16.352, 17.218, 18.087, 18.958, 19.833,
K 20.710, 21.589, 22.470, 23.352, 24.237, 25.123, 26.011, 26.901,
L 27.791, 28.683, 29.577, 30.471, 31.367, 32.264, 33.161, 34.060/
   DATA CT/5.049, 5.029, 5.015, 5.006, 4.999, 4.994, 4.990,
A  4.987, 4.984, 4.982, 4.981, 4.979, 4.979, 9.978, 4.978,
B  4.978, 4.979, 4.980, 4.981, 4.984, 4.986, 4.990, 4.994,
C  4.999, 5.004, 5.010, 5.017, 5.025, 5.033, 5.041, 5.050,
D  5.060, 5.070, 5.081, 5.091, 4.968, 4.968, 4.968, 4.968,
E  4.968, 4.968, 4.968, 4.968, 4.968, 4.968, 4.968, 4.968,
F  4.968, 4.969, 4.969, 4.969, 4.971, 4.972, 4.975, 4.978,
G  4.982, 4.987, 4.993, 5.001, 5.011, 5.022, 5.035, 5.050,
H  5.067, 5.086, 5.107, 5.130, 5.156, 5.183, 5.213, 7.009,
I  7.036, 7.087, 7.148, 7.219, 7.300, 7.390, 7.490, 7.600,
J  7.720, 7.823, 7.921, 8.016, 8.108, 8.195, 8.279, 8.358,
1  8.434, 8.506, 8.575, 8.639, 8.700, 8.757, 8.810, 8.859,
2  8.911, 8.962, 9.012, 9.061, 9.110, 9.158, 9.205, 9.252,
L  9.927, 9.342, 7.057, 7.090, 7.150, 7.233, 7.332, 7.439,
M  7.549, 7.659, 7.766, 7.867, 7.966, 8.053, 8.137, 8.214,
N  8.286, 8.353, 8.415, 8.472, 8.526, 8.576, 8.622, 8.665,
A  8.706, 8.744, 8.780, 8.814, 8.846, 8.876, 8.905, 8.933,
B  8.959, 8.984, 9.008, 9.031, 9.053, 7.276, 7.450, 7.624,
C  7.786, 7.931, 8.057, 8.168, 8.263, 8.346, 8.417, 8.480,
D  8.535, 8.583, 8.626, 8.664, 8.689, 8.728, 8.756, 8.781,
E  8.804, 8.825, 8.844, 8.863, 8.879, 8.895, 8.910, 8.924,
F  8.937, 8.949, 8.961, 8.973, 8.984, 8.994, 9.004, 9.014,
G  7.466, 7.655, 7.832, 7.988, 8.123, 8.238, 8.336, 8.419,
H  8.491, 8.552, 8.605, 8.651, 8.692, 8.727, 8.759, 8.788,
I  8.813, 8.837, 8.858, 8.877, 8.895, 8.912, 8.927, 8.941,
J  8.955, 8.968, 8.980, 8.991, 9.002, 9.012, 9.022, 9.032,
K  9.041, 9.050, 9.058, 7.670, 7.883, 8.063, 8.212, 8.336,
L  8.439, 8.527, 8.604, 8.674, 8.738, 8.800, 8.858, 8.916,
M  8.973, 9.029, 9.084, 9.139, 9.194, 9.248, 9.301, 9.354,
N  9.405, 9.455, 9.503, 9.551, 9.596, 9.640, 9.682, 9.723,
O  9.762, 9.799, 9.835, 9.869, 9.901, 9.932, 8.676, 8.954,
```

```
     A  9.246, 9.574, 9.851, 10.152, 10.444, 10.723, 10.987, 11.233,
     B  11.462,11.674,11.869,12.048,12.214,12.366,12.505,12.634,
     C  12.753,12.863,12.965,13.059,13.146,13.228,13.304,13.374,
     E  13.441,13.503,13.562,13.617,13.669,13.718,13.764,13.808,
     D  13.850,11.310,11.846,12.293,12.667,12.980,13.243,13.466,
     E  13.656,13.815,13.953,14.074,14.177,14.269,14.352,14.424,
     F  14.489,14.547,14.600,14.648,14.692,14.734,14.771,14.807,
     G  14.841,14.873,14.902,14.930,14.956,14.982,15.006,15.030,
     H  15.053,15.075,15.097,15.119, 7.196, 7.350, 7.512, 7.670,
     I  7.815, 7.945, 8.061, 8.162, 8.252, 8.330, 8.398, 8.458,
     J  8.512, 8.559, 8.601, 8.638, 8.672, 8.703, 8.731, 8.756,
     K  8.779, 8.800, 8.820, 8.838, 8.855, 8.871, 8.886, 8.900,
     L  8.914, 8.927, 8.939, 8.950, 8.962, 8.972, 8.983, 8.993/
C       SUBROUTINE PER CALLS SUBROUTINE EQMD FOR CALCULATTION OF MOLE
C       FRACTIONS AND AND THEIR PARTIAL DERATIVES
C
        CALL EQMD(JDR,RR)
        IF(IERR.NE.0)RETURN
C       SECTION 100 CALCULATES AVM,R,H AND U.
        TK=T/180.
        IT=TK
        FR=TK-FLOAT(IT)
        SH(1)=92935.8+4.968*T
        SH(12)=4.968*T
C       WRITE(1,887)SH(1),SH(12)
 887    FORMAT(1X,'SH(1)  SH(12)',2F12.2)
        DO 105 I=2,11
        IN=35*(I-2)+(IT-5)
        SH(I)=(HT(IN)+FR*(HT(IN+1)-HT(IN)))*1800.
105     CONTINUE
        AVM=0.
        H=0.
        DO 110 I=1,12
        IF(X(I).LE.0.000000001)X(I)=0.000000001
        AVM=AVM+X(I)*SM(I)
        H=H+X(I)*SH(I)
 990    FORMAT(1X,'H X SH AVM  HT(I)  DELT',6F10.2)
110     CONTINUE
        H=H/AVM
        R=1.987165/AVM
        RR=R
C       WRITE(1,*)'**RR',RR
        U=H-R*T
        IF(JDR.EQ.0) RETURN
C
        DMT=DXT(1)*SM(1)+DXT(12)*SM(12)
        DHT=X(1)*4.968+DXT(1)*SH(1)+X(12)*4.968+DXT(12)*SH(12)
        DMP=DXP(1)*SM(1)+DXP(12)*SM(12)
        DHP=DXP(1)*SH(1)+DXP(12)*SH(12)
        DMF=DXF(1)*SM(1)+DXF(12)*SM(12)
        DHF=DXF(1)*SH(1)+DXF(12)*SH(12)
        DO 210 I=2,11
        IN=35*(I-2)+(IT-5)
        CP=CT(IN)+FR*(CT(IN+1)-CT(IN))
        DMT=DMT+DXT(I)*SM(I)
```

```
      DHT=DHT+X(I)*CP+DXT(I)*SH(I)
      DMP=DMP+DXP(I)*SM(I)
      DHP=DHP+DXP(I)*SH(I)
      DMF=DMF+DXF(I)*SM(I)
      DHF=DHF+DXF(I)*SH(I)
210   CONTINUE
      DRT=-R*DMT/AVM
      DHT=(DHT-DMT*H)/AVM
      DUT=DHT-R-DRT*T
      DRP=-R*DMP/AVM
      DHP=(DHP-DMP*H)/AVM
      DUP=DHP-DRP*T
      DRF=-R*DMF/AVM
      DHF=(DHF-DMF*H)/AVM
      DUF=DHF-DRF*T
988   FORMAT(1X,'H  DHT  DELT  T',4F15.5)
      RETURN
      END
```

END

DATE

FILMED

8-88

DTIC